

UNIVERSIDADE FEDERAL DE SANTA MARIA
CENTRO DE CIÊNCIAS NATURAIS E EXATAS
PROGRAMA DE PÓS-GRADUAÇÃO EM FÍSICA

Tamíres Zimmer

**CHARACTERIZATION OF SOIL THERMAL DYNAMICS IN NATURAL
PASTURE OVER THE BRAZILIAN PAMPA BIOME: ESTIMATES OF
SOIL THERMAL PROPERTIES.**

Santa Maria, RS
2022

Tamíres Zimmer

**CHARACTERIZATION OF SOIL THERMAL DYNAMICS IN NATURAL PASTURE OVER
THE BRAZILIAN PAMPA BIOME: ESTIMATES OF SOIL THERMAL PROPERTIES.**

Tese de Doutorado apresentada ao programa de Pós-Graduação em Física, Área de Concentração em Áreas Clássicas da Fenomenologia e Suas Aplicações, da Universidade Federal de Santa Maria (UFSM, RS), como requisito parcial para obtenção do grau de **Doutora em Física**.

Prof.^a Débora Regina Roberti

Santa Maria, RS
2022

This study was financed in part by the Coordenação de Aperfeiçoamento de Pessoal de Nível Superior - Brasil (CAPES) - Finance Code 001

Zimmer, Tamíres

Characterization of soil thermal dynamics in natural pasture over the Brazilian Pampa biome: Estimates of soil thermal properties. / Tamíres Zimmer.- 2022.
66 p.; 30 cm

Orientadora: Débora Regina Roberti

Tese (doutorado) - Universidade Federal de Santa Maria, Centro de Ciências Naturais e Exatas, Programa de Pós-Graduação em Física, RS, 2022

1. SOIL TEMPERATURE 2. SOIL HEAT FLUX 3. SOIL THERMAL PROPERTIES 4. CLEARNESS INDEX OF THE ATMOSPHERE 5. PAMPA BIOME I. Roberti, Débora Regina II. Título.

Sistema de geração automática de ficha catalográfica da UFSM. Dados fornecidos pelo autor(a). Sob supervisão da Direção da Divisão de Processos Técnicos da Biblioteca Central. Bibliotecária responsável Paula Schoenfeldt Patta CRB 10/1728.

Declaro, TAMÍRES ZIMMER, para os devidos fins e sob as penas da lei, que a pesquisa constante neste trabalho de conclusão de curso (Tese) foi por mim elaborada e que as informações necessárias objeto de consulta em literatura e outras fontes estão devidamente referenciadas. Declaro, ainda, que este trabalho ou parte dele não foi apresentado anteriormente para obtenção de qualquer outro grau acadêmico, estando ciente de que a inveracidade da presente declaração poderá resultar na anulação da titulação pela Universidade, entre outras consequências legais.

©2022

Todos os direitos autorais reservados a Tamíres Zimmer. A reprodução de partes ou do todo deste trabalho só poderá ser feita mediante a citação da fonte.

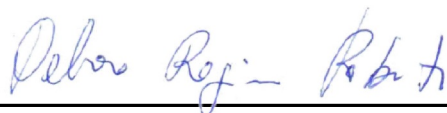
End. Eletr.: tz.tamireszimmer@gmail.com

Tamíres Zimmer

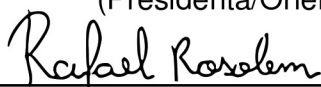
**CHARACTERIZATION OF SOIL THERMAL DYNAMICS IN NATURAL PASTURE OVER
THE BRAZILIAN PAMPA BIOME: ESTIMATES OF SOIL THERMAL PROPERTIES.**

Tese de Doutorado apresentada ao programa de Pós-Graduação em Física, Área de Concentração em Áreas Clássicas da Fenomenologia e Suas Aplicações, da Universidade Federal de Santa Maria (UFSM, RS), como requisito parcial para obtenção do grau de **Doutora em Física**.

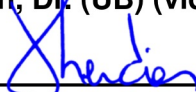
Aprovado em 14 de junho de 2022:



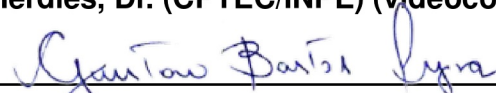
Débora Regina Roberti, Dra. (UFSM)
(Presidenta/Orientadora)



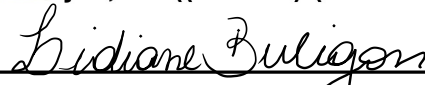
Rafael Rosolen, Dr. (UB) (videoconferência)



Dirceu Herdies, Dr. (CPTEC/INPE) (videoconferência)



Gustavo Bastos Lyra, Dr. ((UFRRJ) (videoconferência)



Lidiane Buligon, Dra. ((UFSM) (videoconferência)

Santa Maria, RS
2022

DEDICATÓRIA

Aos meus pais

AGRADECIMENTOS

À minha família em especial aos meus pais Alberto e Loane, por todo o apoio, compreensão e carinho recebido em qualquer circunstância e por sempre acreditarem em mim e nunca me deixarem desistir.

Ao meu namorado Diego, pelas risadas, choros, desabaços, palavras de incentivo e por toda a compreensão.

À minha orientadora, Profa. Dra. Débora Regina Roberti pela orientação, dedicação, amizade e todo o conhecimento transmitido durante o mestrado e doutorado.

À Profa. Dra. Lidiane Buligon por acompanhar e contribuir com o meu trabalho durante o mestrado e doutorado, e pelos conhecimentos transmitidos desde a graduação.

À minha amiga Vanessa, por toda ajuda, “coorientação” e amizade. Obrigado pelas palavras positivas nos momentos mais difíceis.

À meu amigo Michel, pelo apoio, risadas, estudo desde o segundo semestre da graduação e também por nunca me deixar desistir. Obrigado por me acompanhar há tantos anos em todas as situações.

Aos meus colegas do Laboratório pelo apoio, companheirismo e conhecimentos compartilhados.

Aos meus amigos pela amizade e torcida, mesmo que às vezes a correria do dia a dia impeça os nossos encontros.

Aos meus amores de quatro patas, por me fazerem sorrir todos os dias, independentemente da situação.

Aos professores do Departamento de Física da UFSM.

A UFSM, pela oportunidade de estudo e utilização do espaço físico.

À Coordenação de Aperfeiçoamento de Pessoal de Nível Superior (CAPES) pelo apoio financeiro na forma de bolsa de doutorado.

À todos que de certa forma contribuíram direta ou indiretamente na construção desse trabalho - Muito Obrigada!

Paciência e perseverança tem o efeito mágico de fazer as dificuldades desaparecerem e os obstáculos sumirem.

John Quincy Adams

RESUMO

CARACTERIZAÇÃO DA DINÂMICA TÉRMICA DO SOLO EM PASTAGEM NATURAL SOBRE O BIOMA PAMPA BRASILEIRO: ESTIMATIVAS DAS PROPRIEDADES TÉRMICAS DO SOLO.

AUTORA: Tamíres Zimmer

ORIENTADORA: Débora Regina Roberti

Para caracterizar a dinâmica térmica do solo é necessário determinar suas propriedades térmicas, pois são elas que descrevem como a energia térmica é armazenada e distribuída de acordo com o tempo e a profundidade. Assim, quantificar as temperaturas do solo e da superfície e estimar o armazenamento de calor são fundamentais para estudos de balanço de energia de superfície e este conhecimento é importante para caracterizar o microclima local. Este estudo tem como objetivo quantificar e analisar as propriedades térmicas do solo em campos nativos do bioma Pampa brasileiro por meio de métodos híbridos baseados em dados experimentais e métodos analíticos por meio de dois artigos. No primeiro, investiga-se a influência de condições climáticas como cobertura do céu e umidade do solo (θ) na dinâmica das variáveis térmicas do solo (fluxo de calor, G , e temperatura do solo, T_s) e propriedades térmicas do solo. Os resultados mostraram que os maiores valores de condutividade térmica (λ) e difusividade térmica (k) foram obtidos em períodos com solo úmido. Além disso, observou-se maior variabilidade das propriedades térmicas do solo com o aumento da umidade. A proposta de um novo modelo empírico para $\lambda(\theta)$ forneceu bons resultados para representar o λ experimental e estimar G . O segundo artigo apresenta a estimativa das propriedades térmicas e temperatura do solo obtidas a partir da solução analítica da equação de transferência de calor por condução e condução-convecção. Os resultados obtidos esclarecem melhor a dinâmica térmica do solo ao considerar os processos de condução e convecção de calor no solo em diferentes profundidades. Além disso, as propriedades térmicas do solo mostraram variar em diferentes níveis, além da heterogeneidade vertical nas propriedades térmicas do solo em função da umidade do solo para períodos secos e úmidos. Os resultados do estudo mostram a influência da umidade do solo e das condições climáticas na caracterização termodinâmica do solo.

Palavras-chave: TEMPERATURA DO SOLO. FLUXO DE CALOR NO SOLO. PROPRIEDADES TÉRMICAS DO SOLO. UMIDADE DO SOLO. ÍNDICE DE CLARIDADE DA ATMOSFERA. BIOMA PAMPA.

ABSTRACT

CHARACTERIZATION OF SOIL THERMAL DYNAMICS IN NATURAL PASTURE OVER THE BRAZILIAN PAMPA BIOME: ESTIMATES OF SOIL THERMAL PROPERTIES.

AUTHOR: Tamíres Zimmer
ADVISOR: Débora Regina Roberti

To characterize the soil thermal dynamics, it is necessary to determine its thermal properties because they describe how thermal energy is stored and distributed according to time and depth; this knowledge is important for characterizing the local microclimate. Hence, quantifying soil and surface temperatures and estimating heat storage are pivotal for surface energy balance studies. Given the above, this study aims to quantify and analyze soil thermal properties in native grasslands in the Brazilian Pampa biome through hybrid methods based on experimental data and analytical methods through two articles. In the first, the influence of climatic conditions such as sky cover and soil moisture (θ) on the dynamics of soil thermal variables (soil heat flux, G , and soil temperature, T_s) and soil thermal properties is investigated. The results showed that the highest values of thermal conductivity (λ) and thermal diffusivity (k) were obtained in periods with moist soil. Moreover, greater variability of soil thermal properties with increasing moisture was observed. The proposal of a new empirical model for $\lambda(\theta)$ provided good results to represent the experimental λ and estimate G . The second article presents the estimation of thermal properties and soil temperature obtained from the analytical solution of the heat transfer equation by conduction and conduction-convection. The obtained results shed more light on the thermal dynamics of the soil by considering the conductive and convective processes of heat in the soil at different depths. Moreover, the thermal properties of the soil were shown to vary at different levels, in addition to vertical heterogeneity in the thermal properties of the soil as a function of soil moisture for dry and wet periods. The study results show the influence of soil moisture and climatic conditions on soil thermal dynamic characterization.

Keywords: SOIL TEMPERATURE. SOIL HEAT FLUX. SOIL THERMAL PROPERTIES. CLEARNESS INDEX OF THE ATMOSPHERE. PAMPA BIOME.

LIST OF FIGURES

Figure 2.1 – Illustration of the Pampa biome with delimitation of its territory in South America, Brazil and Rio Grande do Sul State.	13
Figure 2.2 – Illustration of the energy balance components: (a) during the day and (b) during the night.	15
Figure 2.3 – Dependence of thermal conductivity on soil moisture in a porous medium the contact between the grains is limited to small areas (red), and the corresponding cross-sectional area limits the heat flux in a completely dry medium (a). The paths widen considerably with increasing water content, resulting in higher conductivity (b–d).	17

CONTENTS

1	INTRODUCTION	10
1.1	OBJECTIVE.....	12
2	THEORETICAL FOUNDATION	13
2.1	PAMPA BIOME	13
2.2	ENERGY BALANCE	14
2.3	SOIL HEAT FLUX.....	16
2.4	SOIL THERMAL PROPERTIES	17
2.4.1	Thermal conductivity	17
2.4.2	Volumetric heat capacity	18
2.4.3	Thermal diffusivity	18
2.5	CONTRIBUTION OF WATER TO SOIL THERMAL BEHAVIOR.....	18
2.5.1	Soil moisture	19
2.5.2	Soil water availability	19
2.6	ATMOSPHERE CLARITY INDEX	20
3	ARTICLE 1: INFLUENCE OF CLEARNESS INDEX AND SOIL MOISTURE IN THE SOIL THERMAL DYNAMIC IN NATURAL PASTURE IN THE BRAZILIAN PAMPA BIOME	22
4	ARTICLE 2: ESTIMATION OF SOIL THERMAL PROPERTIES USING CONDUCTION AND CONDUCTION - CONVECTION HEAT TRANSFER EQUATIONS IN THE BRAZILIAN PAMPA BIOME	38
5	FINAL CONSIDERATIONS	60
	BIBLIOGRAPHY	62

1 INTRODUCTION

Understanding the complex interaction between soil, vegetation, and the atmosphere is fundamental for describing meteorological, hydrological, and ecological phenomena. Soil is an important natural variable that influences several processes, such as infiltration and heat transfer between soil layers (soil horizons) (ALKHAIER; FLERCHINGER; SU, 2012). In this sense, knowledge of composition and soil land cover and the processes of energy and mass exchange between the surface and subsoil is essential for surface modeling related to surface energy balance closure, models of agricultural production, and climate, among others (HEUSINKVELD et al., 2004; EVETT et al., 2012; KOJIMA et al., 2018). In addition, knowledge of soil thermal properties (soil thermal diffusivity, k , soil thermal conductivity, λ , and soil thermal capacity, c_v) enables an understanding of soil thermal dynamics, which are necessary basic parameters for estimating thermal variables that include soil temperature (T_s) and heat flux (G).

G on the surface can account for about 20% of the energy available over various land covers (KUSTAS; DAUGHTRY, 1990; WILSON et al., 2002; ONCLEY et al., 2007; FOKEN, 2008; WANG; GAO; HORTON, 2010); it is responsible for energy transfer from the surface to the subsoil and is directly related to variations in T_s , soil moisture (θ), and thermal properties. Soil thermal variables such as T_s and G are mainly influenced by weather conditions (ALLEN et al., 1998; ALVALÁ et al., 2002), while thermal properties depend on θ and solar radiation (WANG; GAO; HORTON, 2010; OTUNLA; OLADIRAN, 2013; AN et al., 2016). Both are characterized by diurnal, monthly, seasonal, and annual behavior dynamics. In addition, the thermal properties of the soil depend on factors related to the type of the soil, including texture, porosity (θ_s), density (ρ_s), organic matter content, mineralogical composition, the physical structure of the soil, among others (VRIES; PECK, 1958; JOHANSEN, 1975; CAMPBELL, 1985; LU et al., 2007; CLARKE; AGAB; NICHOLSON, 2008; LIU et al., 2018; LU et al., 2019; XIE et al., 2019). Various studies have shown that climatic conditions related to the amount of solar radiation reaching the surface and soil moisture directly influence the dynamics of energy transfer from the surface to the subsoil (JR; FRIEDL, 2003; OTUNLA; OLADIRAN, 2013; ROXY; SUMITHRANAND; RENUKA, 2014; AN et al., 2016; ZIMMER et al., 2020).

Cloud cover is an important factor in the processes of scattering and absorbing solar radiation in the atmosphere and affects the amount of this radiation that falls on the Earth's surface (ECHER; MARTINS; PEREIRA, 2006); it is also used for the processes of energy transfer both to the atmosphere and the subsoil. Mathematically, various combinations of measurements of incident solar radiation on the surface, surface temperature, soil temperature, soil moisture, and air temperature, together with estimates of the thermal properties of the soil, are used to calculate the G indirectly from the solution of the

heat equation (KIMBALL et al., 1976; HORTON; WIERENGA; NIELSEN, 1983; SILANS; MONTENY; LHOMME, 1997; WANG; BRAS, 1999; VERHOEF, 2004).

Many methods for estimating soil thermal properties have been proposed in the literature. The estimates are generally obtained from analytical solutions of the heat conduction equation (CARSLAW; JAEGER, 1959), where the boundary conditions are described by a sine function or a Fourier series. In the analysis of heat transfer by conduction, the soil is considered vertically homogeneous with a constant thermal diffusivity, and the analytical methods used are amplitude and phase change (VRIES; PECK, 1958; WIERENGA; NIELSEN; HAGAN, 1969), arc tangent (NERPIN; CHUDNOVSKII, 1967), logarithmic (SEEMANN, 1979), harmonic (HORTON; WIERENGA; NIELSEN, 1983), and numerical solutions using the gradient method (HORTON; WIERENGA; NIELSEN, 1983; EVETT et al., 2012; GAO et al., 2017; ROMIO et al., 2019).

Nonetheless, vertical water flow may affect T_{soil} , and thus, thermal properties (e.g., soil heat transfer) are also due to heat convection within pores (SILANS; MONTENY; LHOMME, 1996; GAO; FAN; BIAN, 2003). Solutions for the conduction-convection equation have been developed that consider the vertical heterogeneity of the thermal diffusivity of the soil. Gao, Fan & Bian (2003) proposed a new method for estimating k by deriving the analytical solution of the conduction-convection equation using the harmonic and Laplace transform methods (GAO, 2005). Wang et al. (2012a), Wang et al. (2012b) improved the solution of the conduction-convection equation with a T_s limit described as a Fourier series. Nevertheless, the thermal properties of the soil can also be estimated by empirical models and for specific data sets in different regions and experimental sites around the world.

Therefore, numerous researchers have parameterized thermal properties based on soil parameters measured in laboratory experiments for specific soil samples (CLARKE; AGAB; NICHOLSON, 2008; LU et al., 2019; XIE et al., 2019; ZHAO et al., 2019). However, given scale effects and soil complexity, errors often occur when extrapolating laboratory results to field experiments (BARRIOS; FRANCÉS, 2012; EVETT et al., 2012; AN et al., 2016), mainly because θ depends on field conditions and varies with time and soil depth (FAROUKI, 1986; LU et al., 2007; CHEN; SHAO; LI, 2008; LU et al., 2014). Most empirical models proposed in the literature describe λ as a function of θ (KERSTEN, 1949; VRIES; PECK, 1958; JOHANSEN, 1975; CAMPBELL, 1985; CÔTÉ; KONRAD, 2005; LU et al., 2007; LU et al., 2014; NIKOOSOKHAN; NOWAMOOZ; CHAZALLON, 2016; TONG et al., 2016).

Parameterizations are often used in land surface models to determine the energy and water balance of the surface in different ecosystems, albeit such parameterizations still do not describe all soil properties. Therefore, it is important to develop research that describes the long-term thermal properties of soil in different soil types and climatic zones. Despite climatic information on the energy exchange between soil, plant, and atmosphere being essential to describe these ecosystems, this information is limited and almost non-existent

in some regions, including the Pampa biome. Given this context, this study investigated soil thermal dynamics in two experimental sites characterized by natural pastures in different locations of the Brazilian Pampa biome.

The Pampa biome is characterized by a transitional area between tropical and temperate climates, with hot summers and cold winters, regular rainfall between months, and a region spread between southern Brazil, Uruguay, and northern Argentina. According to (ROESCH et al., 2009), the Pampa has a typical climate for developing forest ecosystems, although the formation of dense forests is uncommon in this region, as grasses predominate. In addition, the Pampa, with its still little-known soil properties, plays an important role in biodiversity conservation (BINKOWSKI, 2009). It is known that the thermal dynamics of the soil in the Pampa biome are of fundamental importance for understanding the local ecosystem, as is the net energy exchange between the surface and atmosphere.

In this context, it is highly challenging to understand how climate variables influence thermal variables and soil thermal properties at different time scales. Describing these soil-plant-atmosphere interactions is extremely difficult, as it is not easy to find studies in the literature with a database of field measurements over long periods, at different seasons, and in similar ecosystems. Monitoring areas in the Pampa is even more difficult, as it is a region that has been little studied in terms of thermal variables and soil thermal properties.

1.1 OBJECTIVE

To quantify and analyze thermal soil properties in native grasslands in the Brazilian Pampa biome using hybrid methods based on experimental data and analytical methods.

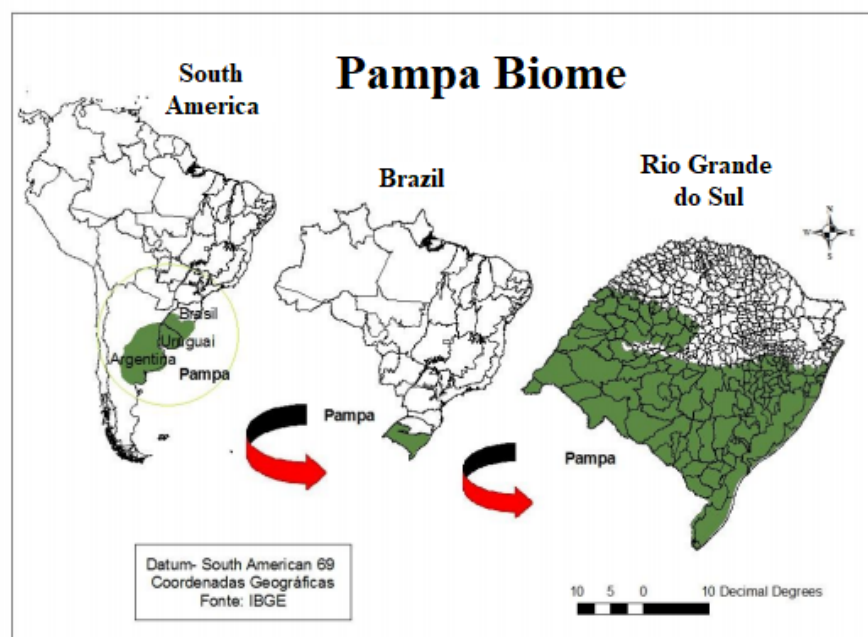
2 THEORETICAL FOUNDATION

This chapter is devoted to a brief overview of the main themes that have supported this study. The overview allows for a better understanding of the parameters used, their properties, and above all, the relationships with the physical properties of the soil analyzed in this thesis.

2.1 PAMPA BIOME

The Pampa biome is located in southern Brazil, part of Argentina, and the entire territory of Uruguay; it occupies an area of roughly 750.000 km² (Figure 2.1). In southern Brazil, the Pampa Biome covers an area of about 176.496 km², which corresponds to 2.07% of the Brazilian territory and 63% of Rio Grande do Sul State (IBGE, 2004; BOLDRINI, 2010).

Figure 2.1 – Illustration of the Pampa biome with delimitation of its territory in South America, Brazil and Rio Grande do Sul State.



Fonte: Adapted from (AZEVEDO, 2013).

These areas have changed since the colonization of Brazil, especially with the introduction of cattle breeding, the expansion of agricultural areas, and the creation of a land structure with medium and large plots. Nevertheless, the Pampa plays an important role in biodiversity conservation, as it is home to a plethora of animal and plant species that are

still little studied (BINKOWSKI, 2009). According to the Ministry of the Environment (ROSA, 2008), there are about 3000 plant species, 100 mammal species, and 500 bird species in the biome. What is more, the Pampa has only recently been recognized as a biome (in 2004) and separated from the Atlantic Forest biome.

The fields of the Pampa biome are characterized by a predominance of grassland vegetation of the low herbaceous type with grass features, which also has shrub vegetation and woodlands (BOLDRINI, 2010). In general, the physiognomy of the fields is determined by the structure of the vegetation. In the Pampa, however, very different field physiognomies can be observed, which are essentially characterized by various factors: soil and relief, climatic conditions, and cultivation. Agriculture is highly developed because of the natural fields, which are an essential resource for its use (NABINGER et al., 2009).

The climate of the Pampa biome is classified as humid subtropical (Cfa) according to the Köppen climate classification (PEEL; FINLAYSON; MCMAHON, 2007), with hot summers and cold winters. During the year, changes in vegetation cover may occur in the fields of the biome, either due to severe weather events or phenomena such as El Niño and La Niña (ENOS). Vegetation in the Pampa biome, therefore, has a well-defined seasonal behavior with a growing season and increased species biomass in the hot seasons (spring and summer) and decreased species biomass in the cold seasons (autumn and winter) (KUPLICH; MOREIRA; FONTANA, 2013; ACOSTA et al., 2019).

2.2 ENERGY BALANCE

The energy balance at the surface, based on the principle of conservation of energy, can be represented by the transfer of energy in the form of heat to warm the atmosphere (sensible heat, H), water vapor condensation, or water evaporation from the surface and transpiration of plants (latent heat, LE) and by energy transfer, conduction to heat the soil (soil heat flux, G). For an ideal surface (relatively flat, homogeneous, large in area, and impermeable to radiation), energy balance is as follows:

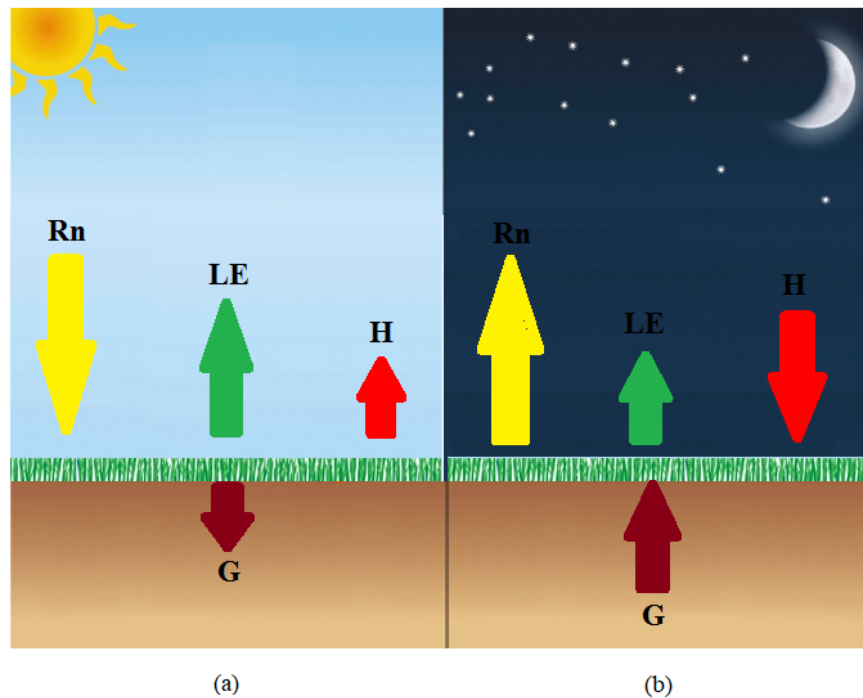
$$Rn - G = H + LE \quad (2.1)$$

where Rn is the net radiation balance at the surface, G is the energy flux in the form of heat in the soil, H is the energy flux in the form of sensible heat and LE is the energy flux in the form of latent heat. The terms on the left and right sides of Eq.(2.1) are defined as available energy ($Rn - G$) and turbulent fluxes ($H + LE$), respectively.

The energy balance allows us to evaluate the changes in the microclimate of the vegetation depending on the stages of development of the plants and conditions of the soil and the atmosphere, as it is based on the balancing of the different types of energy

interacting with the Earth's surface, with solar energy being the main source, and the resulting balance as net radiation (R_n) (BISHT et al., 2005).

Figure 2.2 – Illustration of the energy balance components: (a) during the day and (b) during the night.



Fonte: Prepared by the author.

The R_n is normally positive during the day and negative at night; it defines the difference between energy losses and gains at the surface. During the day (Figure 2.2, a), the soil absorbs solar radiation and, when heated, releases energy to heat the air (H), evaporate water (LE), and heat the deeper soil layers (G). During the night (Figure 2.2, b), the soil continues to rapidly lose energy due to the absence of the Sun and cools more than the adjacent air and deeper soil layers. Since the ground is colder than the adjacent air, the arriving water vapor condenses. In this way, the Earth receives the latent heat (LE) of condensation. The low surface temperature causes heat conduction from the deeper soil layers (G) to be directed upwards, and finally, the warmer air immediately above the soil surface transfers the energy to the soil surface by heat conduction (PEREIRA, 2002).

The closing of the energy balance is often analyzed to assess the quality of the energy fluxes determined with the Eddy Covariance method and indirectly to assess the accuracy of the carbon dioxide measurements (WILSON et al., 2001; CULF; FOKEN; GASH, 2004; LEUNING, 2004; FOKEN, 2008).

2.3 SOIL HEAT FLUX

When a portion of a given substance is heated, the heat generated by the heating tends to spread in all directions until thermal equilibrium is reached. This heat propagation is different for each substance because there can be different interactions between the matter and thermal energy (heat) (TOULOUKIAN et al., 1973).

Among the physical processes of heat propagation, heat conduction predominates in solid substances, and the propagation mechanism does not physically change the properties of the solid substance. Therefore, heat conduction occurs through thermal energy transfer from one particle to another and is generally the most important transfer process in soils. This process is determined by the thermal properties of the soil, which in turn are strongly dependent on soil moisture (θ) (PREVEDELLO, 2015).

Heat conduction in solids was originally analyzed by Fourier, whose name is associated with the linear transport equations used to describe heat conduction. The first law of heat conduction, known as Fourier's law, states that the heat flow in a homogeneous body is proportional to the temperature gradient and can be written as follows:

$$G = -\lambda \frac{\partial T}{\partial z} \quad (2.2)$$

where G (W m^{-2}) is the soil heat flux (i.e. the amount of heat conducted per unit cross-section per unit time), λ ($\text{W m}^{-1}\text{K}^{-1}$) is the thermal conductivity, which is a function of θ ($\text{m}^3 \text{m}^{-3}$), T (K) is the soil temperature, and z (m) is the depth of the soil surface. The negative sign means that heat flows from the point of higher temperature to the point of lower temperature (HORTON; WIERENGA; NIELSEN, 1983).

The soil heat flux is defined as the amount of energy used to heat the soil, and it cannot be measured directly, although its concept has important physical significance because it is linked to a measurable scalar quantity (temperature) since the temperature distribution within the material is given as a function of position and time.

G represents the fraction of R_n that is transferred to the lower soil layers and generally results in an increase in energy in the middle of the night or a decrease during the day. In energy balance research, G quantification is of utmost importance as it represents the energy input/output of a given medium, thus contributing to the increase and/or decrease in LE and H fluxes and, consequently, the increase and/or decrease in evaporation and transpiration rates.

2.4 SOIL THERMAL PROPERTIES

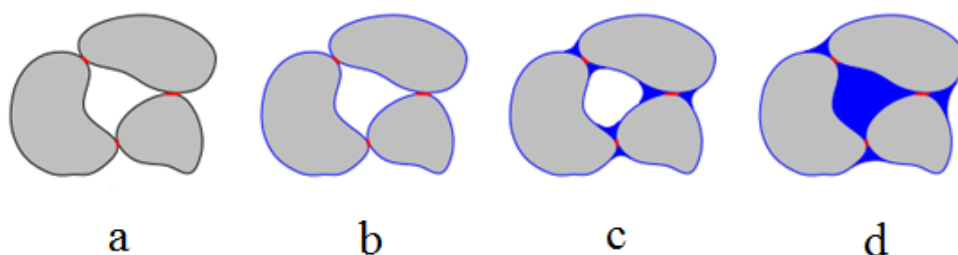
2.4.1 Thermal conductivity

Thermal conductivity (λ) is the amount of energy that soil can transfer through a unit area per unit time under a temperature gradient in the direction of that heat flow (FAROUKI, 1981). It is also a critical thermal property that determines the soil's ability to transfer energy in the form of heat.

The thermal conductivity of soil is one of the most important parameters related to heat exchange and plays a key role in verifying the thermal hydrodynamics of soil. Since soil is a granular medium composed of solid, liquid, and gaseous components, its thermal conductivity depends on the volumetric proportions of these components, the size and arrangement of the solid particles, and the contact area between solid and liquid and, in particular, the soil moisture (CAMPBELL; LONGWORTH, 1970).

Heat conduction in dry porous media occurs almost exclusively via the contact zones between solid particles (Figure 2.3, a). Figure 2.3 (c) illustrates the heat transfer by conduction in pore media, but under wetter medium conditions, where the presence of water trapping the solid particles leads to an effective increase in the contact area that can transfer heat, so that λ increases rapidly. With increasing humidity (Figure 2.3, d), λ continues to increase as the air, which has low conductivity, can no longer transfer heat (PREVEDELLO, 2015).

Figure 2.3 – Dependence of thermal conductivity on soil moisture in a porous medium the contact between the grains is limited to small areas (red), and the corresponding cross-sectional area limits the heat flux in a completely dry medium (a). The paths widen considerably with increasing water content, resulting in higher conductivity (b–d).



Fonte: Prepared by (ROTH, 1995).

2.4.2 Volumetric heat capacity

The heat capacity (c_v) per unit volume of soil is the energy in the form of heat required to change the temperature of that unit volume by 1 °C. It is calculated as the product of the specific heat of the soil (C_s) and the specific density of the soil (ρ_s) (FAROUKI, 1986):

$$c_v = \rho_s C_s \quad (2.3)$$

The volumetric heat capacity of a soil depends on the following factors: the factors inherent in the soil itself and the factors that can be managed or controlled to some extent. The factors or properties inherent in the soil itself are related to mineralogical composition and organic matter (WIERENGA; NIELSEN; HAGAN, 1969). Factors that influence soil heat capacity and can be controlled externally are volumetric moisture and soil density, although they are difficult to measure. Soil management also influences c_v by causing soil compaction, increasing density, and reducing porosity (WIERENGA; NIELSEN; HAGAN, 1969).

2.4.3 Thermal diffusivity

Soil thermal diffusivity (k) determines the rate at which temperature spreads through the soil, varying in time and space, and dictates the relationship between the ability to store and conduct thermal energy in the soil (REICHARDT; TIMM, 2004). The relationship is given by the ratio between the thermal conductivity (λ) and soil volumetric heat capacity (c_v) (FAROUKI, 1986), as

$$k = \frac{\lambda}{c_v} \quad (2.4)$$

Thermal diffusivity is also a function of soil moisture, density, and composition (REICHARDT; TIMM, 2004), and it increases at higher θ values until reaching a maximum value. From this point, the water content λ no longer increases at the same rate as c_v , and the thermal diffusivity, therefore, decreases (CAMPBELL; LONGWORTH, 1970).

2.5 CONTRIBUTION OF WATER TO SOIL THERMAL BEHAVIOR

Soil can be considered a medium that can store water very efficiently, and this storage can occur over long periods so that plants can use it. Water enters the soil through precipitation, irrigation, runoff, and the capillary rise and leaves through drainage, runoff, and evapotranspiration. The physical properties of the pore space, such as porosity,

connectivity between pores, and permeability influence the transport of fluids in the soil. The water movement in the soil is usually in liquid and/or vapor form, which leads to changes in the thermal properties of the soil due to variations in the amount and state of water. This fact is due to the temperature gradients in the soil that cause the movement of water in the medium (FAROUKI, 1986).

2.5.1 Soil moisture

Soil moisture (θ) can be described as the amount of water that the soil stores (REICHARDT, 1990); θ is the ratio between the volume of water present in a soil sample and the volume of the sample:

$$\theta = \frac{V}{V_T} = \frac{\rho_A(m_u - m_s)}{V_T} \quad (2.5)$$

where θ is the soil moisture ($\text{m}^3 \text{m}^{-3}$), V is the volume occupied by water (m^3), V_T is the total volume of the sample (m^3), ρ_A is the density of water (kg m^{-3}), m_s is the mass of solids (kg), and m_u is the wet mass of the soil sample (kg). The measurement of soil moisture (θ) can also be expressed as a percentage (%).

2.5.2 Soil water availability

Soil water availability refers to the capacity of a soil to retain water available to plants. After heavy rainfall or irrigation, the soil will drain until field capacity is reached. Field capacity (θ_{FC}) is the amount of water that a well-drained soil should hold against gravitational forces or the amount of water remaining when downward drainage has markedly decreased. In the absence of a water supply, the water content in the root zone decreases due to water uptake by the crop. As water uptake progresses, the remaining water is held to the soil particles with greater force, lowering its potential energy and making it more difficult for the plant to extract it. Eventually, a point is reached where the crop can no longer extract the remaining water. The water uptake becomes zero when wilting point (θ_{WP}) is reached (ALLEN et al., 1998).

As the water content above θ_{FC} cannot be held against the forces of gravity and will drain and as the water content below θ_{WP} cannot be extracted by plant roots, the total available water in the root zone is the difference between the water content at field capacity and wilting point (ALLEN et al., 1998); it is mathematically expressed by the equation:

$$TAW = 1000(\theta_{FC} - \theta_{WP})Z_r \quad (2.6)$$

where TAW (mm) is the total available soil water in the root zone, θ_{FC} ($\text{m}^3 \text{m}^{-3}$) is the water content at field capacity, θ_{WP} ($\text{m}^3 \text{m}^{-3}$) is the water content at wilting point, and Z_r (m) is the rooting depth.

Although water is theoretically available until θ_{WP} , the crop water uptake is reduced well before the wilting point is reached. As the soil water content decreases, water becomes more strongly bound to the soil matrix and more difficult to extract. When the soil water content drops below a threshold value, soil water can no longer be transported quickly enough towards the roots to respond to the transpiration demand, and the crop begins to experience stress (ALLEN et al., 1998). The fraction of TAW that a crop can extract from the root zone without suffering water stress is the readily available soil water (RAW) and given by the equation:

$$RAW = p(TAW) \quad (2.7)$$

where p is the average fraction of total available soil water that can be depleted from the root zone before moisture stress occurs. The factor p differs from one crop to another (ALLEN et al., 1998).

2.6 ATMOSPHERE CLARITY INDEX

According to Marthews, Malhi & Iwata (2012), the clarity index (κ) is defined as the ratio between the shortwave radiation (R_g) received from the sun/sky on a horizontal surface and the radiation reaching the upper part of the atmosphere (R_0), which is calculated according to the equation:

$$\kappa = \frac{R_g}{R_0} \quad (2.8)$$

Equation (2.8) depends on the time, the day of the year, and the location (latitude). The clarity index is dimensionless and ranges from 0 to 1 (where 1 corresponds to 100%). This value expresses the atmospheric transmittance (i.e., how much of the incident radiation at the top of the atmosphere actually reaches the Earth's surface). In addition, κ varies according to the amount of clouds and aerosols in the atmosphere, resulting in an increase or decrease in the direct or diffuse components of solar radiation reaching the surface. This fact also makes it possible to classify cloud cover according to its degree of cloudiness (TAVARES, 2005).

The radiation reaching the top of the atmosphere (R_0) can be calculated with the classical equation described by Iqbal (1983), which is calculated as a function of the solar constant (S_0), the radius of the Earth's orbital vector (E_0), the local latitude (ϕ), the solar

declination (δ), and the zenith angle (Z) as follows:

$$R_0 = S_0 E_0 \cos(Z) \quad (2.9)$$

with

$$E_0 = 1 + 0,0033 \cos\left(\frac{2\pi d_n}{365}\right) \quad (2.10)$$

where d_n is the day of the year according to the Julian calendar. For the solar zenith angle (Z), which is the angle between the vector connecting the centers of the Earth and the Sun and the local zenith, the following equation is used:

$$\cos(Z) = \sin\phi \sin\delta + \cos\phi \cos\delta \cos H \quad (2.11)$$

where δ is the solar declination and considered the (celestial) latitude at which the Sun is located, which may vary from 0° to $\pm 23^\circ$ during the year; it is calculated as follows:

$$\delta = 23,45 \sin\left[\frac{360(284 + d_n)}{365}\right] \quad (2.12)$$

The hour angle (H), which is a measure of the Sun's position in the equatorial hour coordinate system, takes values between -90° and $+90^\circ$. The value $H = 0^\circ$ is assigned to the solar midpoint, while negative values refer to the period before the solar midpoint and positive values to the later period (PLANA-FATTORI; CEBALLOS, 1996).

3 ARTICLE 1: INFLUENCE OF CLEARNESS INDEX AND SOIL MOISTURE IN THE SOIL THERMAL DYNAMIC IN NATURAL PASTURE IN THE BRAZILIAN PAMPA BIOME

Geoderma 378 (2020) 114582



Contents lists available at ScienceDirect

Geoderma

journal homepage: www.elsevier.com/locate/geoderma



Influence of clearness index and soil moisture in the soil thermal dynamic in natural pasture in the Brazilian Pampa biome



Tamires Zimmer^{a,*}, Lidiane Buligon^{a,2}, Vanessa de Arruda Souza^{a,1}, Leugim Corteze Romio^b, Débora Regina Roberti^{a,*}

^a Universidade Federal de Santa Maria (UFSM), Santa Maria, RS, Brazil

^b Universidade Federal do Pampa (UNIPAMPA), Itaquí, RS, Brazil

ARTICLE INFO

Editor Name: Morgan Cristine L.S.

Keywords:
Soil thermal properties
Soil heat flux
Soil temperature
Thermal conduction
Empirical model

ABSTRACT

The soil thermal characterization is necessary to describe the storage and propagation of energy between surface and subsoil. Different weather conditions may influence soil energy exchange processes. Previous studies showed that the variables related to solar radiation and soil moisture (θ) have a significant influence on soil thermal dynamics. In this study, we analyzed the influence of these conditions in the dynamic of soil thermal variables (soil heat flux, G , soil temperature at 0.05 m, T_{s5} , and at 0.15 m, T_{s15}) and soil thermal properties (thermal conductivity, λ , thermal diffusivity, k , and thermal capacity, c_v) obtained in two natural pasture experimental sites located over the Pampa biome in southern Brazil: Pedras Altas (PAS) and Santa Maria (SMA), with two datasets for both sites. The solar global radiation (R_g), represented by the clearness index, and the soil moisture were used to classify the dataset for different sky cover and dry and wet soil. We estimated the soil thermal properties using analytical methods and experimental data. We analyze the dependence of $\lambda(\theta)$ and we proposed a new empirical model to $\lambda(\theta)$ whose hypothesis takes into account a mathematical expression related to the physical phenomenon. Our results showed that, for both sites, the average daily experimental G values were negative and higher in wet soil than in dry soil (in absolute values), while an opposite behavior was found in daily T_{s5} and T_{s15} . In a daily cycle, the hysteresis phenomenon was observed between G and R_g , and between air and soil temperatures. The clearness index influenced the pattern of these hystereses, independent of dry or wet soil period. The higher values of λ and k were found for wet soil periods in both sites. In general, λ and k values presented a variation of until 10% and 33% between the dataset, respectively. This variation in k induced the bigger variability in c_v . The new empirical model for $\lambda(\theta)$ showed good results to represent the experimental λ and to estimate G , consequently has the potential for use in studying numerical algorithms for describing coupled heat and mass transfer processes. The results obtained here allowed a description of the soil thermal regime in the natural pasture over Brazilian Pampa biome and can also be incorporated into global land surface models that aim to represent the behavior of energy exchange between the soil-surface-atmosphere.

1. Introduction

Understanding the complex interaction between soil, vegetation, and the atmosphere is fundamental to describe meteorological, hydrological, and ecological phenomena (Alkhaier et al., 2012). The knowledge of soil energy exchange processes as well as of the thermal properties of each type of soil is essential for modeling of soil-plant-atmosphere interaction, surface energy balance closure, models of weather forecasting and agricultural production, among others (Evelt et al., 2012; Heusinkveld et al., 2004; Kojima et al., 2018).

The soil heat flux (G) is responsible for energy transfer from the surface to the subsoil and can represent about 20% of the energy available on different land cover (Foken, 2008; Kustas et al., 2000; Oncley et al., 2007; Wang et al., 2010; Wilson et al., 2002). G is directly related to changes in soil temperature variation and the soil thermal properties: thermal conductivity (λ), thermal diffusivity (k), and thermal capacity (c_v) and is characterized by dynamics of diurnal, monthly, seasonal and annual behavior. These variables define the soil thermal regime.

Natural pastures have global importance in economic and climatic

* Corresponding authors at: Departamento de Física, Universidade Federal de Santa Maria – UFSM, 97105900 Santa Maria, RS, Brasil.

E-mail addresses: tz.tamireszimmer@gmail.com (T. Zimmer), debora@ufsm.br (D.R. Roberti).

¹ Departamento de Física.

² Departamento de Matemática.

<https://doi.org/10.1016/j.geoderma.2020.114582>

Received 23 November 2019; Received in revised form 8 June 2020; Accepted 9 July 2020

Available online 30 July 2020

0016-7061/ © 2020 Elsevier B.V. All rights reserved.

scenery. Although climatic information on energy exchanges between the soil–plant–atmosphere is essential to describe these ecosystems, this information is limited and almost nonexistent in some regions, such as the Pampa biome. The Pampa biome is characterized by a transition area between the tropical and temperate climate, with hot summers, cold winters, and shallow soils. This biome is located in Uruguay, southern Brazil, and part of Argentina. The climate characteristics play a significant role in the plant species composition, which is dominated by grasses favoring the livestock (Boldrini et al., 2015; Nabinger et al., 2009; Pillar et al., 2009). Understand the soil thermal dynamics in these conditions is a fundamental piece in preservation and conservation studies over the Pampa native vegetation.

Previous studies showed that the soil thermal regime is related to many factors linked to vegetation cover and weather conditions. Alvalá et al. (2002) showed that the soil heat flux is smaller at the forest than at the pasture, with greater differences in dry periods. Allen et al. (1998) suggest to use a linear relationship between soil heat flux and net radiation, but many studies demonstrated that this relationship depends on soil properties, vegetation and time of day (Bryś et al., 2020; Kustas et al., 2000; Purdy et al., 2016; Santanello and Friedl, 2003). Moreover, An et al. (2016), Otunla and Oladiran (2013), and Wang et al. (2010) estimated soil thermal properties with different methods and showed that the performance of these methods varies with weather and soil conditions, such as sky cover and/or soil moisture. Therefore, these studies indicate that soil moisture and variables related to solar radiation are the main factors that influence the dynamics of soil thermal variables and properties. Here, we analyzed the soil thermal regime of Brazilian Pampa biome over different clearness index of the atmosphere and soil moisture conditions.

Many methodologies to estimate the soil properties have been proposed in the literature. In general, the estimates are obtained from analytical solutions of the heat conduction equation (Carslaw and Jaeger, 1959), mainly by the methods of amplitude, phase shift (De Vries, 1963; Wierenga et al., 1969), arctangent (Nerpin and Chudnovskii, 1967), logarithmic (Seemann, 1979), harmonic (Horton et al., 1983), conduction – convection (Gao et al., 2008; Wang et al., 2012), and using numerical solutions, through the gradient method (Evet et al., 2012; Gao et al., 2017; Horton et al., 1983). In addition, many studies describe the dependence of soil thermal properties with soil moisture (θ). An example are parameterizations for λ (θ), which have shown that λ has a pattern until a certain soil moisture value, with a larger standard deviation after this limit (Campbell, 1985; Côté and Konrad, 2005; De Vries, 1963; Johansen, 1975; Kersten, 1949; Liu et al., 2018; Lu et al., 2007, 2014; Nikoosokhan et al., 2015; Romio et al., 2019; Tong et al., 2016; Yan et al., 2019; Zhao et al., 2019). These studies are usually carried out using soil parameters measured in laboratory experiments for soil samples (Clarke et al., 2008; Lu et al., 2019; Xie et al., 2019; Zhao et al., 2009). However, due to scale effects and the soil complexity, errors are often generated when laboratory

results are extrapolated to field experiments (An et al., 2016; Barrios and Francés, 2012; Evett et al., 2012). These parameterizations are frequently used in land surface models to determine the surface energy and water budget in different ecosystems, but such parameterizations still do not describe all the soil complexity over field conditions. According to Yan et al. (2019), to develop new models or verify the ones available in the literature a soil thermal conductivity database should be established and large datasets should be used. Therefore, it is important to develop research to describe the long term soil thermal properties in different soil types and climates. In this study, the soil thermal properties will be estimated over the Brazilian Pampa biome.

The goal of this paper is to analyze the influence of clearness index and soil moisture in soil thermal variables on different time scale over Brazilian Pampa biome. Besides, it is analyzed the influence of the soil moisture in soil thermal properties variability. Two experimental sites were used in this study, Pedras Altas (PAS) and Santa Maria (SMA), totaling two years of field measurements in each site.

2. Materials and methods

2.1. Experimental sites and instrumentation

The two experimental sites are located over the Pampa biome in the State of Rio Grande do Sul (RS), Brazil, specifically, in Pedras Altas (PAS) and in Santa Maria (SMA). The PAS experimental site is located in 31°43.556' S; 53°32.036' W; 395-m elevation, in a private farm near the city of Pedras Altas. The SMA site is located in 29°43'27.502" S; 53°45'36.097" W; 88-m elevation, in an experimental area of the Federal University of Santa Maria (UFSM), near the Santa Maria city. The vegetation in experimental sites is used as pasture for beef cattle and mainly consists of native grasses. The typical climate of these regions is classified as humid subtropical Cfa according to Köppen (Peel et al., 2007).

The textural class of soil is sandy loam and clay loam in PAS and SMA, respectively. The soil textural characteristics of both sites are described in Rubert et al. (2018). In this study, for the PAS site we used the average values of the soil physical properties at 0.05 m and 0.15 m depths: field capacity, $\theta_{FC} = 0.28 \text{ m}^3 \text{ m}^{-3}$; permanent wilting point, $\theta_{WP} = 0.10 \text{ m}^3 \text{ m}^{-3}$; soil porosity, $\theta_s = 0.42 \text{ m}^3 \text{ m}^{-3}$; and soil bulk density, $\rho_s = 1405 \text{ kg m}^{-3}$. For SMA these properties were measured at 0.10 m depth: $\theta_{FC} = 0.31 \text{ m}^3 \text{ m}^{-3}$; $\theta_{WP} = 0.11 \text{ m}^3 \text{ m}^{-3}$; $\theta_s = 0.45 \text{ m}^3 \text{ m}^{-3}$; and $\rho_s = 1397 \text{ kg m}^{-3}$.

For both sites, the meteorological and soil variables were measured in the frequency of 1 min^{-1} and after processed in one-hour averages. The instruments used in this study are described in Table 1. For more information about the sites description and instrumentation see Rubert et al. (2018). Precipitation (P_{rec}) was collected by the automatic stations of the National Institute of Meteorology (INMET). The nearest INMET station from the PAS site is located in the city of Bagé, 67 km away

Table 1
Instrumentation at the experimental sites used in this study.

Variable (symbol) [unit]	Sensor model and manufacturer	Sensor height (m)	Site
Net Radiation (R_n) [W m^{-2}]	CNR2/Campbell Scientific	3	PAS
Net Radiation (R_n) [W m^{-2}]	CNR4/Kipp&Zonen	3	SMA
Global Solar Radiation (R_g) [W m^{-2}]	LI200S/LI-COR	3	PAS
Global Solar Radiation (R_g) [W m^{-2}]	CNR4/Kipp&Zonen	3	SMA
Air temperature (T_a) [$^{\circ}\text{C}$]	CS215-L/Campbell Scientific	3	PAS
Air temperature (T_a) [$^{\circ}\text{C}$]	HMP155/Vaisala	3	SMA
Soil heat flux (G) [W m^{-2}]	HFP01/Hukseflux	–0.10	PAS; SMA
Soil temperature (T_s) [$^{\circ}\text{C}$]	T108/Campbell Scientific	–0.05; –0.15	PAS; SMA
Soil moisture (θ) [$\text{m}^3 \text{ m}^{-3}$]	CS616/Campbell Scientific	–0.10	PAS; SMA
<i>Automatic weather station</i>			
Precipitation (P_{rec}) [mm]	TE525MM/Campbell Scientific	3	Bagé
Precipitation (P_{rec}) [mm]	TR525USW/Texas Electronics	6	Santa Maria

(code OMM: 86992, location: 31.34° S, 54.01° W, 226-m elevation) and for the SMA site, the nearest INMET station is approximately 4 km (code OMM: 86977, location: 29.72° S, 53.72° W, 103-m elevation).

The study period was from 1 September 2014 to 31 August 2016 for both sites. Unfortunately, the measurement system failed for the following period: from 1 September to 31 December 2014 for soil measurements and from 23 to 27 November 2014, from 1 January to 24 February 2015 for atmospheric measurements in SMA site; from 17 September to 5 November 2015 for soil and atmospheric measurements in PAS site. In this study, the methodology to estimate the soil thermal properties (Section 2.3) needs an hourly soil temperature dataset without gaps. Except in the period that the measurements system failed, the soil temperature dataset presented gaps no longer than three hours, which were filled by linear interpolation.

2.2. Classification of experimental data

The experimental dataset was subdivided using the daily clearness index of the atmosphere (κ) and the daily mean soil moisture (θ). The κ over shortwave wavelengths is defined as the ratio between the daily integrated shortwave radiation received on a horizontal surface near the soil surface (global solar radiation, R_g) and the daily shortwave radiation that would theoretically be received on the same horizontal surface above the atmosphere (Liou, 2002).

According to Kuye and Jagtap (1992), the clearness index is classified as:

- (i) CS = clear sky if $\kappa \geq 0.65$;
- (ii) CP = partly cloudy sky if $0.35 < \kappa < 0.65$;
- (iii) CD = cloudy sky if $\kappa \leq 0.35$.

The soil was classified according to its moisture using the soil moisture threshold value (θ_i) as follows:

- (i) W = wet soil if $\theta \geq \theta_i$;
- (ii) D = dry soil if $\theta < \theta_i$.

Where θ_i was calculated by the difference between the experimental measurement field capacity (θ_{FC}) and the readily available water (RAW), as presented in Allen et al. (1998). RAW is calculated by:

$$RAW = p \cdot (TAW) \quad (1)$$

where TAW ($m^3 m^{-3}$) is the total available water that a crop can extract from the root zone of a plant without suffering from water stress, and p is the average fraction of total available soil water that can be depleted from the root zone before moisture stress. The factor p depends on the crop. For extensive grazing, characteristic of the study area, $p = 0.60$. The TAW is obtained by the difference between experimental θ_{FC} and permanent wilting point (θ_{WP}), following Allen et al. (1998).

From the above classifications the daily mean of observed data were separated: clear sky with dry soil (CSD); clear sky with wet soil (CSW); partly cloudy sky with dry soil (CPD); partly cloudy sky with wet soil (CPW); cloudy sky with dry soil (CDD) and cloudy sky with wet soil (CDW). These classifications for the experimental data were performed for the period from 1 September 2014 to 31 August 2016 in both sites to analyze the influence of the clearness index and soil moisture on the soil thermal variables.

2.3. Model: Classical thermal conduction equation

The one-dimension heat conduction equation in an isotropic medium is described by:

$$\frac{\partial T}{\partial t} = \frac{1}{c_v} \frac{\partial}{\partial z} \left(\lambda \frac{\partial T}{\partial z} \right) \quad (2)$$

where T is the soil temperature (K), t is the time (s), c_v is the soil thermal capacity ($J m^{-3} K^{-1}$), λ is the soil thermal conductivity ($W m^{-1} K^{-1}$), and z is the depth of the soil surface (m). The term in brackets of Eq. (2), known as the Fourier law of heat conduction (Carslaw and Jaeger, 1959), is defined as the soil heat flux, G ($W m^{-2}$), in a depth z . That is, the soil heat flux is proportional to the vertical soil temperature gradient,

$$G = \lambda \frac{\partial T}{\partial z}. \quad (3)$$

Assuming that c_v and λ are independent of depth and time, Eq. (2) can be rewritten by:

$$\frac{\partial T}{\partial t} = k \frac{\partial^2 T}{\partial z^2} \quad (4)$$

where k is the soil thermal diffusivity, given by $k = \lambda c_v^{-1}$ ($m^2 s^{-1}$).

According to Carslaw and Jaeger (1959), the problem for transient heat transfer, as given by Eq. (4), subject to the initial and boundary conditions, defined respectively by:

$$T(z, 0) = f(z) \quad (5)$$

$$T(0, t) = \bar{T}_0 + A_0 \sin(\omega t + \varphi_0) \quad (6)$$

where \bar{T}_0 is the mean soil surface temperature, A_0 is the amplitude of the soil surface temperature wave, φ_0 is the phase shift of the soil surface temperature, and ω is the angular velocity of the Earth's rotation ($rad h^{-1}$) ($\omega = 2\pi/\tau$, with τ denoting the period of the fundamental cycle, 1 day).

The solution of Eq. (4) for homogeneous soil of semi-infinite thickness with daily mean temperature (\bar{T}) and repeating periodic surface temperature oscillations is (Carslaw and Jaeger, 1959),

$$T(z, t) = \bar{T}(z) + A_i e^{-\sqrt{\frac{\omega}{2k}}(z-z_i)} \sin\left(\omega t + \varphi_i - (z - z_i) \sqrt{\frac{\omega}{2k}}\right) \quad (7)$$

where $i = 1$ represents the depth of the first soil temperature measurement, z_i , and $i = 2$ the depth of the second soil temperature measure, z_2 , $\bar{T}(z)$ is the daily mean soil temperature at depth z , A_i are the temperature amplitudes and φ_i the phase shifts. The term $\sqrt{\frac{\omega}{2k}}$ is defined as the inverse of damping depth, d (m), ($d = \sqrt{\frac{2k}{\omega}}$) (Campbell and Norman, 1998).

The soil thermal diffusivity (k), as proposed by Horton et al. (1983), can be expressed as follows:

$$k_a = \frac{\omega(z_1 - z_2)^2}{2 \left[\ln \left(\frac{A_1}{A_2} \right) \right]^2} \quad (8)$$

and

$$k_p = \frac{\omega(z_1 - z_2)^2}{2(\varphi_1 - \varphi_2)^2} \quad (9)$$

where the sub-index a refers to the amplitude method and the sub-index p to the phase shift method. Thus, by replacing Eq. (7) in Eq. (3) and using Eqs. (8) or (9), we calculate the soil heat flux as a function of depth and time, given by the equation:

$$G(z, t) = \lambda \left[\frac{\Delta T}{\Delta z} + \sqrt{2} A_i \sqrt{\frac{\omega}{2k}} e^{-\sqrt{\frac{\omega}{2k}}(z-z_i)} \sqrt{\frac{\omega}{2k}} \sin\left(\omega t + \varphi_i + \frac{\pi}{4} - (z - z_i) \sqrt{\frac{\omega}{2k}}\right) \right] \quad (10)$$

for $i = 1, 2$, representing the depths z_1 and z_2 , respectively. $\Delta T/\Delta z$ is the gradient of the daily mean soil temperature ($K m^{-1}$).

The estimate of the soil thermal conductivity can be calculated from Eq. (10) using Eqs. (8) or (9), identifying by λ_a and λ_p when the amplitude and the phase shift method is used, respectively. The thermal

soil capacity was determined by the following mathematical relationships:

$$c_{v(a)} = \frac{\lambda_a}{k_a} \quad (11)$$

$$c_{v(p)} = \frac{\lambda_p}{k_p} \quad (12)$$

The estimation of the soil thermal properties in each soil moisture classification (dry and wet periods) of the experimental data (Section 2.2) from 1 September 2014 to 31 August 2016 in both sites was obtained using the modeling described below. The soil thermal diffusivity, k ($\text{m}^2 \text{s}^{-1}$), is estimated using the experimental data of soil temperature and the mathematical methods of the amplitude (k_a) and phase shift (k_p) with the Eqs. (8) and (9). The parameters A_1 , A_2 , φ_1 and φ_2 were adjusted to Eq. (7) from the daily average experimental data of the soil temperature in the depths $z_1=0.05$ m and $z_2=0.15$ m, using the least-squares method. Thus, were obtained the value of k_a and the value of k_p for the entire dataset. The hourly experimental λ was estimated from the inversion of Eq. (10) using the hourly experimental values of soil temperature and soil heat flux with the values of k estimated using amplitude and phase shift methods. Consequently, λ was obtained by amplitude and phase shift method for an hourly interval. The experimental c_v was obtained by Eqs. (11) and (12) using an average value of λ for both methods.

2.4. Conductivity as a function of the soil moisture

In the previous section, a methodology was presented to calculate the soil thermal conductivity (λ) as a function of soil heat flux (G) from experimental data. These values of λ were used as input data for empirical adjustments of the relationships between λ and θ . In the literature, there are many models to describe the $\lambda(\theta)$, in this work we use the models proposed by Lu et al. (2014), Tong et al. (2016) and a new empirical model proposed. The models are described below.

2.4.1. Lu et al. (2014) model

The model for the $\lambda(\theta)$ proposed by Lu et al. (2014) uses an exponential function to express the nonlinear behavior of λ as a function of θ , texture and soil bulk density (ρ_s):

$$\lambda(\theta) = \lambda_{dry} + e^{(\beta - \gamma \theta^\alpha)} \quad (13)$$

where λ_{dry} is the soil thermal conductivity of a dry soil sample ($\text{W m}^{-1} \text{K}^{-1}$) and parameters α and β are shape factors of the $\lambda(\theta)$ curve, which is related to soil texture and ρ_s . The λ_{dry} is estimated from soil porosity (θ_s) by the linear equation proposed by Lu et al. (2007):

$$\lambda_{dry} = -0.56\theta_s + 0.51 \quad (14)$$

A linear relationship between the clay fraction (f_{cl}) and the parameter α of the Eq. (13) is established as follows:

$$\alpha = 0.67f_{cl} + 0.24 \quad (15)$$

The parameter β is estimated by ρ_s and the sand fraction (f_{sa}) with the following multiple regression equation:

$$\beta = 1.97f_{sa} + 1.87\rho_s - 1.36f_{sa}\rho_s - 0.95 \quad (16)$$

2.4.2. Tong et al. (2016) model

The model proposed by Tong et al. (2016) uses an empirical method to calculate λ as a function of θ based on Jury and Horton (2004), through the equation:

$$\lambda(\theta) = a - be^{(-c\theta)} \quad (17)$$

where a , b and c are empirical parameters. The parameters a and b are determined by nonlinear regression.

2.4.3. New empirical model

The Eqs. (13)–(17) use physical soil properties or adjustments of empirical equations to estimate $\lambda(\theta)$. We propose a new empirical model for $\lambda(\theta)$, based mainly on Lu et al. (2014) (Eq. (13)) model, which takes into account the behavior of the curve of the available experimental dataset, as follows:

$$\lambda(\theta) = \lambda_{dry} + \beta \cdot e^{\left(\frac{\gamma}{(\theta - \theta_{min})^\alpha}\right)} \quad (18)$$

where λ_{dry} is the thermal conductivity of a soil sample close to minimum soil moisture ($\text{W m}^{-1} \text{K}^{-1}$); the parameter β is related to the asymptotic values of the λ , that is values at which λ is estimated for θ greater than RAW , and also depends on the smaller value of the experimental λ (λ_{dry}); θ_{min} is the minimum soil moisture of the experimental dataset; the $\gamma > 0$ and $\alpha > 0$ are parameters to be adjusted.

2.5. Model evaluations

The empirical models for $\lambda(\theta)$ analyzed in this study were calibrated from 1 September 2014 to 31 August 2015 for the PAS site as follows:

- **Fitting 1:** Eq. (13) proposed by Lu et al. (2014) uses the parameters λ_{dry} , α and β of Eqs. (14), (15) and (16), respectively, with θ_s , f_{cl} , f_{sa} and ρ_s obtained in the experimental site, described in Section 2.1;

- **Fitting 2:** Eq. (13) proposed by Lu et al. (2014) adjusted to the values of $\lambda(\theta)$ obtained with the experimental dataset, generating the parameters λ_{dry} , α and β by least-squares method;

- **Fitting 3:** Eq. (17) proposed by Tong et al. (2016) adjusted to the values of $\lambda(\theta)$ obtained with the experimental dataset, generating the parameters a , b and c by least-squares method;

- **Fitting 4:** Eq. (18) new empirical model adjusted to the values of $\lambda(\theta)$ obtained with the experimental dataset, generating the parameters γ and α by the least-squares method. The parameter λ_{dry} was obtained directly from the dataset corresponding to the θ_{min} . The β parameter value calculated using the Ford-Walford method (Ford, 1933; Walford, 1946).

To analyses the dataset, fit the curves, and calibrate the empirical models we used the MATLAB (Mathworks Inc.). The lsqcurvefit function from Optimization Toolbox™ was used to solve the least-squares method.

The results generated by the calibrated Fittings were evaluated by the following statistical indices: Pearson's correlation (r) (coefficient of determination $R^2 = r^2$), root mean square error (RMSE), bias, and percent bias (Pbias) according to the equations below:

$$r = \frac{\sum (x_e - \bar{x}_e)(x_m - \bar{x}_m)}{\sqrt{(\sum (x_e - \bar{x}_e)^2)(\sum (x_m - \bar{x}_m)^2)}} \quad (19)$$

$$RMSE = \sqrt{\frac{\sum (x_e - x_m)^2}{n}} \quad (20)$$

$$bias = \frac{\sum (x_m - x_e)}{n} \quad (21)$$

$$Pbias = \frac{bias}{\left(\frac{1}{n}\right) \sum x_e} \times 100 \quad (22)$$

where x_e represents the experimental value, x_m is the modeled value, \bar{x} is the average of observations and n number of observations.

The Average value of λ for the calibration period and the empirical models of $\lambda(\theta)$ calibrated were validated throughout Eq. (3), estimating G using the hourly experimental values of soil temperature and soil moisture from 1 September 2015 to 31 August 2016 for PAS site and from 1 September 2014 to 31 August 2016 for SMA site. The results obtained are compared to hourly experimental soil heat flux (G) for the same period, using the statistical index R^2 (Eq. (19)) and RMSE (Eq. (20)). The statistical indexes of bias and Pbias work only when the means of the model and observations have the same signal for the entire

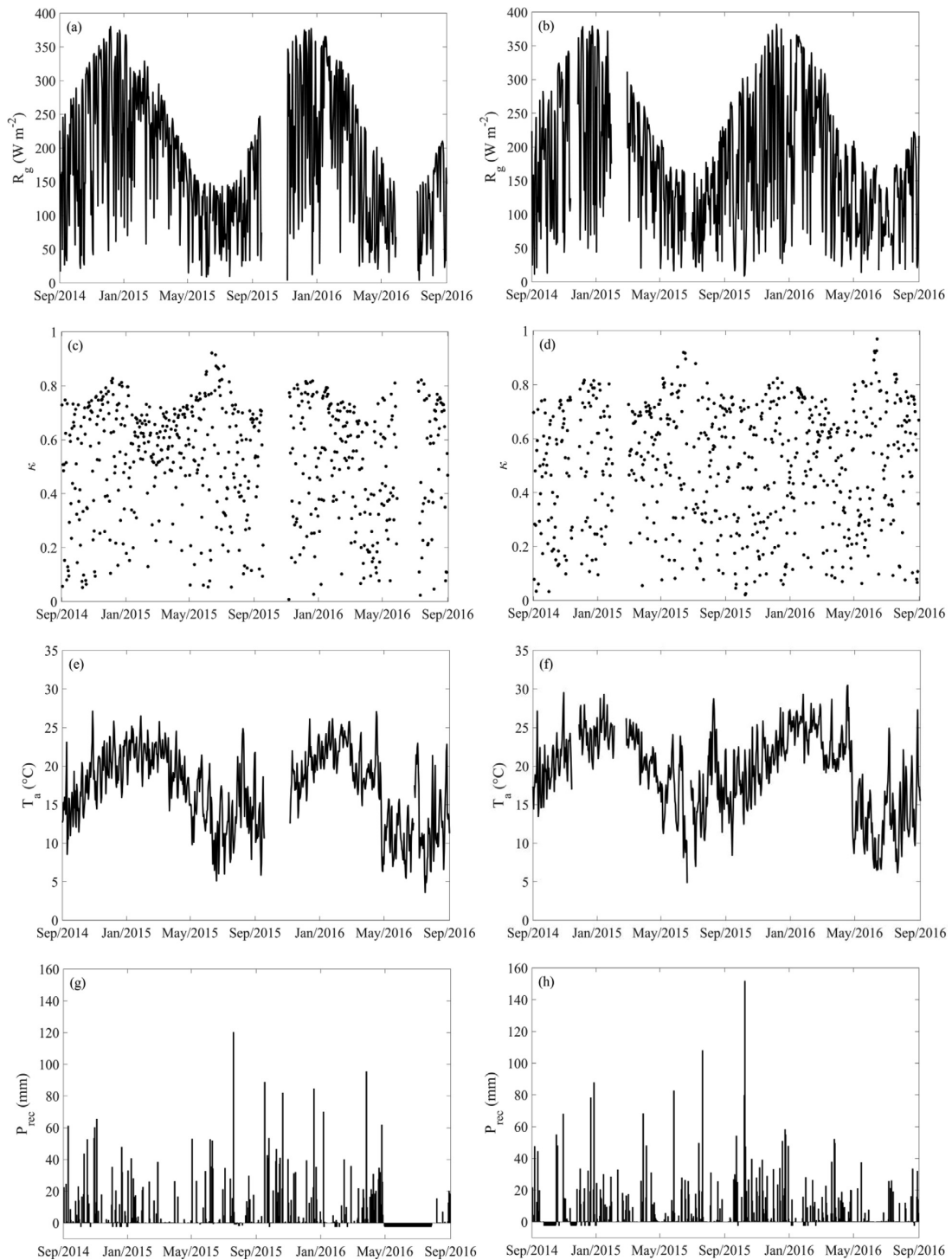


Fig. 1. (a, b) Daily average of the global solar radiation (R_g); (c, d) clearness index of the atmosphere (κ); (e, f) air temperature (T_a); (g, h) daily accumulated precipitation (P_{rec}) for PAS in left panel and SMA for right panel. The periods without precipitation measurements are represented with negative values.

dataset (Gustafson and Yu, 2012). G has positive and negative values, therefore the $bias$ and $Pbias$ do not represent correct statistical values. For this reason, they will not be used in this analysis.

3. Results and discussion

3.1. Atmospheric variables

The southern region of Brazil is constantly influenced by cold and warm fronts (Cavalcanti, 2009). Furthermore, the oscillations associated with climatic events, such as the El Niño-Southern Oscillation (ENSO) that occurs in the Equatorial Pacific, also influence the precipitation in this region, consequently affecting the air temperature and incident global solar radiation (Grimm, 2004; Grimm et al., 1998).

The daily averages of global solar radiation (R_g), clearness index of the atmosphere (κ) and air temperature (T_a) are shown in Fig. 1 for PAS and SMA sites. A well-defined seasonal behavior during the year to R_g and T_a in both sites can be observed. The highest values of R_g occur during the spring/summer season (September-March) with peaks close to 380 W m^{-2} , and the lowest values were between autumn/winter (April-August) with maximum peaks in this period of 200 W m^{-2} . It represents a difference of almost 50% between the seasons. The κ showed variation throughout the study period, and the highest values were found from November to January and from June to July (Fig. 1(c, d)). For PAS and SMA the CS represented 28.58% and 21.75%, CP represented 40.62% and 34.71% and CD, 30.80% and 43.54% respectively. Therefore, the CP condition is predominant in both sites, occurring in all seasons while CS predominate in spring/summer and CD in autumn/winter, as shown in Fig. A.1.

The air temperature is higher from November to March, arriving near $30 \text{ }^\circ\text{C}$ (spring/summer). The lowest T_a values occur during the autumn/winter seasons, with negative values at the beginning of the morning, causing average daily temperatures of approximately $4 \text{ }^\circ\text{C}$.

Precipitation regime in southern Brazil is well distributed throughout the year (Fig. 1(g, h)). From September 2014 to August 2015, the precipitation was 1922 mm at SMA and 1753 mm at PAS; from September 2015 to August 2016, it was 2050 mm at SMA and 1788 mm at PAS. These values were greater than the climatological average for both sites (1300 mm for PAS and 1617 mm for SMA). The high values, especially 2015/2016, are due to the El Niño phenomenon, which tends to increase the precipitation rate in the southern region of Brazil. The most detailed analysis of atmospheric variables to the SMA and PAS sites are presented in Rubert et al. (2018).

3.2. Soil variables

Both sites have similar vegetation cover but significant differences in soil structure that affect the soil hydraulic and thermal properties (Rubert et al., 2018). The mean value of θ for the entire period was higher in the SMA site ($\theta = 0.22 \text{ m}^3 \text{ m}^{-3}$) than in PAS ($\theta = 0.18 \text{ m}^3 \text{ m}^{-3}$) (Fig. 2(a, b)). This result is associated with the soil type, which in SMA has a higher water holding capacity than at PAS (Rubert et al., 2018). The PAS site showed higher soil moisture variability throughout the year, where θ values ranged from 0.06 to $0.35 \text{ m}^3 \text{ m}^{-3}$. The value of soil moisture threshold (θ_t), used to classify the dataset, was found as $\theta_t = 0.19 \text{ m}^3 \text{ m}^{-3}$ to SMA and $\theta_t = 0.18 \text{ m}^3 \text{ m}^{-3}$ to PAS. For PAS, 58.79% of the days, the soil moisture was greater than θ_t , while in SMA 80.31% (wet period in Table 2).

The daily soil temperature amplitude at 0.05 m (T_{s5}) (measured as the half of the difference between the minimum and maximum value of each day) (Fig. 2(e, f)) showed greater variation during the spring/summer seasons (September-March) when there is greater global solar radiation (R_g) in the surface (Fig. 1(a, b)). The PAS site presents greater amplitude variations when compared to SMA (Fig. 2(g, h)). During the analyzed period, the amplitude of variation for T_{s5} and T_{s15} was approximately $25 \text{ }^\circ\text{C}$ and $19 \text{ }^\circ\text{C}$, respectively, at both sites. The average soil

temperature over the entire period for the two experimental sites at both depths was $\approx 19 \text{ }^\circ\text{C}$ (Fig. 2(g, h) and Table 2). Sandy soils tend to have higher daily thermal amplitudes in the superficial layers and smaller in depth. This behavior is because sandy soils have higher porosity, with less contact between soil particles, thus hampering the conduction process. Clay soils, on the other hand, are more efficient in conducting heat, with lower daily thermal amplitude (Fig. 2 (g, h)) (Sepaskhah and Boersma, 1979).

In Table 2 are shown the average of atmospheric and soil variables in the different dataset classifications in the PAS and SMA sites (Section 2.2). In both sites, the wet classification is predominant. We can observe the lower values of T_{s5} and T_{s15} for the CDW, for both sites, are due to the lower clearness index values of the atmosphere. The soil temperature is higher in the dry period for all clearness index classification in both depths. For PAS site the soil temperature gradient presented negative values for the entire period and for the classifications CSD and CSW because in CS conditions the surface temperature is higher than the deeper layers. For SMA the soil temperature gradient presented positive values for all periods, except for CSD and CSW classifications.

3.3. Soil heat flux

Fig. 2(c, d) presents the seasonal behavior of the G throughout the year in both sites. The highest values of G were observed during the spring/summer seasons (September-March), and are related to the increase of incidence of R_g (Fig. 1(a, b) and Fig. A.3). In the autumn/winter seasons (April-August), in general, the daily G average was negative, i.e., the subsoil warms the surface layers. It is may be related to the reduction of global solar radiation incident on the surface (Fig. 1(a, b)) and with the lowest clearness index of the atmosphere, observed in the period (Fig. 1(c, d) and Fig. A.3).

The values of G from entire, wet and dry periods are negative, with greater values for wet period (in absolute values) for both sites. In most data classifications, the G values also are negative, but for CSD, the G invert the sign (positive values) in both sites. The signal for G and $\Delta T \Delta z^{-1}$ are opposite, except for the entire period in the PAS site. This last result can be affected by the missing data in the 2015 spring season when the CS classification is dominant (Fig. A.1) and G is positive (Table 2). Allen et al. (1998) suggested G represents approximately 10% of R_g , however this result was not observed in PAS and SMA site.

In Fig. 3, G was plotted against R_g , T_a , T_{s5} , and T_{s15} , using the mean daily cycles in different clearness index range and dry soil classification for PAS and SMA sites. The variables are made dimensionless by their maximum values in order to compare the pattern formed by the hysteretic behavior (Rubert et al., 2018; Zheng et al., 2014; Zuecco et al., 2016). For wet soil classifications, the behavior among the variables was similar to dry soil (Fig. A.2).

Hysteresis loops showed clockwise behavior for the T_{s5} and T_{s15} variables, while for R_g and T_a the behavior was counterclockwise. In general, larger differences are obtained between CS and CD, and for the CP the relations are similar to CS. The hysteresis phenomenon is mainly observed between G and R_g , since the hysteresis loop has a circular shape, with time-lag between the maximum values of R_g and G of approximately 2 h. R_g for CS and CP conditions show the maximum peak at approximately 12 h local time, for CD the maximum peak occurs in the afternoon at approximately 14 h local time.

The relation of G with T_{s5} and T_a for all classifications and T_{s15} for CD presents a linear shape, showing a better relation of G with these variables. The maximum values of G , T_{s5} , and T_a occurred around 15 h local time and T_{s15} around 20 h local time. We can observe that the curve during the night for CD at T_{s5} and T_{s15} is more inclined, representing the small variation of the soil temperature in each soil depth throughout the night. For the deeper soil temperature (T_{s15}), the hysteresis phenomenon is more evident (circular shape) in CS and CP cases. The relationship of G with θ did not present hysteresis behavior (data

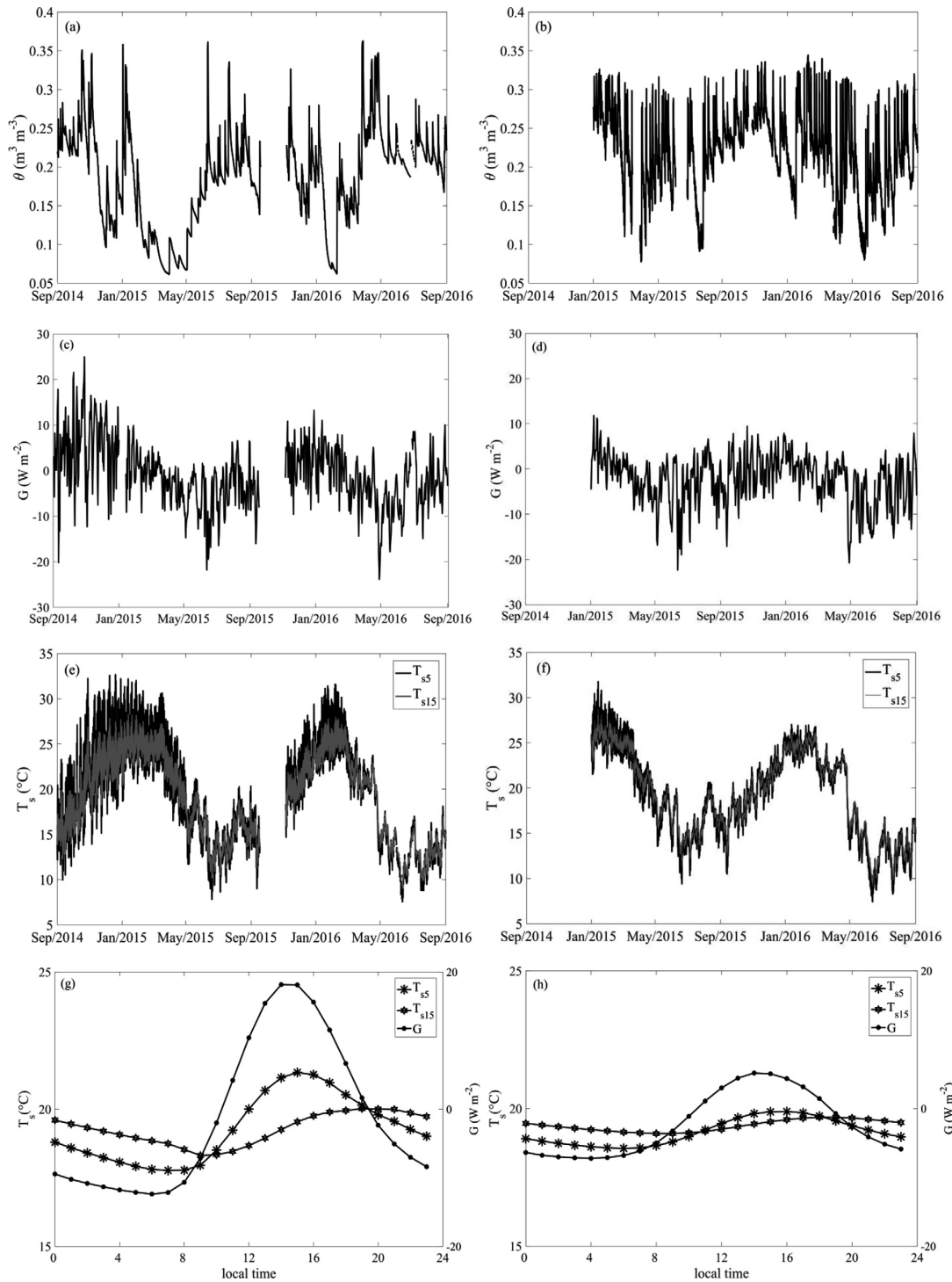


Fig. 2. (a, b) Hourly soil moisture (θ); (c, d) daily mean of soil heat flux (G); (e, f) hourly soil temperature (T_s); (g, h) diurnal cycles of soil temperature and soil heat flux from 1 September 2014 to 31 August 2016 for PAS in the left panel and SMA for the right panel.

Table 2

Average of soil heat flux values, G (W m^{-2}), net radiation, R_n (W m^{-2}), soil temperature at $z = 0.05$ m, T_{s5} ($^{\circ}\text{C}$), soil temperature at $z = 0.15$ m, T_{s15} ($^{\circ}\text{C}$), and the temperature gradient, $\Delta T \Delta z^{-1}$ ($^{\circ}\text{C m}^{-1}$), for the dataset classifications.

	% days	G	R_n	T_{s5}	T_{s15}	$\Delta T \Delta z^{-1}$
<i>Pedras Altas (PAS)</i>						
Entire period	100	-1.10	107.10	19.29	19.26	-0.31
Dry period	41.21	-0.31	130.27	22.00	22.15	1.49
Wet period	58.79	-1.67	90.12	17.21	17.27	0.54
CSD	18.03	3.35	187.40	24.82	24.31	-5.06
CSW	10.55	6.26	195.87	22.81	22.21	-5.97
CPD	16.42	-2.74	103.15	20.52	20.60	0.78
CPW	24.20	-1.77	97.00	16.18	16.28	1.02
CDD	6.76	-4.18	43.85	18.93	19.18	2.45
CDW	24.04	-4.58	37.22	15.76	16.05	2.90
<i>Santa Maria (SMA)</i>						
Entire period	100	-2.30	105.70	19.14	19.37	2.31
Dry period	19.69	-0.55	165.88	22.83	22.92	0.98
Wet period	80.31	-2.69	91.09	18.32	18.58	2.97
CSD	11.92	0.18	200.65	23.92	23.89	-0.33
CSW	9.83	0.66	191.05	23.37	23.33	-0.34
CPD	5.06	-1.58	137.82	20.92	21.11	1.89
CPW	29.65	-4.27	115.45	17.91	18.29	3.86
CDD	2.71	-1.61	55.00	21.71	21.90	1.94
CDW	40.83	-2.56	47.72	16.93	17.19	2.62

not shown) since θ does not depend on the daily behavior but rather on the precipitation cycle.

3.4. Soil thermal properties

The mean values of the soil thermal properties obtained with the amplitude and phase shift method for different classifications of the soil moisture at the PAS and SMA sites are shown in Table 3. The soil thermal diffusivity presents different values between the methods. In general, the values of k_a are greater than k_p , except in wet period for PAS. The k values presented a variation of around 33% (from $4.19 \times 10^{-7} \text{ m}^2 \text{ s}^{-1}$ to $6.25 \times 10^{-7} \text{ m}^2 \text{ s}^{-1}$).

Otunla and Oladiran (2013) estimated k for a soil with a texture of loamy sand in Nigerian for 13 days during the transition from the dry season to the rainy season, finding average values of $4.49 \times 10^{-7} \text{ m}^2 \text{ s}^{-1}$ and $5.93 \times 10^{-7} \text{ m}^2 \text{ s}^{-1}$ for the amplitude and phase shift, respectively. Wang et al. (2010) found average values of k equals to $2.06 \times 10^{-7} \text{ m}^2 \text{ s}^{-1}$ (amplitude method) and $4.24 \times 10^{-7} \text{ m}^2 \text{ s}^{-1}$ (phase shift method) for 7 days of data in a soil predominantly medium loam with a high proportion of silt located in China. However, An et al. (2016), studying a semi-arid area in China with silt sandy soil at 0.05–0.10 m depth for two months, estimated k using the amplitude and phase shift methods as 12.0×10^{-7} and $10.0 \times 10^{-7} \text{ m}^2 \text{ s}^{-1}$ for clear sky, and 8.0×10^{-7} and $7.8 \times 10^{-7} \text{ m}^2 \text{ s}^{-1}$ for rainy, for each method respectively. In addition, the authors found k values equal to $7.6 \times 10^{-7} \text{ m}^2 \text{ s}^{-1}$ for low soil moisture content with high water movement in the soil profile and $7.5 \times 10^{-7} \text{ m}^2 \text{ s}^{-1}$ high soil moisture content with low water movement in the soil profile, that is, same value for both methods.

The soil thermal conductivity showed similar values for the two methods in both sites. The values of λ were found between $1.00 \text{ W m}^{-1} \text{ K}^{-1}$ and $1.14 \text{ W m}^{-1} \text{ K}^{-1}$. According to Chen and Duthia (2001), the maximum λ value is $1.9 \text{ W m}^{-1} \text{ K}^{-1}$. However, Abu-Hamdeh and Reeder (2000) in laboratory studies with sandy soil from Jordan (soil similar to our study), when evaluating the effect of different soil properties, found the λ ranged from 0.58 to $1.94 \text{ W m}^{-1} \text{ K}^{-1}$. From our results, the wet periods presented higher λ values, approximately 10% for PAS and 5% for SMA (Table 3). These results should be associated with the increase of soil moisture, which in turn causes a greater energy transport in the heat form, because the porous part of the soil, which in the dry period was filled with air, will be filled with water, allowing a

greater heat flux by conduction (Sepaskhah and Boersma, 1979). Therefore, the variability of λ among soils of different composition can be attributed to differences in heat conduction in the soil materials themselves and the formation of water bridges between soil particles (Zhao et al., 2019). The results showed here are similar to other studies reported in the literature (Usovich et al., 2016; Zaibon et al., 2019; Zhao et al., 2016).

The values of soil thermal capacity, c_v , vary from $1.78 \times 10^6 \text{ J m}^{-3} \text{ K}^{-1}$ to $2.62 \times 10^6 \text{ J m}^{-3} \text{ K}^{-1}$. Being $c_v = \lambda/k$, this variation in c_v is mainly associated with k variability.

We use the damping depth, d , in (Eq. (7)), calculated using k_p , to analyze the influence of soil moisture in the variation of daily soil temperature (amplitude and phase). The results indicate that the amplitude of soil temperature fluctuations at 0.15 m is around 45% of the amplitude at the 0.05 m for wet and 40% in dry periods for both sites. In these conditions, the phase is approximately $\pi/3$ rad for dry and $\pi/4$ for wet periods (Table A.1). These results are in accordance with the behavior shown in Fig. 2(g, h) and they confirm that the soil moisture influence the flow of energy through.

3.5. Soil thermal conductivity vs soil moisture

According to the results shown in Table 3, the λ values are influenced by soil moisture. The soil thermal conductivity increases with increasing soil moisture on a daily scale, as shown in Fig. 4 for the PAS site. Tong et al. (2016) and Wang et al. (2005) obtained a similar result. For dry periods, the soil thermal conductivity increases quickly when θ values are small. However, for wet periods the λ values exhibit great variability. This behavior occurs when the values of θ are above $0.18 \text{ m}^3 \text{ m}^{-3}$, i.e., above the θ_i value. Roxy et al. (2014) observed a similar behavior and found a limit value (peak) near $\theta = 0.22 \text{ m}^3 \text{ m}^{-3}$. These limits values found in both studies can be explained because the heat conduction in dry porous media occurs principally through the contact zones between the solid particles. Low values of soil moisture mean low contact between particles. As θ increases, water begins to fill the spaces previously occupied by air, forming water bridges between the solid particles of the soil, and consequently, λ increases rapidly due to the greater contact between the particles (Ewing and Horton, 2007; Sepaskhah and Boersma, 1979; Tarnawski and Gori, 2002). This process continues until most of the solid particles are connected. Subsequently, the increase of λ with the increase of θ depends to a large extent on the displacement of air by the water and, as a result, the increase of λ becomes slower, tending to an asymptotic value. However, the experimental data behavior shows great variability in λ in this situation, as seen in Fig. 4.

The empirical parameters for the four Fittings considered in this study are shown in Table 4 with the statistical indices. For Lu et al. (2014) model, we used the experimental and unadjusted soil parameters (Fitting 1). Subsequently, the calibration was performed using the $\lambda(\theta)$ experimental data (Fitting 2). The α values found were close for both Fittings, whereas for λ_{dry} and β the values differ by almost 50%. Lu et al. (2014) found values of λ_{dry} ranging from 0.22 to $0.29 \text{ W m}^{-1} \text{ K}^{-1}$, β between 1.48 and 1.86, and α ranging from 0.24 to 0.53 for different soil types. In addition, for similar soil of this study (sand soil), Lu et al. (2014) found $\lambda_{dry} = 0.29 \text{ W m}^{-1} \text{ K}^{-1}$, $\alpha = 0.24$ and $\beta = 1.86$, similar to the results obtained here using Fitting 1. However, Fitting 2 presented more reliable estimates of $\lambda(\theta)$ resulting in a R^2 equal to 0.67 and lower RMSE.

The fit for Tong et al. (2016) model (Fitting 3), presented lower RMSE and higher R^2 when compared to the Fittings 1 and 2. These authors evaluated different soil types and obtained the values of a parameter ranging in an interval from 1.51 to 2.64, and values of b ranging from 1.40 to 2.04, similar to those found by Jury and Horton (2004). The c parameter in Tong et al. (2016) ranged from 2.96 to 6.04, with an average of 3.90, which was fixed for all soils, this methodology was also performed by Jury and Horton (2004). The c values for

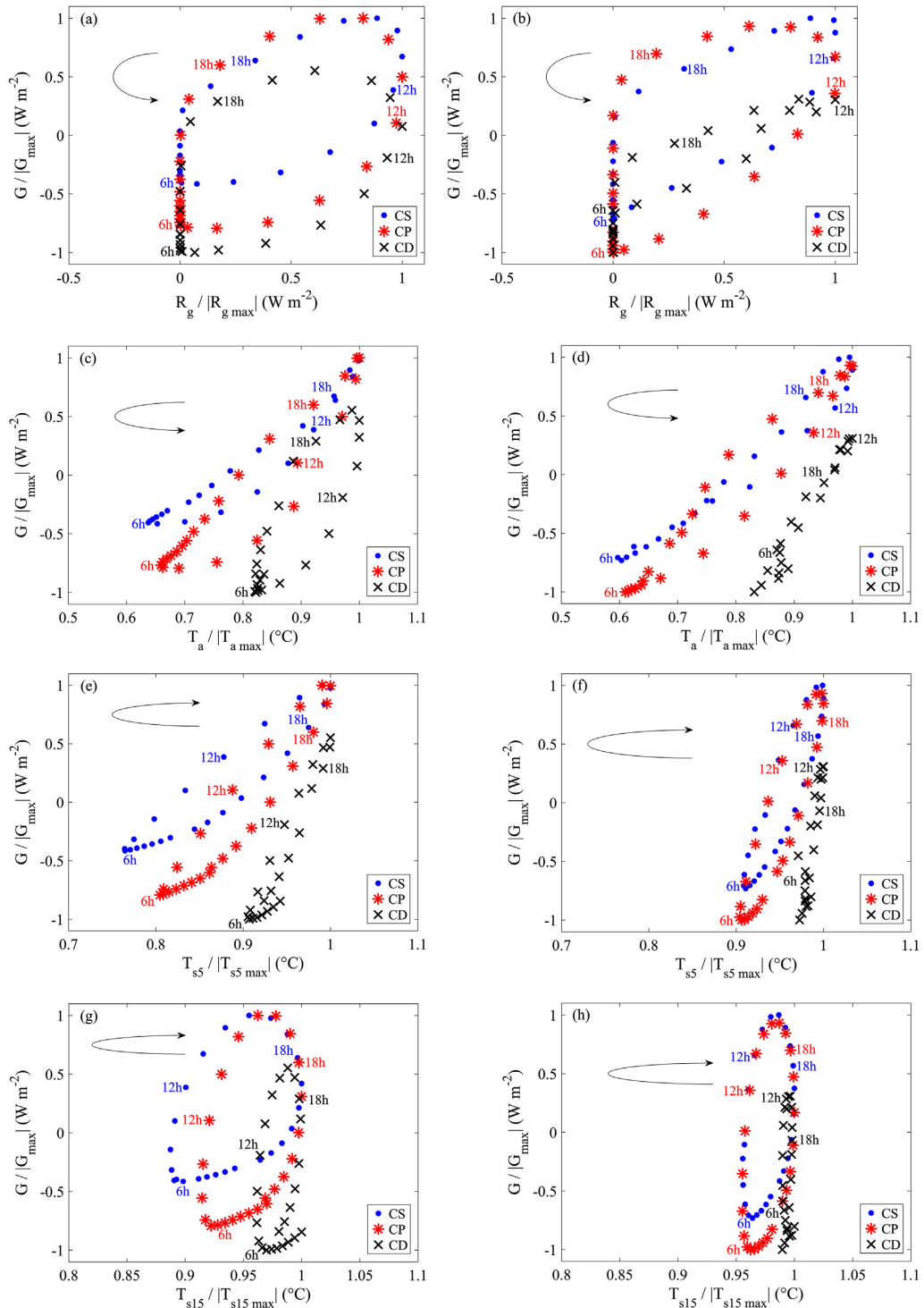


Fig. 3. Dimensionless soil heat flux (G) response curves vs: (a, b) global solar radiation (R_g), (c, d) air temperature (T_a), (e, f) soil temperature at 0.05 m (T_{s5}) and (g, h) 0.15 m (T_{s15}) for PAS site in the left panel and SMA site for the right panel. The arrow indicates the directions morning (6 h to 12 h) and afternoon (12 h to 18 h).

Table 3

Average soil thermal conductivity values, λ ($\text{W m}^{-1} \text{K}^{-1}$), soil thermal diffusivity, k ($\text{m}^2 \text{s}^{-1}$), soil thermal capacity, c_v ($\text{J m}^{-3} \text{K}^{-1}$), by the Amplitude Method and the Phase Shift Method for the different classifications of the soil moisture in both sites.

	Amplitude Method				Phase Shift Method	
	$k_a(10^{-7})$	λ_a	$c_{v(a)}(10^6)$	$k_p(10^{-7})$	λ_p	$c_{v(p)}(10^6)$
	<i>Pedras Altas (PAS)</i>					
Entire period	5.25	1.05 ± 0.51	2.01	4.97	1.05 ± 0.51	2.12
Dry period	5.14	1.00 ± 0.46	1.95	4.19	1.00 ± 0.46	1.78
Wet period	5.46	1.10 ± 0.54	2.01	5.62	1.10 ± 0.54	2.62
	<i>Santa Maria (SMA)</i>					
Entire period	5.62	1.10 ± 0.49	1.95	5.53	1.10 ± 0.49	1.98
Dry period	5.43	1.09 ± 0.44	2.00	5.25	1.09 ± 0.44	2.07
Wet period	6.25	1.14 ± 0.51	1.82	5.96	1.14 ± 0.51	1.91

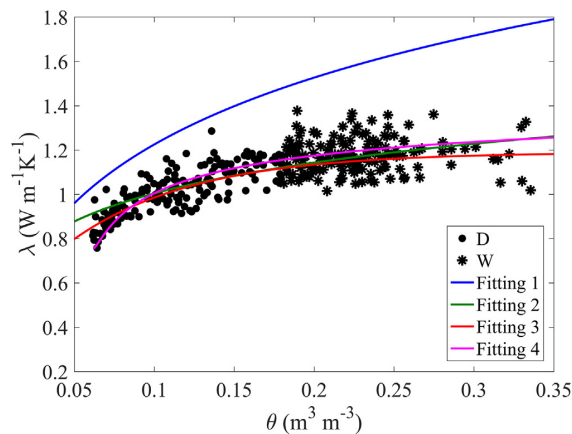


Fig. 4. Daily average soil thermal conductivity (λ) and soil moisture (θ) for the different classifications of the soil moisture and Fittings 1, 2, 3 and 4 for the PAS site from September 2014 to August 2015.

adjusted data in this study were much higher than those reported by Tong et al. (2016), whereas the values of a and b were smaller (Table 4).

Fitting 4 obtained the best statistical indices since it uses an equation that generates a curve closer to the observed data. It should be observed for all Fittings that were calibrated here presented good results when compared by statistical errors (Table 4 and Fig. 4).

All fittings were compared to the λ values obtained with daily experimental data in Fig. 5. We can observe two groups of data: one for wet soil and another for dry soil. Therefore, the statistical indices were calculated for dry and wet soil conditions (Table 5). The dry condition presented the best R^2 , between 0.54 and 0.76. However, due to the dispersion of the λ for wet condition, the models do not represent the experimental λ ($R^2 \sim 0$).

Table 6 shows the statistical indices for the G obtained experimentally and estimated soil heat flux using the average and Fittings λ models. In general, a good representation of the experimental data in all models is observed for both sites, with R^2 greater than 0.84. The lowest accuracy was found for Fitting 1, which uses measured values of soil

physics parameters. The best result was obtained by the Fitting 4 (uses the new empirical model) with the highest R^2 and the lowest $RMSE$ for both sites. Although the values of statistical indices using Average are similar to Fitting 4, this new empirical model describes thermal conductivity in different soil moisture range and their parameters present physical meaning (Section 2.4.3).

4. Conclusion

In this paper, the influence of the atmospheric clearness index and soil moisture on the soil thermal dynamic were investigated for two experimental sites located in the natural pasture over Brazilian Pampa biome. In general, for both sites, the average of daily G was negative, representing the subsurface is heating the surface, with higher absolute values in wet soil than in dry soil. However, the average of daily T_{s5} and T_{s15} was higher in dry soil. Moreover, in a daily cycle, 5% more energy flow from 0.05 m to 0.15 m in wet periods than in dry periods. The atmospheric clearness index influenced the shape of the hysteresis loop between G and R_g , T_a , T_{s5} , and T_{s15} , independent of dry or wet soil period. For both sites, a good relation between hourly G and T_{s5} and T_a was found, while between G and R_g and T_{s15} a shift was observed.

The average values of the estimated soil thermal properties, to classical methods and experimental data, were close to those found in the literature. The values of soil thermal diffusivity and soil thermal conductivity are higher in wet soil, independent of the clearness index classification. The behavior of soil thermal conductivity with soil moisture was analyzed. The λ increases with soil moisture increase until around it reaches θ_c value, above this threshold the λ presents a great variability.

The empirical models for $\lambda(\theta)$ were evaluated to estimate the soil heat flux using the Fourier Law in SMA and PAS sites. We verified that for high values of soil moisture, the different models do not represent well the experimental data due to the variability of the dataset. The new empirical model presented the best performance for both sites, according to statistical indices analyzed. Therefore, for the modeling and estimation of the soil thermal conductivity as well as the estimation of the soil heat flux, it is recommended to use the new empirical model for similar soil studied here. Moreover, this equation can be used in different soil types after a parameters calibration.

The analyses performed in this study showed that the atmospheric

Table 4

Statistical indexes and the parameters calculated and/or adjusted using the Fittings 1, 2, 3 and 4 for the estimation of soil thermal conductivity at the PAS site from September 2014 to August 2015.

	R^2	$RMSE$ ($\text{W m}^{-1} \text{K}^{-1}$)	$bias$ ($\text{W m}^{-1} \text{K}^{-1}$)	$Pbias$ (%)	λ_{dry}	β	α	γ	θ_{min}	a	b	c
Fitting 1	0.47	0.31	0.29	27.26	0.27	1.71	0.24	–	–	–	–	–
Fitting 2	0.67	0.05	–0.010	–1.17	0.44	1.05	0.21	–	–	–	–	–
Fitting 3	0.70	0.04	–0.010	–1.15	–	–	–	–	–	1.19	0.75	13
Fitting 4	0.76	0.03	0.004	0.50	0.75	0.74	0.52	0.20	0.06	–	–	–

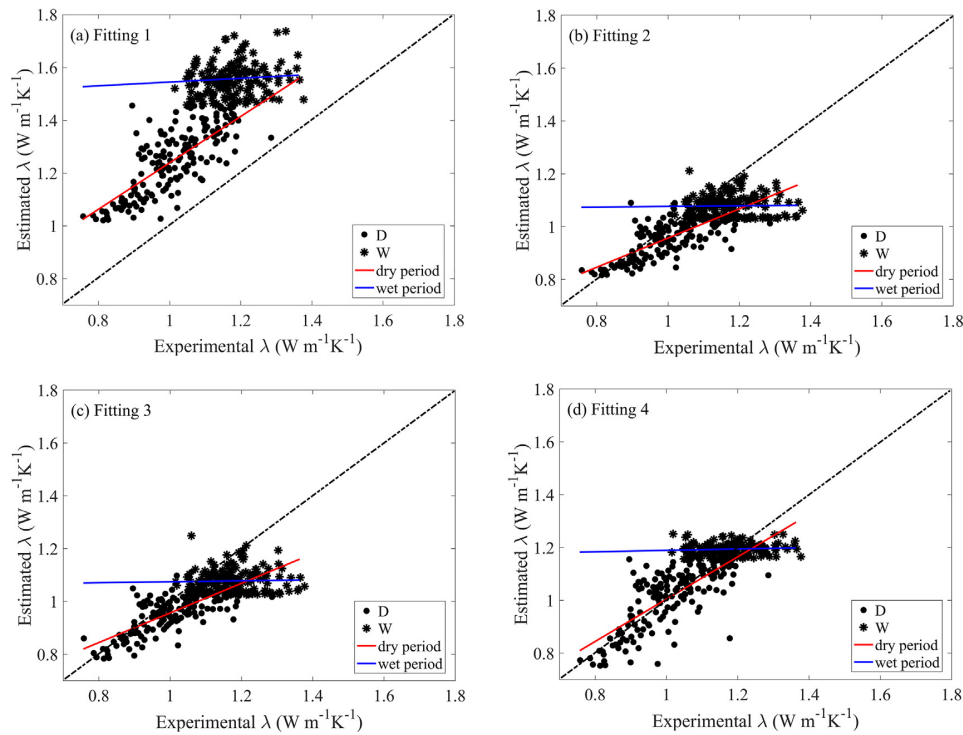


Fig. 5. Comparison of the λ estimated by the (a) Fitting 1, (b) Fitting 2, (c) Fitting 3 (d) Fitting 4 vs λ experimental for the different classifications of the soil moisture for the PAS site from September 2014 to August 2015. The linear regression for the dry and wet periods and the 1:1 line (dotted black line) are presented.

Table 5

Statistical indexes between soil thermal conductivity experimental data (through Eq. (10)) and estimated by Fitting 1, 2, 3 and 4, grouping for dry and wet periods for the PAS site from September 2014 to August 2015.

	Dry period				Wet period			
	R ²	RMSE (W m ⁻¹ K ⁻¹)	bias (W m ⁻¹ K ⁻¹)	Pbias (%)	R ²	RMSE (W m ⁻¹ K ⁻¹)	bias (W m ⁻¹ K ⁻¹)	Pbias (%)
Fitting 1	0.54	0.25	0.23	23.27	0.04	0.39	0.38	32.55
Fitting 2	0.57	0.08	-0.04	-4.87	0.06	0.13	-0.09	-8.16
Fitting 3	0.67	0.08	-0.04	-4.91	0.04	0.13	-0.09	-8.26
Fitting 4	0.76	0.07	0.01	1.61	0.08	0.02	0.01	1.63

Table 6

Statistical indexes for the validation using G obtained experimentally at 0.10 m and modeled with Eq. (3) using the empirical models of $\lambda(\theta)$ for PAS and SMA (Fittings). Average is $\lambda = 1.08 \text{ W m}^{-1} \text{ K}^{-1}$.

	PAS*		SMA**	
	R ²	RMSE(W m ⁻²)	R ²	RMSE(W m ⁻²)
Average	0.94	2.86	0.96	1.38
Fitting 1	0.84	4.65	0.89	2.78
Fitting 2	0.95	2.51	0.96	1.49
Fitting 3	0.95	2.49	0.96	1.42
Fitting 4	0.97	2.47	0.97	1.32

* Period from 1 September 2015 to 31 August 2016.

** Period from 1 September 2014 to 31 August 2016.

clearness index and the soil moisture influence the dynamic of soil thermal on different temporal scales. Specifically, the clearness index influence mainly the relationship between G and atmospheric and soil variables, i.e., in a daily cycle, while the soil moisture influence mainly the value of soil variables and the estimation of soil thermal properties, i.e, seasonal behavior, besides to influence the energy flow through the soil. Moreover, the analyses allowed a regional description of the soil thermal regime in the natural pasture over Brazilian Pampa biome. Similar analyses in different soil types and biomes are needed to improve our understanding of this issue.

Declaration of Competing Interest

The authors declare that they have no known competing financial interests or personal relationships that could have appeared to influence the work reported in this paper.

Acknowledgments

The authors acknowledge the National Council for Scientific and Technological Development (CNPq, Brazil), the Coordination for the Improvement of Higher Education Personnel (CAPES, Brazil), and the Foundation for Research of Rio Grande do Sul State (FAPERGS).

Appendix A. Supplementary data

Supplementary data to this article can be found online at <https://doi.org/10.1016/j.geoderma.2020.114582>.

References

Abu-Hamdeh, Reeder, 2000. Soil thermal properties: Effects of density, moisture, salt

- concentration and organic matter. *Soil Sci. Soc. Am. J.* 64, 1285–1290. https://doi.org/10.1007/978-3-319-70548-4_39.
- Alkhaier, F., Su, Z., Flerchinger, G.N., 2012. Reconnoitering the effect of shallow groundwater on land surface temperature and surface energy balance using MODIS and SEBS. *Hydrol. Earth Syst. Sci.* 16, 1833–1844. <https://doi.org/10.5194/hess-16-1833-2012>.
- Allen, R.G., Pereira, L.S., Raes, D., Smith, M., Ab, W., 1998. *Allen FAO1998. Irrig. Drain. Pap. 56* <https://doi.org/10.1016/j.eja.2010.12.001>. FAO 300.
- Alvalá, R.C.S., Giello, R., Da Rocha, H.R., Freitas, H.C., Lopes, J.M., Manzi, A.O., Von Randow, C., Dias, M.A.F.S., Cabral, O.M.R., Waterloo, M.J., 2002. Intradial and seasonal variability of soil temperature, heat flux, soil moisture content, and thermal properties under forest and pasture in Rondônia. *J. Geophys. Res. D Atmos.* 107, 1–20.
- An, K., Wang, W., Zhao, Y., Huang, W., Chen, L., Zhang, Z., Wang, Q., Li, W., 2016. Estimation from soil temperature of soil thermal diffusivity and heat flux in subsurface layers. *Boundary-Layer Meteorol.* 158, 473–488. <https://doi.org/10.1007/s10546-015-0096-7>.
- Barrios, M., Francés, F., 2012. Spatial scale effect on the upper soil effective parameters of a distributed hydrological model. *Hydrol. Process.* 26, 1022–1033. <https://doi.org/10.1002/hyp.8193>.
- Boldrini, I., Overbeck, G., Trevisan, R., 2015. Biodiversidade de plantas, in: *Os Campos Do Sul. UFRRGS: Porto Alegre, Brazil*, pp. 53–70.
- Bryś, K., Bryś, T., Sayegh, M.A., Ojrzynska, H., 2020. Characteristics of heat fluxes in subsurface shallow depth soil layer as a renewable thermal source for ground coupled heat pumps. *Renew. Energy* 146, 1846–1866. <https://doi.org/10.1016/j.renene.2019.07.101>.
- Campbell, G. S., 1985. *Soil Physics with BASIC: Transport Models for Soil–Plant Systems*. 1st November 1985.
- Campbell, G.S., Norman, J.M., 1998. *An Introduction to Environmental Biophysics, Climate Change 2013 - The Physical Science Basis*. Springer, New York, New York, NY. <https://doi.org/10.1007/978-1-4612-1626-1>.
- Carslaw, H.S., Jaeger, J.C., 1959. *Conduction of heat in solids*, 2d ed. Clarendon Press, Oxford.
- Cavalcanti, Iracema Fonseca de Albuquerque and Ferreira, Nelson Jesus and Dias, Maria Assunção Paus da Silva and Silva, M.G.A.J. da, 2009. *Tempo e clima no Brasil*.
- Chen, F., Dudhia, J., 2001. Coupling an Advanced Land Surface-Hydrology Model with the Penn State–NCAR MM5 Modeling System. Part I: Model Implementation and Sensitivity. *Mon. Weather Rev.* 129, 569–585.
- Clarke, B.G., Agab, A., Nicholson, D., 2008. Model specification to determine thermal conductivity of soils. *Proc. Inst. Civ. Eng. - Geotech. Eng.* 161, 161–168. <https://doi.org/10.1680/geng.2008.161.3.161>.
- Côté, J., Konrad, J.-M., 2005. A generalized thermal conductivity model for soils and construction materials. *Can. Geotech. J.* 42, 443–458. <https://doi.org/10.1139/t04-106>.
- De Vries, D.A., 1963. *Thermal properties of soils*. *Phys. plant Environ.* 210–235.
- Evvett, S.R., Agam, N., Kustas, W.P., Colaizzi, P.D., Schwartz, R.C., 2012. Soil profile method for soil thermal diffusivity, conductivity and heat flux: Comparison to soil heat flux plates. *Adv. Water Resour.* 50, 41–54. <https://doi.org/10.1016/j.advwatres.2012.04.012>.
- Ewing, R.P., Horton, R., 2007. Thermal conductivity of a cubic lattice of spheres with capillary bridges. *J. Phys. D: Appl. Phys.* 40, 4959–4965. <https://doi.org/10.1088/0022-3727/40/16/031>.
- Foken, T., 2008. Eddy flux measurements the energy balance closure problem: An Overview. *Ecol. Appl.* 18, 1351–1367. <https://doi.org/10.1890/06-0922.1>.
- Ford, E., 1933. An Account of the Herring Investigations Conducted at Plymouth during the Years from 1924 to 1933. *J. Mar. Biol. Assoc. United Kingdom* 19, 305–384. <https://doi.org/10.1017/S0025315400055910>.
- Gao, Z., Horton, R., Wang, L., Liu, H., Wen, J., 2008. An improved force-restore method for soil temperature prediction. *Eur. J. Soil Sci.* 59, 972–981. <https://doi.org/10.1111/j.1365-2389.2008.01060.x>.
- Gao, Z., Russell, E.S., Missik, J.E.C., Huang, M., Chen, X., Strickland, C.E., Clayton, R., Arntzen, E., Ma, Y., Liu, H., 2017. A novel approach to evaluate soil heat flux calculation: An analytical review of nine methods. *J. Geophys. Res.* 122, 6934–6949. <https://doi.org/10.1002/2017JD027160>.
- Grimm, A.M., 2004. How do La Niña events disturb the summer monsoon system in Brazil? *Clim. Dyn.* 22, 123–138. <https://doi.org/10.1007/s00382-003-0368-7>.
- Grimm, A.M., Ferraz, S.E.T., Gomes, J., 1998. Precipitation anomalies in southern Brazil associated with El Niño and La Niña events. *J. Clim.* 11, 2863–2880. [https://doi.org/10.1175/1520-0442\(1998\)011<2863:PAISBA>2.0.CO;2](https://doi.org/10.1175/1520-0442(1998)011<2863:PAISBA>2.0.CO;2).
- Jr, G., William, I., Yu, S., 2012. Generalized approach for using unbiased symmetric metrics with negative values: Normalized mean bias factor and normalized mean absolute error factor. *Atmos. Sci. Lett.* 262–267. <https://doi.org/10.1002/asl.393>.
- Heusinkveld, B.G., Jacobs, A.F.G., Holslag, A.A.M., Berkowicz, S.M., 2004. Surface energy balance closure in an arid region: Role of soil heat flux. *Agric. For. Meteorol.* 122, 21–37. <https://doi.org/10.1016/j.agrformet.2003.09.005>.
- Horton, R., Wierenga, P.J., Nielsen, D.R., 1983. Evaluation of methods for determining the apparent thermal diffusivity of soil near the surface. *Soil Sci. Soc. Am. J.* 47, 25. <https://doi.org/10.2136/sssaj1983.03615995004700010005x>.
- Johansen, O., 1975. *Thermal Conductivity of Soils, Draft Translation Report 637*. Ph.D. Diss. *Nor. Univ. Sci. Technol.*, pp. 291.
- Jury, William A and Horton, R., 2004. *Soil Physics*. John Wiley & Sons.
- Kersten, M., 1949. Laboratory research for the determination of the thermal properties of soils. *ACFEL Tech. Rep.* 23. Univ of Minnesota, Minneapolis.
- Kojima, Y., Heitman, J.L., Sakai, M., Kato, C., Horton, R., 2018. Bulk density effects on soil hydrologic and thermal characteristics: A numerical investigation. *Hydrol. Process.* 32, 2203–2216. <https://doi.org/10.1002/hyp.13152>.
- Kustas, W.P., Prueger, J.H., Hatfield, J.L., Ramalingam, K., Hipps, L.E., 2000. Variability in soil heat flux from a mesquite dune site. *Agric. For. Meteorol.* [https://doi.org/10.1016/S0168-1923\(00\)00131-3](https://doi.org/10.1016/S0168-1923(00)00131-3).
- Kuye, A., Jagtap, S.S., 1992. Analysis of solar radiation data for Port Harcourt. *Nigeria. Sol. Energy* 49, 139–145. [https://doi.org/10.1016/0038-092X\(92\)90148-4](https://doi.org/10.1016/0038-092X(92)90148-4).
- Liou, K.-N., 2002. *An introduction to atmospheric radiation*, Second. ed. Elsevier.
- Liu, Z., Xu, J., Li, X., Wang, J., 2018. Mechanisms of biochar effects on thermal properties of red soil in south China. *Geoderma*. <https://doi.org/10.1016/j.geoderma.2018.02.045>.
- Lu, S., Lu, Y., Peng, W., Ju, Z., Ren, T., 2019. A generalized relationship between thermal conductivity and matric suction of soils. *Geoderma*. <https://doi.org/10.1016/j.geoderma.2018.09.057>.
- Lu, S., Ren, T., Gong, Y., Horton, R., 2007. An improved model for predicting soil thermal conductivity from water content at room temperature. *Soil Sci. Soc. Am. J.* 71, 8. <https://doi.org/10.2136/sssaj2006.0041>.
- Lu, Y., Lu, S., Horton, R., Ren, T., 2014. An empirical model for estimating soil thermal conductivity from texture, water content, and bulk density. *Soil Sci. Soc. Am. J.* 78, 1859. <https://doi.org/10.2136/sssaj2014.05.0218>.
- Nabinger, C., Ferreira, E., Freitas, A., Carvalho, P.C., Sant'Anna, D., 2009. Produção animal com base no campo nativo: Aplicações de resultados de pesquisa., in: *Campos Sulinos—Conservação e Uso Sustentável Da Biodiversidade*. Ministério do Meio Ambiente: Brasília, Brazil, pp. 175–199.
- Neppin, S V and Chudnovskii, A.F., 1967. *Physics of the soil: Israel program for scientific translations*.
- Nikoosokhan, S., Nowamooz, H., Chazallon, C., 2015. Effect of dry density, soil texture and time-spatial variable water content on the soil thermal conductivity. *Geotech. Geoenviron. Eng.* 149, 149–158. <https://doi.org/10.1080/17486025.2015.1048313>.
- Onceley, S.P., Foken, T., Vogt, R., Kohsik, W., DeBruin, H.A.R., Bernhofer, C., Christen, A., van Gorsel, E., Grantz, D., Feigenwinter, C., Leber, I., Liebenthal, C., Liu, H., Mauder, M., Pitacco, A., Ribeiro, L., Weidinger, T., 2007. The energy balance experiment EBEX-2000. Part I: Overview and energy balance. *Boundary-Layer Meteorol.* 123, 1–28. <https://doi.org/10.1007/s10546-007-9161-1>.
- Otunla, T.A., Oladiran, E.O., 2013. Evaluation of soil thermal diffusivity algorithms at two equatorial sites in West Africa. *Ann. Geophys.* 56. <https://doi.org/10.4401/ag-6170>.
- Peel, M., Finlayson, C., Brian, L., McMahon, T.A., 2007. Updated world map of the Köppen–Geiger climate classification. *Hydrol. Earth Syst. Sci.* 4, 439–473.
- Pillar, V.D., Müller, S., Castilhos, Z.M., Jacques, A.V., 2009. *Conservação e uso Sustentável da Biodiversidade*, 3rd ed. Brasília, Brazil, Ministério do Meio Ambiente.
- Purdy, A.J., Fisher, J.B., Goulden, M.L., Famiglietti, J.S., 2016. Ground heat flux: An analytical review of 6 models evaluated at 88 sites and globally. *J. Geophys. Res. Biogeosciences* 121, 3045–3059. <https://doi.org/10.1002/2016JG003591>.
- Romio, L.C., Roberti, D.R., Buligon, L., Zimmer, T., Degrazia, G.A., 2019. A numerical model to estimate the soil thermal conductivity using field experimental data. *Appl. Sci.* 9, 13.
- Roxy, M.S., Sumithranand, V.B., Renuka, G., 2014. Estimation of soil moisture and its effect on soil thermal characteristics at Astronomical Observatory. Thiruvananthapuram, south Kerala 1793–1807. <https://doi.org/10.1007/s12040-014-0509-x>.
- Rubert, G.C., Roberti, D.R., Pereira, L.S., Quadros, F.L.F., de Velho, H.F.C., de Moraes, O.L.L., 2018. Evapotranspiration of the Brazilian Pampa biome: Seasonality and influential factors. *Water (Switzerland)* 10, 1–18. <https://doi.org/10.3390/w10121864>.
- Santanello, J.A., Friedl, M.A., 2003. Diurnal covariation in soil heat flux and net radiation. *J. Appl. Meteorol.* 42, 851–862. [https://doi.org/10.1175/1520-0450\(2003\)042<0851:DCISHF>2.0.CO;2](https://doi.org/10.1175/1520-0450(2003)042<0851:DCISHF>2.0.CO;2).
- Seemann, J., 1979. *Measuring technology*. Springer - Verlag, *Agrometeorology* https://doi.org/https://doi.org/10.1007/978-3-642-67288-0_9.
- Sepaskhab, A.R., Boersma, L., 1979. Thermal conductivity of soils as a function of temperature and water content. *Soil Sci. Soc. Am. J.* 43, 439–444. <https://doi.org/10.2136/sssaj1979.03615995004300030003x>.
- Tarnawski, V.R., Gori, F., 2002. Enhancement of the cubic cell soil thermal conductivity model. *Int. J. Energy Res.* 26, 143–157. <https://doi.org/10.1002/er.772>.
- Tong, B., Gao, Z., Horton, R., Li, Y., Wang, L., 2016. An empirical model for estimating soil thermal conductivity from soil water content and porosity. *J. Hydrometeorol.* 17, 601–613. <https://doi.org/10.1175/jhm-d-15-0119.1>.
- Usowicz, B., Lipiec, J., Lukowski, M., Marczewski, W., Usowicz, J., 2016. The effect of biochar application on thermal properties and albedo of loess soil under grassland and fallow. *Soil Tillage Res.* <https://doi.org/10.1016/j.still.2016.03.009>.
- Walford, L.A., 1946. *A New Graphic Method of Describing the Growth of Animals* 90, 141–147.
- Wang, K., Wang, P., Liu, J., Sparrow, M., Haginoya, S., Zhou, X., 2005. Variation of surface albedo and soil thermal parameters with soil moisture content at a semi-desert site on the western Tibetan Plateau. *Boundary-Layer Meteorol.* 116, 117–129. <https://doi.org/10.1007/s10546-004-7403-z>.
- Wang, L., Gao, Z., Horton, R., 2010. Comparison of six algorithms to determine the soil apparent thermal diffusivity at a site in the loess plateau of China. *Soil Sci.* 175, 51–60. <https://doi.org/10.1097/SS.0b013e3181cdda3f>.
- Wang, L., Gao, Z., Horton, R., Lenschow, D.H., Meng, K., Jaynes, D.B., 2012. An analytical solution to the one-dimensional heat conduction-convection equation in soil. *Soil Sci. Soc. Am. J.* 76, 1978–1986. <https://doi.org/10.2136/sssaj2012.0023n>.
- Wierenga, P. J. Nielsen, D. R. and Hagan, R.M., 1969. *Thermal Properties of a Soil Based Upon Field and Laboratory Measurements* 354–360.
- Wilson, K., Goldstein, A., Falge, E., Aubinet, M., Baldocchi, D., Berbigier, P., Bernhofer, C., Ceulemans, R., Dolman, H., Field, C., Grelle, A., Ibrom, A., Law, B.E., Kowalski, A., Meyers, T., Moncrieff, J., Monson, R., Oechel, W., Tenhunen, J., Valentini, R., Verma,

- S., 2002. Energy balance closure at FLUXNET sites. *Agric. For. Meteorol.* [https://doi.org/10.1016/S0168-1923\(02\)00109-0](https://doi.org/10.1016/S0168-1923(02)00109-0).
- Xie, X., Lu, Y., Ren, T., Horton, R., 2019. Soil temperature estimation with the harmonic method is affected by thermal diffusivity parameterization. *Geoderma* 353, 97–103. <https://doi.org/10.1016/j.geoderma.2019.06.029>.
- Yan, H., He, H., Dyck, M., Jin, H., Li, M., Si, B., Lv, J., 2019. A generalized model for estimating effective soil thermal conductivity based on the Kasubuchi algorithm. *Geoderma*. <https://doi.org/10.1016/j.geoderma.2019.06.031>.
- Zaibon, S., Anderson, S.H., Veum, K.S., Haruna, S.I., 2019. Soil thermal properties affected by topsoil thickness in switchgrass and row crop management systems. *Geoderma*. <https://doi.org/10.1016/j.geoderma.2019.05.005>.
- Zhao, G.Z., Wang, W.K., Hou, L.L., Li, Y.L., 2009. Determination of thermal parameter of aerated zone in the arid and semi-arid region. *Hydrogeol. Eng. Chin.* 36, 107–110.
- Zhao, J., Ren, T., Zhang, Q., Du, Z., Wang, Y., 2016. Effects of biochar amendment on soil thermal properties in the North China plain. *Soil Sci. Soc. Am. J.* 80, 1157–1166. <https://doi.org/10.2136/sssaj2016.01.0020>.
- Zhao, Y., Si, B., Zhang, Z., Li, M., He, H., Hill, R.L., 2019. A new thermal conductivity model for sandy and peat soils. *Agric. For. Meteorol.* <https://doi.org/10.1016/j.agrformet.2019.04.004>.
- Zheng, H., Wang, Q., Zhu, X., Li, Y., Yu, G., 2014. Hysteresis responses of evapotranspiration to meteorological factors at a diel timescale: Patterns and causes. *PLoS One* 9, 1–10. <https://doi.org/10.1371/journal.pone.0098857>.
- Zuecco, G., Penna, D., Borga, M., van Meerveld, H.J., 2016. A versatile index to characterize hysteresis between hydrological variables at the runoff event timescale. *Hydrol. Process.* 30, 1449–1466. <https://doi.org/10.1002/hyp.10681>.

APPENDIX A. SUPPLEMENTARY MATERIALS

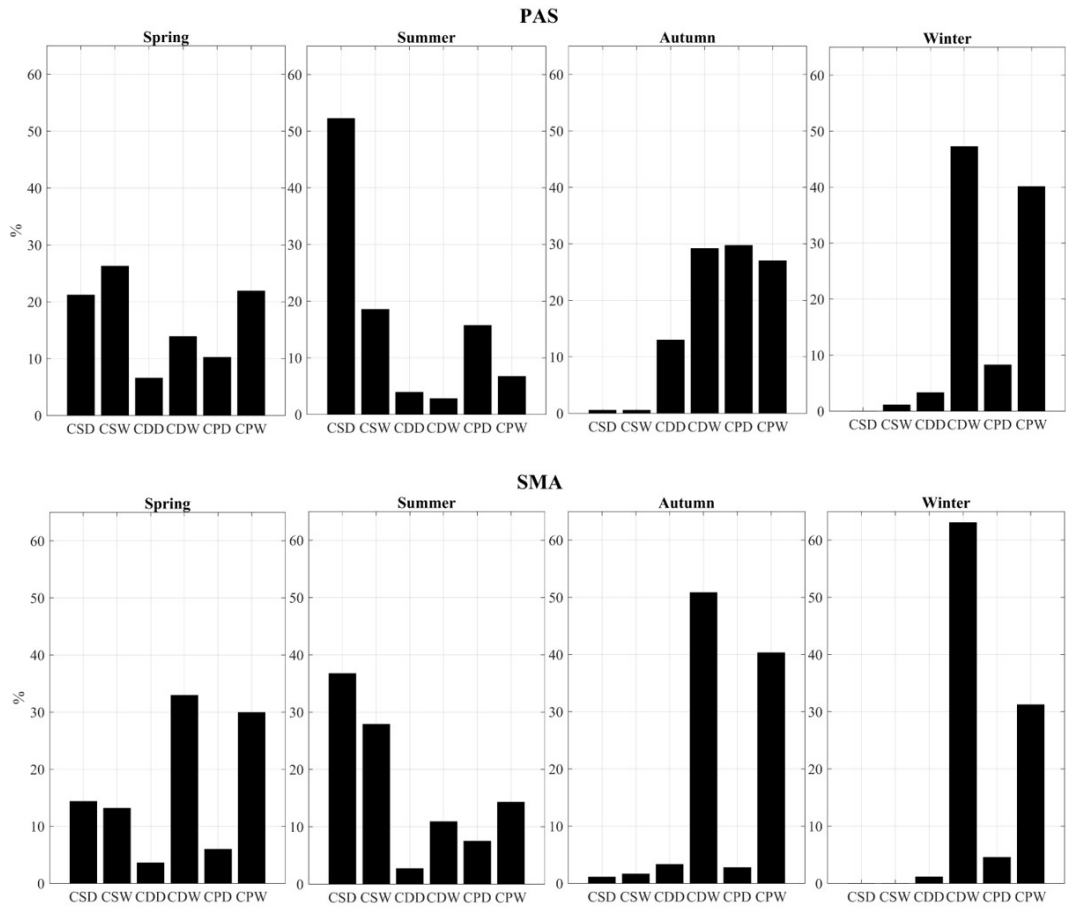


Fig.A.1. Distribution of data classification per season.

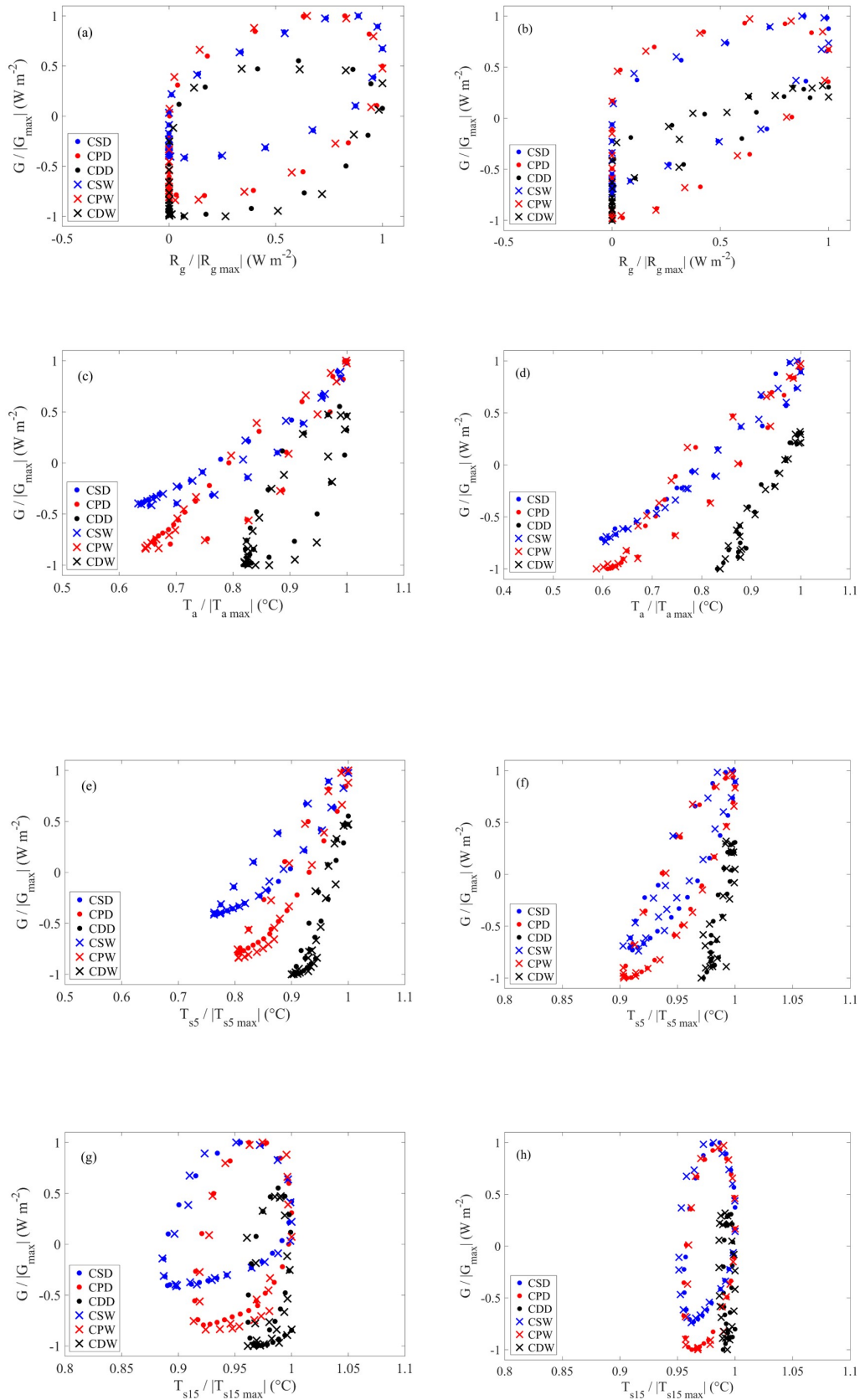


Fig.A.2. Dimensionless soil heat flux (G) response curves vs: (a, b) global solar radiation (R_g), (c, d) air temperature (T_a), (e, f) soil temperature at 0.05m (T_{s5}) and (g, h) 0.15 m (T_{s15}) for PAS site in the left panel and SMA site for the right panel.

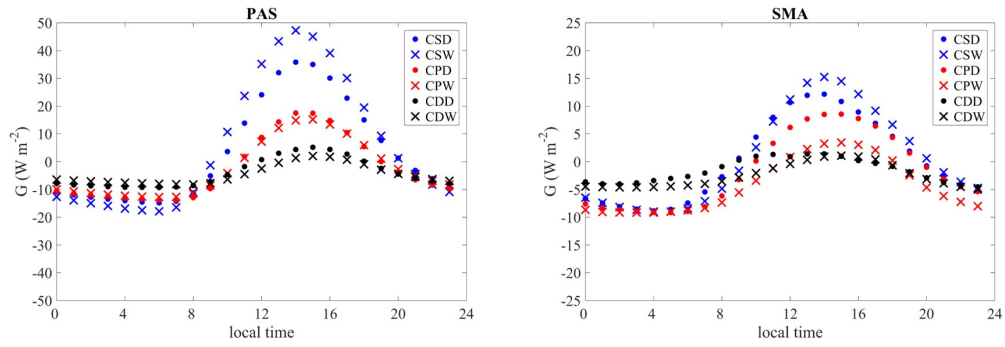


Fig.A.3. Diurnal cycles of soil heat flux (G) for each data classification.

Table A.1

Damping depth, d , calculated using k_p from Table 3; Exponential decay amplitude of soil temperature, $A^* = e^{-(z-z_i)/d}$ and phase $\Phi = (z - z_i)/d$ using $z = 0.15$ m and $z_i = 0.05$ m; for PAS and SMA sites in dry and wet periods.

	period	k_p ($\text{m}^2 \text{s}^{-1}$),	d (m)	A^*	Φ (rad)
PAS	dry	4.19×10^{-7}	0.107	0.39	$\approx \pi/3$
	wet	5.62×10^{-7}	0.124	0.45	$\pi/4$
SMA	dry	5.25×10^{-7}	0.120	0.43	$\pi/3$
	wet	5.96×10^{-7}	0.128	0.46	$\approx \pi/4$

4 ARTICLE 2: ESTIMATION OF SOIL THERMAL PROPERTIES USING CONDUCTION AND CONDUCTION - CONVECTION HEAT TRANSFER EQUATIONS IN THE BRAZILIAN PAMPA BIOME

1

ORIGINAL ARTICLE

Journal Section

Estimation of soil thermal properties using conduction and conduction - convection heat transfer equations in the Brazilian Pampa biome

Tamíres Zimmer¹ | Vanessa de Arruda Souza¹ | Leugim Corteze Romio² | Lidiane Buligon¹ | Gustavo Pujol Veeck¹ | Michel Baptistella Stefanello¹ | Débora Regina Roberti¹

¹Departamento de Física, Universidade Federal de Santa Maria, Santa Maria, RS, Brazil

²Universidade Federal do Pampa (UNIPAMPA), Campus Caçapava do Sul, RS, Brazil

Correspondence

Débora Regina Roberti, Departamento de Física, Universidade Federal de Santa Maria, Santa Maria, RS, Brazil
Email: debora@ufsm.br

Funding information

Soil temperature, composition, and structure directly affect the heat transfer mechanisms in soil. Understanding the thermal behavior of soil is fundamental for describing the processes of mass and energy exchange in the soil-plant-atmosphere system. In addition, estimating thermal property values is necessary to determine the amount of heat transferred, stored, or transmitted by conduction and convection between the soil surface and deeper layers. Nonetheless, estimating thermal properties using heat transfer models and soil moisture is still a challenge. Therefore, this paper used two soil heat transfer models (the conduction and conduction-convection methods) to estimate soil thermal properties. Experimental data were collected in a natural pasture area in the Pampa biome in southern Brazil. The results showed that soil thermal diffusivity (k) has an inverse seasonal variation with soil temperature (T_s). The k and soil thermal conductivity (λ) values are higher when the depth of the levels and soil moisture (θ) increase, confirming the vertical variation of thermal properties. The parameter W , which considers the additional effects of soil heterogeneity and thermal convection due to the vertical movement of water in the soil, decreases in periods of higher T_s . Increasing values of W led to an increase in the variability of k with depth. The conduction-convection method pro-

¹Article configured in the journal's technical standards to be submitted.

vides the best estimates for T_s with $R^2 = 0.99$ for deeper layers. However, we found that both models gave similar results for near-surface layers since, in this case, the conduction process was responsible for most of the heat transfer from the surface to the ground. The results obtained here allowed us to evaluate heat transfer at different depths and estimate thermal properties as a function of soil moisture in a natural pasture area in the Brazilian Pampa biome. Furthermore, the results can be integrated into global land surface models intended to represent the behavior of the energy exchange between soil, surface, and the atmosphere.

KEYWORDS

Soil temperature; soil thermal properties; soil moisture; conduction-convection method; Pampa biome.

1 | INTRODUCTION

Soil temperature (T_s) is an environmental variable that plays a critical role in energy balance applications, including land surface modeling and numerical weather and climate predictions (Holmes et al., 2008; Alkhaier et al., 2012). In addition, T_s also affects soil physical and chemical properties and biochemical processes (Rahi and Jensen, 1975; Andry et al., 2009), as well as plant growth (Mellander et al., 2004; Wu et al., 2012), organic matter decomposition and mineralization rates (Wang et al., 2006; Guntiñas et al., 2012), CO_2 release (Peng et al., 2009; Graham, 2010; Xu et al., 2012; Onwuka and Nwangwu, 2016), among others.

Knowledge of soil thermal properties (thermal diffusivity, k , thermal conductivity, λ , and thermal capacity, c_v) enables a better understanding of soil thermal dynamics, as these are fundamental parameters required for estimating T_s and soil heat flux (G) and consequently for establishing the energy balance. The thermal properties of the soil depend on factors related to the nature of the soil, such as texture, organic matter content, mineralogical composition, and the physical structure of the soil, among other factors (De Vries and Peck, 1958; Johansen, 1975; Campbell, 1985; Lu et al., 2007; Liu et al., 2008; Clarke et al., 2008; Lu et al., 2014; Zhao et al., 2019; Lu et al., 2019; Xie et al., 2019). In addition, evidence has shown the dependence of soil thermal properties on soil moisture (θ) and climatic conditions such as sky cover (Wang et al., 2010; Otunla and Oladiran, 2013; An et al., 2016; Zimmer et al., 2020). These studies have shown that θ and solar radiation influence the dynamics of thermal variables and soil properties. Zimmer et al. (2020) analyzed the influence of these conditions on the dynamics of soil thermal variables (heat flux, G , soil temperature at 0.05 m, T_{s5} and 0.15 m, T_{s15}) and soil thermal properties in areas with natural pastures. The results showed that the highest λ and k values were obtained in periods with wet soil at both sites. In addition, greater variability in soil thermal properties was observed with increasing soil moisture. The proposal of a new empirical model for $\lambda(\theta)$ provided good results for representing the experimental λ and G estimation.

In general, thermal properties are estimated using the one-dimensional heat conduction equation, assuming an isotropic and thermally homogeneous medium (Carslaw and Jaeger, 1959). When analyzing heat transfer under these conditions, it is assumed that hydraulic permeability does not depend on the orientation and thermal diffusivity is

independent of position. In this case, both properties can be considered constant, which means that the problem is described in a simplified way, leading to known solutions. The main analytical methods are amplitude and phase shift (De Vries and Peck, 1958; Wierenga et al., 1969), arctangent (Nerpin and Chudnovskii, 1967), logarithmic (Seemann, 1979) and harmonic (Horton et al., 1983), while numerical solutions are primarily based on the gradient method (Horton et al., 1983; Evett et al., 2012; Gao et al., 2017; Romio et al., 2019). However, heat transfer in the soil is also determined by the heat convection within the pores (de Silans et al., 1996; Gao et al., 2003), and thus the vertical water flux affects T_s and, consequently, the soil thermal properties. Research describing and solving the problem considers both processes (i.e., heat transfer by conduction and convection), as presented by Gao et al. (2003); Gao (2005). In these studies, k and liquid water (W) flux density were estimated, assuming that each term of the conduction-convection equation represents independent processes. In other models proposed by Gao et al. (2008a), Wang et al. (2012a,b) assumed that the thermal diffusivity of the soil varies vertically, so the additional term generated is added to the liquid water flux density term. Unlike previous models, W is associated with heat conduction and convection processes due to the presence of water in the soil, and in this case, the estimates obtained do not allow separate quantification of each physical effect.

Theoretical studies of heat transfer in soils generally consider the soil a homogeneous medium and assume that the entire heat transfer process proceeds uniformly through the porous medium. However, soils are porous media that are inherently heterogeneous. The depth of heat penetration into the soil and daily and seasonal amplitude of temperature variations influence the thermal properties of the soil. For models formulated considering the vertical heterogeneity of the soil, T_s and G measurements at different depths must be considered, while the influence of soil water content requires θ measurements. *In situ* measurement of these variables can be done using sensors and automatic data acquisition systems, albeit this method requires skilled labor for installation, maintenance, and data acquisition, which are essential for adequate soil thermal characterization (Costello and Horst, 1991). Nevertheless, estimating thermal properties that combine heat and moisture transfer in soil remains challenging. This is either because of the difficulty of obtaining experimental data or because the more complex equation is mathematically difficult to solve. Therefore, for this study, an experimental setup with temperature, heat flux, and soil moisture measurements at different soil depths was developed to shed more light on the thermal dynamics of the soil and to estimate its thermal properties by considering the processes of heat transfer by conduction and convection. By implementing different solutions, the thermal properties of the soil are estimated and the influence of different physical processes in the modeled measurements is quantified.

The experimental area is located in a region with fields and native vegetation in the Brazilian Pampa biome. The site was chosen because of its economic and environmental importance in southern Brazil, as it includes a large area for livestock production. Therefore, studying soil thermal dynamics in an area of natural pasture is essential to improve the characterization of the Brazilian Pampa biome and quantify the processes associated with the closure of the energy balance. In this context, this study aimed to estimate the thermal properties of the soil using the heat transfer equations using the conduction (CM) and conduction-convection (CCM) methods. Experimental data on soil temperature, heat flux, and moisture measured at different depths were used to calibrate and validate the models. The time series of experimental field data covers the period from 3 April 2020 to 30 September 2021 and is important for seasonal analysis.

This study analyzes the variability of soil thermal variables and properties at different time scales (daily and seasonal) and the influence of the vertical movement of water in the soil on soil thermal characterization. From the CCM solution, k and W are estimated to quantify the influence of the convection process, and these estimates are compared with those obtained from the conduction equation. The vertical variation of soil thermal properties as a function of soil moisture was analyzed under dry and wet conditions. The study identifies and quantifies the influence

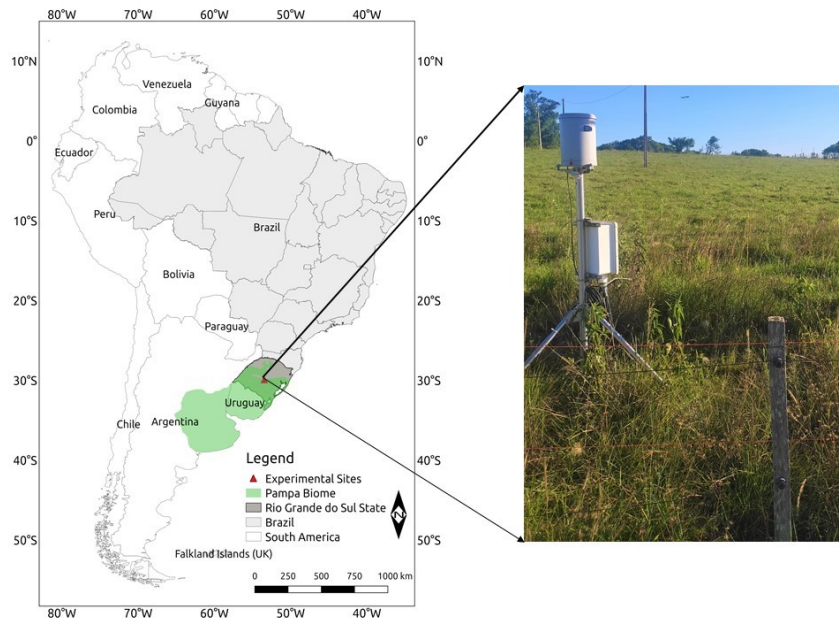
of depth and the daily and seasonal amplitude of temperature and moisture variations on soil thermal properties. It, therefore, offers potential for investigating numerical algorithms describing coupled processes of heat transfer and soil.

2 | MATERIALS AND METHODS

2.1 | Experimental data and instrumentation

The SMA site is located in the municipality of Santa Maria, Rio Grande do Sul State, southern Brazil (29°43'27.502" S; 53°45'36.097" W; 88 m elevation), in an experimental area of the Federal University of Santa Maria (UFSM) (Figure 1). The study area has natural vegetation of the Pampa biome, mainly composed of native grasses used as pasture for beef cattle. According to Köppen (Peel et al., 2007), the region is classified as having a humid subtropical climate (Cfa) with well-distributed rainfall throughout the year, high temperatures in summer (daily averages of 30°C), and low temperatures in winter with daily averages of 4°C.

FIGURE 1 – Location of the experimental area.



The soil classification is clay loam with an average of 41.08% sand, 23.10% clay, and 35.82% silt between the surface and 0.45 m depth. The average values of soil physical properties at 0.05, 0.10, 0.25 and 0.45 m depth are: field capacity, $\theta_{FC} = 0.31 \text{ m}^3 \text{ m}^{-3}$, permanent wilting point, $\theta_{WP} = 0.11 \text{ m}^3 \text{ m}^{-3}$, soil porosity, $\theta_s = 0.47 \text{ m}^3 \text{ m}^{-3}$, and soil density, $\rho_s = 1355 \text{ kg m}^{-3}$. For more information on the experimental site, see Rubert et al. (2018) and Zimmer et al. (2020).

Soil temperature (T_s) was measured using the T108 sensor (Campbell Scientific Inc., Logan, Utah, USA) at depths of 0.05 (T_{s5}), 0.09 (T_{s9}), 0.13 (T_{s13}), 0.17 (T_{s17}), 0.21 (T_{s21}), 0.30 (T_{s30}), 0.34 (T_{s34}), and 0.38 m (T_{s8}). Soil heat flux (G)

was measured using the sensor HFPO1 (Hukseflux Thermal Sensor B.V., Delft, The Netherlands) at depths of 0.09 (G_9), 0.17 (G_{17}), and 0.34 m (G_{34}). Soil moisture (θ) was measured with a CS616 reflectometer (Campbell Scientific Inc., Logan, Utah, USA) at depths of 0.09 (θ_9), 0.17 (θ_{17}), and 0.34 m (θ_{34}). Precipitation (P_{rec}) was measured with a rain gauge (TR525USW, Texas Electronics, USA) at 2 m height. A diagram showing the position of the sensors and the analysed levels is provided in Figure 2. The data were measured at a frequency of 1 min^{-1} and then processed to one-hour averages.

The study period was from 3 April 2020 to 30 September 2021. The measurement system failed from 12 to 20 November 2020, 25 to 27 March 2021 and from 27 to 29 July 2021 due to technical issues. The soil temperature dataset was populated using linear interpolation whenever the gap interval was equal to or less than two hours, and if gaps were longer than two hours, the data were not considered in the analyses. The soil was classified by its moisture using the soil moisture threshold value (θ_t) according to:

- (i) W = wet soil if $\theta \geq \theta_t$;
- (ii) D = dry soil if $\theta < \theta_t$.

where $\theta_t = (\theta_{FC}) - p \cdot (TAW)$ and TAW are obtained by the difference between θ_{FC} and θ_{WP} ; the p factor depends on the crop, according to Allen et al. (1998). For more information on the method, see Zimmer et al. (2020).

2.2 | Thermal conduction equation

The equation describing heat transfer in soil by conduction in a one-dimensional isotropic medium is given by:

$$\frac{\partial T}{\partial t} = \frac{1}{c_v} \frac{\partial}{\partial z} \left(\lambda \frac{\partial T}{\partial z} \right) \quad (1)$$

where T is the soil temperature (K), t is the time (s), c_v is the soil thermal capacity ($\text{J m}^{-3} \text{K}^{-1}$), λ is the soil thermal conductivity ($\text{W m}^{-1} \text{K}^{-1}$), and z is the depth of the soil surface (m). The term in brackets of Eq.(1), known as Fourier's law of heat conduction (Carslaw and Jaeger, 1959), is defined as the soil heat flux, G (W m^{-2}), in a z depth.

Assuming that c_v and λ are independent of depth and time, Eq.(1) can be rewritten as:

$$\frac{\partial T}{\partial t} = k \frac{\partial^2 T}{\partial z^2} \quad (2)$$

where $k = \lambda c_v^{-1}$ ($\text{m}^2 \text{s}^{-1}$) is the soil thermal diffusivity.

According to Carslaw and Jaeger (1959), a solution for the transient heat transfer problem governed by Eq.(2), for a homogeneous soil of semi-infinite thickness with average daily temperature repeating periodic surface temperature oscillations, is represented by the initial and boundary conditions, respectively:

$$T(z, 0) = f(z) \quad (3)$$

$$T(0, t) = \bar{T}_0 + A_0 \sin(\omega t + \varphi_0) \quad (4)$$

is given by

$$T(z, t) = \bar{T}(z) + A_i e^{-(z-z_i)\alpha} \sin(\omega t + \varphi_i - (z - z_i)\alpha) \quad (5)$$

where \bar{T}_0 is the mean soil surface temperature, A_0 is the amplitude of the soil surface temperature wave, φ_0 is the phase shift of the soil surface temperature, ω is the angular velocity of the Earth's rotation (rad h⁻¹) ($\omega = 2\pi/\tau$, with τ denoting the period of the fundamental cycle, 1 day), $\bar{T}(z)$ is the daily mean soil temperature at depth z , the sub-index i represents the level z_i of soil temperature measurement, A_i are the temperature amplitudes, φ_i phase shifts and $\alpha^{-1} = \sqrt{\frac{2k}{\omega}}$ (m) is the damping depth of the temperature wave (Campbell and Norman, 1998). From Eq.(5), Horton et al. (1983) proposed the amplitude and phase shift method to calculate the soil thermal diffusivity (k), as given by the following equations:

$$k_a = \frac{\omega(z_1 - z_2)^2}{2[\ln(\frac{A_1}{A_2})]^2} \quad (6)$$

and

$$k_p = \frac{\omega(z_1 - z_2)^2}{2(\varphi_1 - \varphi_2)^2} \quad (7)$$

where the sub-index a refers to the amplitude method and the sub-index p to the phase shift method, $i = 1$ represents the depth of the first soil temperature measurement (z_1) and $i = 2$ is the depth of the second soil temperature measurement (z_2). The values for A_i and φ_i , $i = 1$ e 2 , are obtained by fitting the temperature data at the respective depths.

The expression for the soil heat flux G (W m⁻²) written as a function of depth and time is obtained by substituting Eq.(5) in Fourier's law (Carslaw and Jaeger, 1959), therefore:

$$G(z, t) = \lambda \left(\frac{\Delta T}{\Delta z} + \sqrt{2} A_i \sqrt{\frac{\omega}{2k}} e^{-(z-z_i)\sqrt{\frac{\omega}{2k}}} \sin \left(\omega t + \varphi_i + \frac{\pi}{4} - (z - z_i) \sqrt{\frac{\omega}{2k}} \right) \right) \quad (8)$$

with $\Delta T/\Delta z$ the temperature gradient (K m⁻¹) and $i = 1, 2$, represent the depths z_1 and z_2 , respectively.

Therefore, the soil thermal conductivity (λ) estimation can be obtained by fitting Eq.(8) and using Eqs.(6) or (7). The method used to estimate λ by λ_a and λ_p for the amplitude and phase shift method, respectively, is identified. Soil heat capacity is determined by the following mathematical relationships: $c_{v_a} = \lambda_a k_a^{-1}$ (amplitude method) and $c_{v_p} = \lambda_p k_p^{-1}$ (phase shift method).

2.3 | Thermal conduction-convection equation

The conduction-convection equation for one-dimensional heat transfer from the soil in the presence of constant net flux (Gao et al., 2003, 2008a) is given by:

$$\frac{\partial T}{\partial t} = k \frac{\partial^2 T}{\partial z^2} + W \frac{\partial T}{\partial z} \quad (9)$$

where the parameter W considers the addition of the effect of soil heterogeneity and thermal convection by the vertical movement of water in the soil. Specifically,

$$W = \frac{\partial k}{\partial z} - \frac{c_w}{c_v} \eta \theta \quad (10)$$

η is the liquid infiltration rate (m s^{-1}) (i.e., Darcy's velocity; positive downwards), θ is the soil moisture ($\text{m}^3 \text{m}^{-3}$), and c_w is the heat capacity of water ($4.18 \times 10^6 \text{ J m}^{-3} \text{K}^{-1}$). The first term of the Eq.(10), $\frac{\partial k}{\partial z}$, as the vertical gradient of soil diffusivity derived from the conductive process and the second term $-\frac{c_w}{c_v} \eta \theta$ as the water flux density resulting from the convective process; therefore, the authors define the total term W as the liquid water flux density.

Following a procedure similar to the one described in Section 4.3.2, Gao (2005) proposed the following solution for Eq.(9):

$$T(z, t) = \bar{T}(z) + A_i e^{-(z-z_i)\alpha M} \sin(\omega t + \varphi_i - (z - z_i)\alpha N) \quad (11)$$

where

$$M = \frac{\alpha}{\omega} \left\{ W + \frac{1}{\sqrt{2}} \left[W^2 + \left(W^4 + \frac{4\omega^4}{\alpha^4} \right)^{1/2} \right]^{1/2} \right\} \quad (12)$$

$$N = \sqrt{2} \left(\frac{\omega}{\alpha} \right) \left[W^2 + \left(W^4 + \frac{4\omega^4}{\alpha^4} \right)^{1/2} \right]^{-1/2} \quad (13)$$

The equation for the thermal diffusivity of the soil (k) and flow density of liquid water (W) were derived from Eq. (11) and expressed as:

$$k_{cc} = - \frac{\omega(z_1 - z_2)^2 \ln(A_1/A_2)}{(\varphi_1 - \varphi_2) [(\varphi_1 - \varphi_2)^2 + \ln^2(A_1/A_2)]} \quad (14)$$

$$W = \frac{\omega(z_1 - z_2)}{(\varphi_1 - \varphi_2)} \left[\frac{2 \ln^2(A_1/A_2)}{(\varphi_1 - \varphi_2)^2 + \ln^2(A_1/A_2)} - 1 \right] \quad (15)$$

where the sub-index cc refers to the conduction-convection method.

Once again, substituting in Fourier's law of heat conduction (Carslaw and Jaeger, 1959) Eq.(11), the heat flux in the soil is obtained by:

$$G(z, t) = \lambda \left(\frac{\Delta T}{\Delta z} + M A_i e^{-(z-z_i)M} \sin(\omega t + \varphi_i - (z - z_i)N) \right) - N A_i e^{-(z-z_i)M} \cos(\omega t + \varphi_i - (z - z_i)N) \quad (16)$$

Therefore, the soil thermal conductivity (λ) can be estimated from Eq.(16) using Eqs.(14) and (15). The notation λ_{cc} will be used to identify the method of conduction - convection. The reason $c_{vcc} = \lambda_{cc} k_{cc}^{-1}$ is used to estimate the soil heat capacity and liquid infiltration rate (η) by the equation:

$$\eta = \frac{c_v \omega (z_1 - z_2)}{c_w (\varphi_1 - \varphi_2)} \left[1 - \frac{2 \ln^2(A_1/A_2)}{(\varphi_1 - \varphi_2)^2 + \ln^2(A_1/A_2)} \right] \quad (17)$$

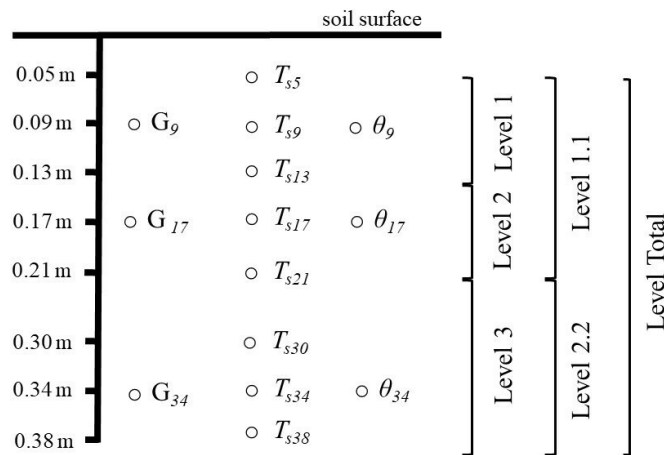
It is important to note that the inclusion of the convective term generated the dependence of k , and consequently

λ , with the estimates for amplitudes and phase shift at depths z_1 and z_2 .

2.4 | Data processing

The experimental setup with temperature, heat flux, and moisture measurements at different soil depths was used to estimate the thermal properties and evaluate their dependence on the measurement depth and water content.

FIGURE 2 – Configuration of the positions of the sensors installed on the ground with the different levels analyzed. The G represents soil heat flux sensors, T_s for soil temperature sensors, and θ for soil moisture sensors.



For this purpose, three different analyses were carried out with the configuration of the sensors installed in the soil (Figure 2):

- **Analysis 1:** the measurements were divided into three levels corresponding to the following depths:

Level 1 - $z_1 = 0.05$ m to $z_2 = 0.13$ m using T_{s5} , T_{s13} , θ_9 , and G_9 ;

Level 2 - $z_2 = 0.13$ m to $z_3 = 0.21$ m using T_{s13} , T_{s21} , θ_{17} , and G_{17} ;

Level 3 - $z_3 = 0.30$ m to $z_4 = 0.38$ m using T_{s30} , T_{s38} , θ_{34} , and G_{34} .

- **Analysis 2:** the measurements were divided into two levels corresponding to the following depths:

Level 1.1 - $z_1 = 0.05$ m to $z_2 = 0.21$ m using T_{s5} , T_{s21} , θ_9 , and G_9 ;

Level 2.2 - $z_2 = 0.21$ m to $z_3 = 0.38$ m using T_{s21} , T_{s38} , θ_{34} , and G_{34} .

- **Analysis 3:** The measurements were divided into a total level corresponding to the following depth:

Total Level - $z_1 = 0.05$ m to $z_2 = 0.38$ m using T_{s5} , T_{s38} , θ_{17} , and G_{17} .

The sinusoidal functions $T(z_i, t) = \bar{T}_i + A_i \sin(\omega t + \varphi_i)$, ($t > 0$; $i = 1, 2, 3, 4$) resulting from Eq.(5), when $z = z_i$, was used to approximate the temporal variation curves of soil temperature collected at 0.05, 0.13, 0.21, 0.30 and 0.38 m depths. The values of A_i and φ_i ($i = 1, 2, 3$ and 4) were determined for each level obtained by Analysis 1, 2 and 3. The temporal variations of k ($m^2 s^{-1}$) were determined using Eqs.(6), (7) and (14). The parameter W ($m^2 s^{-1}$) was determined using Eq.(15), where A_i and φ_i have already been described. Using the hourly experimental T_s and G values for each level proposed in Analyses 1, 2 and 3 and with the previously obtained k values, λ ($W m^{-1} K^{-1}$)

is calculated from the fit of Eqs.(8) and (16). Consequently, λ was determined by the amplitude, phase shift, and conduction-convection method. The c_v value was obtained with an average value of λ and k for each level determined by the analyses and methods used. MATLAB (Mathworks Inc.) was used to analyze the data set and fit the sinusoidal functions, and the Optimisation Toolbox™ function 'lsqcurvefit' was used to solve the least-squares method.

The values of the fitted parameters and the soil thermal properties estimated at each analyzed level were used to obtain the simulated T_s at levels different from those used in Analyses 1, 2, and 3 and then validated via statistical indices with the experimental T_s at the respective sub-level simulated. To obtain the simulated T_s data, Eq.(5) for the amplitude and phase shift method and Eq.(11) for the conduction-convection method were employed for the same data period (3 April 2020 to 30 September 2021). In this sense, we identified each validation performed as follows:

- Validation 1:

Sub-Level – T_{s9} : uses k_a , k_p , k_{cc} , and the parameters set in Level 1 (Analysis 1) and experimental T_{s9} ;

Sub-Level – T_{s17} : uses k_a , k_p , k_{cc} , and the parameters set in Level 2 (Analysis 1) and experimental T_{s17} ;

Sub-Level – T_{s34} : uses k_a , k_p , k_{cc} , and the parameters set in Level 3 (Analysis 1) and experimental T_{s34} .

- Validation 2:

Sub-Level – T_{s9} : uses k_a , k_p , k_{cc} , and the parameters set in Level 1.1 (Analysis 2) and experimental T_{s9} ;

Sub-Level – T_{s17} : uses k_a , k_p , k_{cc} , and the parameters set in Level 1.1 (Analysis 2) and experimental T_{s17} ;

Sub-Level – T_{s34} : uses k_a , k_p , k_{cc} , and the parameters set in Level 2.2 (Analysis 2) and experimental T_{s34} .

- Validation 3:

Sub-Level – T_{s9} : uses k_a , k_p , k_{cc} , and the parameters set in Total Level (Analysis 3) and experimental T_{s9} ;

Sub-Level – T_{s17} : uses k_a , k_p , k_{cc} , and the parameters set in Total Level (Analysis 3) and experimental T_{s17} ;

Sub-Level – T_{s34} : uses k_a , k_p , k_{cc} , and the parameters set in Total Level (Analysis 3) and experimental T_{s34} .

The results obtained through validation were evaluated using the following statistical indices: Pearson's correlation (r) (coefficient of determination $R^2 = r^2$) and root mean square error (RMSE), according to the equations below:

$$r = \frac{\sum(x_e - \bar{x}_e)(x_m - \bar{x}_m)}{\sqrt{\sum(x_e - \bar{x}_e)^2 \sum(x_m - \bar{x}_m)^2}} \quad (18)$$

$$RMSE = \sqrt{\frac{\sum(x_e - x_m)^2}{n}} \quad (19)$$

where x_e stands for the experimental value, x_m for the modelled value, and n for the number of observations.

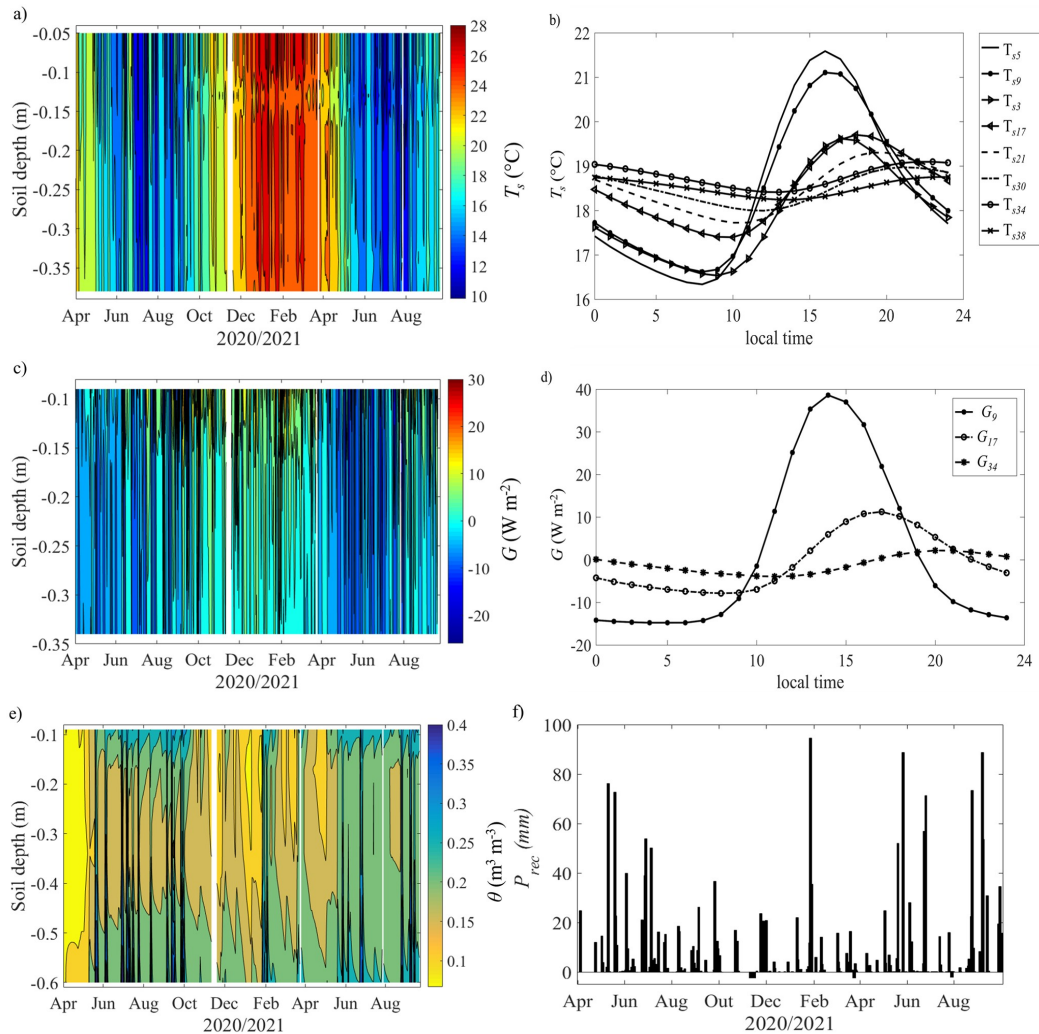
3 | RESULTS AND DISCUSSION

3.1 | Soil variables

The (T_s) showed higher values in the spring/summer (October–March) than in the autumn/winter (April–September) (Figure 3a), which can be attributed to the stronger solar radiation reaching the Earth's surface. During the analyzed period, the largest amplitudes of variation of T_s occurred during the day to a depth of 0.17 m (i.e., T_{s5} , T_{s9} , T_{s13} , and T_{s17} ; Figures 3a, 3b). We can also observe that the amplitudes decreased and a shift in the phase of T_s at increasing depths. This is because the energy flow in the form of heat from the surface to the subsurface decreases (Figures 3c

and 3d). The minimum hourly values for T_{s5} and T_{s9} were $\approx 7^\circ\text{C}$, with a maximum of $\approx 34^\circ\text{C}$ for T_{s13} , a minimum of $\approx 9^\circ\text{C}$ and a maximum of $\approx 30^\circ\text{C}$ for T_{s17} ; for the other temperatures (T_{s21} , T_{s30} , T_{s34} , and T_{s38}), the minimum was $\approx 11^\circ\text{C}$ and the maximum was $\approx 28^\circ\text{C}$. The T_s between the different depths showed variability in the diurnal cycle of $\approx 3^\circ\text{C}$ (Figure 3b). The mean value of T_s was $\approx 19^\circ\text{C}$ at all depths.

FIGURE 3 – a) Contour plots of daily average soil temperature (T_s , $^\circ\text{C}$), c) soil heat flux (G , W m^{-2}), and e) soil moisture (θ , $\text{m}^3 \text{m}^{-3}$); b) daily cycle of T_s and d) G ; f) daily accumulated precipitation (P_{rec} , mm). The periods without precipitation measurements are represented by negative values.



The soil heat flux (G) shows a seasonal behaviour. The highest values of G were observed in the spring/summer seasons (October–March) at all depths (Figure 3c), with greater daily variability for the first depth of 0.09 m (G_9) (Figure 3d). During the autumn/winter seasons (April–September), the daily average of G was generally negative (i.e., the subsoil warms the surface). This result is related to the decrease in solar radiation at the surface. The same result was also obtained by Romio et al. (2019) and Zimmer et al. (2020), who also analyzed G in similar regions of the Pampa

biome.

Soil moisture (θ) had great variability throughout the year and at all depths (Figure 3e), with daily mean θ values ranging from 0.06 to 0.35 $\text{m}^3 \text{m}^{-3}$. The average value of θ for the whole period and both depths analyzed was $\approx 0.19 \text{ m}^3 \text{m}^{-3}$. This result is related to the clayey soil and, therefore, higher water retention capacity. On the days when precipitation accumulations were observed, the average θ values at the analyzed depths reached 0.35 $\text{m}^3 \text{m}^{-3}$. By following the method of Allen et al. (1998), we calculated the value of the average soil moisture threshold (θ_t) for all analyzed levels, resulting in $\theta_t = 0.19 \text{ m}^3 \text{m}^{-3}$. Thus, the experimental site has dry soils on 30% of the days and wet soils on 70%.

Southern Brazil has had a well-distributed rainfall regime over the years, as observed in the precipitation data obtained in this study (Figure 3f). Nonetheless, the accumulated precipitation of 1817.3 mm (from 3 April 2020 to 30 September 2021) was lower than the climatological average for the region (2700 mm). During this period, the La Niña phenomenon occurred with weak/moderate intensity, leading to lower precipitation in the region (NOAA, 2022); the highest daily precipitation was on 28 January 2021 (summer), with 95 mm.

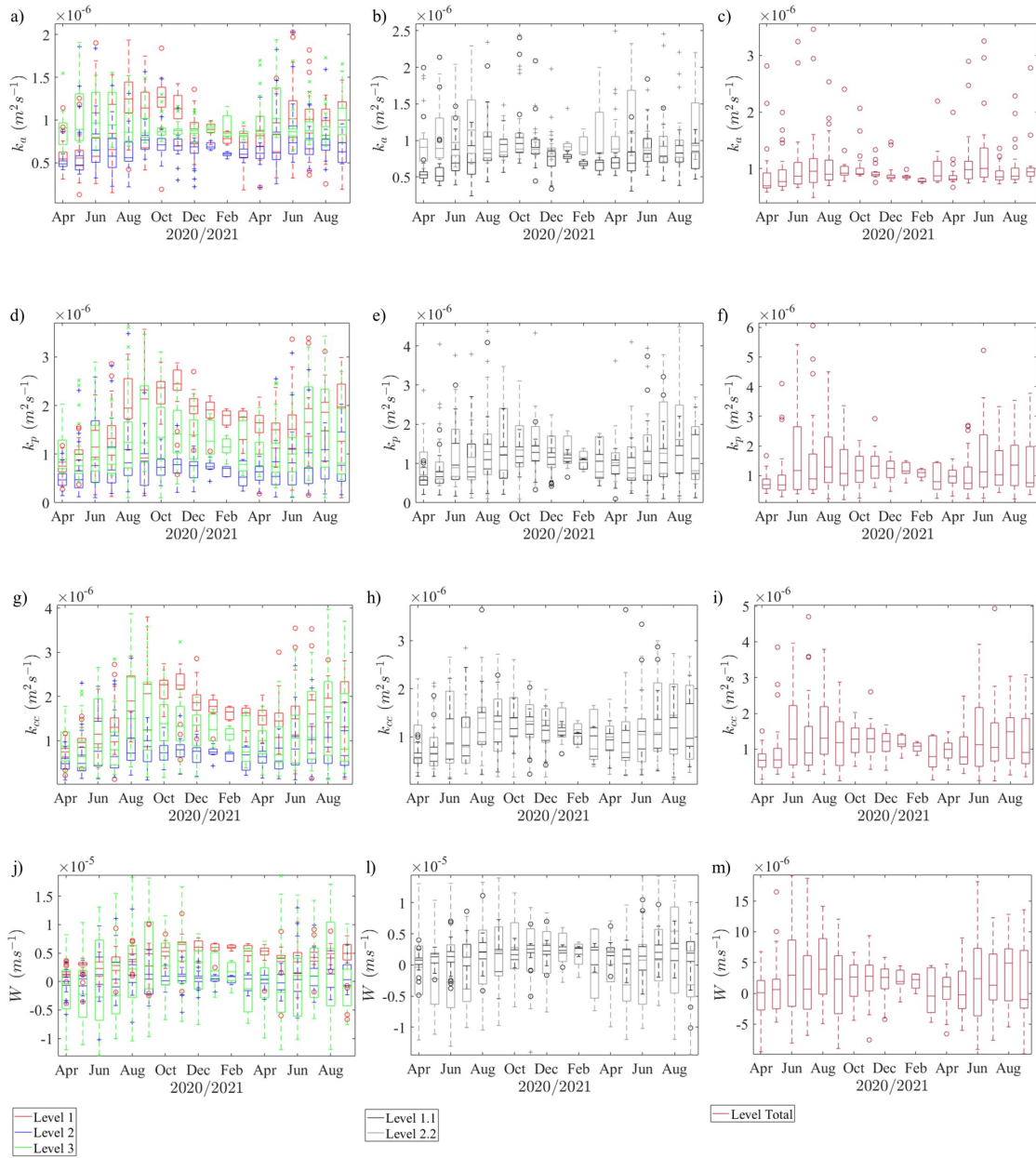
3.2 | Soil thermal properties

The temporal variations in soil thermal diffusivity (k , $\text{m}^2 \text{s}^{-1}$) for the amplitude (k_a), phase shift (k_p), and conduction-convection (k_{cc}) methods for different soil levels obtained by Analyses 1, 2 and 3 are shown in Figure 4. We can observe that k tends to have an inverse seasonal variation with the soil temperature (T_s) at all analyzed levels and methods (Figure 3a). In general, the lowest daily k values occur in periods with higher T_s (December–April), while the highest k values occur in periods with lower T_s and higher θ (Figure 3e).

The minimum, mean, and maximum values of k calculated for Analyses 1, 2 and 3 are listed in Table 1. The mean k values were higher with increasing depth of the levels in Analyses 1 and 2 (Table 1) and directly related to the increased soil moisture (Table 4). The most significant variations in k occurred in Analysis 1 (Figure 4) for both methods, from the shallowest to the deepest level, showing that soil thermal diffusivity is vertically heterogeneous. We can also observe that the k_p and k_{cc} values are higher and similar to those obtained by k_a (Figure 4 and Table 1). These results are consistent because the k_p and k_{cc} values depend mainly on the phase of the soil temperature (i.e., $\phi_1 - \phi_2$ of Eq. (7)), while k_a estimates mainly depend on the amplitude.

If one only analyzes the conduction process, the thermal diffusivity determined by the phase shift method must correspond to the one determined by the amplitude method. However, this is not the case because the upward or downward effects of water flow are reflected in lower temperature amplitudes, which may cause the values determined by the phase shift method to be higher or lower than those determined by the amplitude method (Liu et al., 2019). Therefore, the discrepancy between the phase and amplitude methods may be caused by water movement or convection heat transfer (Liu et al., 2019). The conduction-convection method showed the highest values compared to the other methods (Table 1); the same result was also found by An et al. (2016), who estimated soil thermal diffusivity for different depths and environmental conditions in a semi-arid region, reporting values ranging from 0.75×10^{-6} to $1.20 \times 10^{-6} \text{ m}^2 \text{ s}^{-1}$. Otunla and Oladiran (2013) estimated k for sandy clay soil (loamy sand) using different methods and obtained values between 0.25×10^{-6} and $0.84 \times 10^{-6} \text{ m}^2 \text{ s}^{-1}$. Wang et al. (2010) demonstrated mean k values of $0.20 \times 10^{-6} \text{ m}^2 \text{ s}^{-1}$ for the amplitude method and $0.42 \times 10^{-6} \text{ m}^2 \text{ s}^{-1}$ for the phase shift method using 7-day data in a medium clay soil in China. Considering the results from the different authors, the values estimated in this study are within the range of thermal diffusivity for the soil type of the experimental site, as they range from 0.68×10^{-6} to $1.65 \times 10^{-6} \text{ m}^2 \text{ s}^{-1}$ for the different methods and different sampling depths, confirming the validity of the methods for the different levels.

FIGURE 4 – Estimated soil thermal diffusivity: (a, b, c) by the amplitude method (k_a); (d, e, f) phase shift method (k_p); (g, h, i) conduction-convection method (k_{cc}); (j, l, m) liquid water flux density (W), for Analysis 1 with Level 1, 2 and 3 in the left panels; Analysis 2 with Levels 1.1 and 2.2 in the middle panels; Analysis 3 with Total Level in the right panels.



Liquid water flux density values (W , $m^2 s^{-1}$) varied between levels and time (Figure 4 and Table 2). In general, W did not show a clearly defined seasonality. However, for Level 1, the W variation showed a slight trend with the

TABLE 1 – Minimum, mean, and maximum values of soil thermal diffusivity (k , $\text{m}^2 \text{s}^{-1}$) estimated by the amplitude (k_a), phase shift (k_p), and conduction-convection (k_{cc}) methods for Analyses 1, 2 and 3.

Analysis	Level	k_a (10^{-6})			k_p (10^{-6})			k_{cc} (10^{-6})		
		min	mean	max	min	mean	max	min	mean	max
1	1	0.14	0.68	2.03	0.10	0.74	3.86	0.12	0.76	3.80
	2	0.16	0.92	2.02	0.10	1.24	3.48	0.11	1.33	2.86
	3	0.61	1.02	1.94	0.10	1.57	3.49	0.11	1.65	3.97
2	1.1	0.24	0.79	2.40	0.10	1.02	4.08	0.13	1.04	2.87
	2.2	0.62	1.05	2.45	0.10	1.14	4.37	0.16	1.34	3.00
3	Total	0.48	1.07	3.46	0.24	1.22	6.05	0.11	1.31	4.70

seasonal variation of T_s (Figure 3a). The calculated values of the W for Analysis 3 (Figure 4) tended to decrease during the periods with the highest values of T_s , leading to lower θ (Figure 3e). This fact could be related to greater water evaporation from the soil surface (Wang et al., 2010). Gao et al. (2008a) reported that under evaporation conditions, there is an upward flow of water (liquid and vapor) that responds to the progressive drying of the surface. According to Wang et al. (2010), the net flow of water causes a net flow of convection heat. Therefore, heat transfer must include a vertical convective heat transfer component. We can also observe that W represents $\sim 70\%$ of the data with a downward flow for the winter season (June–September) (Figure 4m), periods with higher θ . The minimum, mean, and maximum values of W for the analyses are listed in Table 2. The minimum W value is $-1.44 \times 10^{-5} \text{ m}^2 \text{ s}^{-1}$ (upward flow) in Analysis 2 (Level 2.2), and the maximum value is $1.92 \times 10^{-5} \text{ m}^2 \text{ s}^{-1}$ (downward flow) in Analysis 1 (Level 3). The mean W value for the shallowest ground levels were less than $0.1 \times 10^{-5} \text{ m}^2 \text{ s}^{-1}$.

TABLE 2 – Minimum, average and maximum values of liquid water flux density (W , $\text{m}^2 \text{ s}^{-1}$), average values of the vertical gradient of soil thermal diffusivity ($\frac{\partial k}{\partial z}$, $\text{m}^2 \text{ s}^{-1}$) and the mean value of the convective term ($\frac{c_w}{c_v} \eta \theta$, m s^{-1}) for Analysis 1, 2 and 3.

Analysis	Level	$W(10^{-5})$			$\frac{\partial k}{\partial z}(10^{-5})$	$\frac{c_w}{c_v} \eta \theta$
		min	mean	max	mean	mean
1	1	-0.66	0.11	1.19	2.50	2.40
	2	-1.02	0.40	1.30	8.92	8.52
	3	-1.40	0.53	1.92	10.03	9.50
2	1.1	-1.01	0.16	1.11	6.41	6.25
	2.2	-1.44	0.52	1.43	10.05	9.53
3	Total	-0.98	0.19	1.91	8.26	8.07

In Analysis 1 and 2, as the depth of the layer increases, the water flux resulting from the convective process increases due to the downward movement of water (Table 2), so the water infiltration rate increases. The most significant variation in the vertical gradient of soil thermal diffusivity ($\frac{\partial k}{\partial z}$) was found for Level 3 and Level 2.2 in Analyses

1 and 2, respectively (Table 2).

The average values of soil thermal conductivity (λ , $\text{W m}^{-1}\text{K}^{-1}$) for all methods (λ_a , λ_p and λ_{cc}) and analyses performed in this study were very similar (Table 3). λ ranged from 1.11 to 1.70 $\text{W m}^{-1}\text{K}^{-1}$ for both methods, lower in near-surface layers and higher in deeper levels. In Analysis 2, the results were about 30% lower when comparing both levels and methods, showing that λ varies with depth. These data are related to θ being higher at greater depths (Figure 3e). For Total Level, the conduction-convection method showed the lowest value of λ compared to the other methods (amplitude and phase shift) (Table 3). Lu et al. (2014), analysed 17 different soil types and found λ values ranging from 0.2 to 2.3 $\text{W m}^{-1}\text{K}^{-1}$. The authors report that λ not only varies for different soil types, but this variation can also occur for the same soil type, which could be related to soil moisture and density. Similar results were found in this study for the soil profile investigated at the SMA site.

TABLE 3 – Mean values of the thermal conductivity and thermal capacity of the soil according to the amplitude method (λ_a , $\text{W m}^{-1}\text{K}^{-1}$; c_{va} , $\text{J m}^{-3}\text{K}^{-1}$), phase shift method (λ_p , $\text{W m}^{-1}\text{K}^{-1}$; c_{vp} , $\text{J m}^{-3}\text{K}^{-1}$) and conduction-convection method (λ_{cc} , $\text{W m}^{-1}\text{K}^{-1}$; c_{vcc} , $\text{J m}^{-3}\text{K}^{-1}$) for Analyses 1, 2 and 3.

Analysis	Level	λ_a	c_{va} (10^6)	λ_p	c_{vp} (10^6)	λ_{cc}	c_{vcc} (10^6)
1	1	1.14±0.36	1.67	1.15±0.36	1.55	1.18±0.36	1.55
	2	1.17±0.68	1.27	1.17±0.68	0.94	1.22±0.68	0.91
	3	1.19±0.70	1.16	1.19±0.70	0.70	1.23±0.70	0.74
2	1.1	1.11±0.54	1.40	1.11±0.54	1.10	1.13±0.54	1.08
	2.2	1.62±0.64	1.54	1.62±0.64	1.42	1.65±0.64	1.23
3	Total	1.70±0.74	1.59	1.70±0.74	1.39	1.47±0.74	1.12

Soil heat capacity values (c_v , $\text{J m}^{-3}\text{K}^{-1}$) ranged from 0.70×10^6 to 1.67×10^6 $\text{J m}^{-3}\text{K}^{-1}$ (Table 3). c_v increased linearly with increasing soil height in Analysis 2. This may be related to c_v providing the energy needed to increase T_s . Roxy et al. (2014) analyzed the variation of c_v with soil water content for one year's data in India and found that increased θ leads to higher c_v values and, thus, there is a linear relationship between these variables.

3.3 | Soil Thermal Properties as a Function of Soil Moisture

3.3.1 | Soil thermal diffusivity and liquid water flux density

The variations of soil thermal diffusivity (k , m^2s^{-1}) determined by the amplitude (k_a), phase shift (k_p), and conduction-convection (k_{cc}) methods and liquid water flux density (W , m^2s^{-1}) as a function of soil moisture (θ) for dry (D) and wet (W) soil periods are shown in Figures 5, 6 and 7 and Table 4. The parameters k and W increased at higher θ for both levels analyzed. We also observed an increase in the variability of thermal diffusivity at lower depths, especially for periods with wet soil. This could be related to the increasing W values and deeper water movement in the subsurface due to higher η ; similar findings were found by Wang et al. (2010). Another possible reason is that k and W depend not only on θ but also on other factors, such as the infiltration rate of the fluid, as suggested by Gao et al. (2003). Verhoef et al. (1996) and Gao (2005) reported that k values increase with soil moisture. According to Gao (2005), this behavior is also confirmed for W . All methods analyzed in this study indicate that the highest value of k does not occur at maximum θ (Figures 5-7), but when θ is between 0.15 and 0.23 m^3m^{-3} , k and W do not change for a small

variation in the values of θ . This finding is similar to other studies (Gao, 2005; Gao et al., 2008a; Wang et al., 2010; Hu et al., 2016), which reported that k increases as the dry soil (D) ($\theta < 0.19 \text{ m}^3 \text{ m}^{-3}$) becomes wetter, albeit approaches a constant value or even decreases as the soil continues to increase in θ . However, for soils subject to evaporative drying, k tends to increase from the surface downwards, meaning the lowest k value is at the dry surface and higher k values occur at the wet surface (Table 4).

FIGURE 5 – Daily soil thermal diffusivity estimated as a function of soil moisture (θ) for dry (D) and wet (W) periods: a) by amplitude (k_a), b) phase shift (k_p), and c) conduction-convection (k_{cc}) methods for Analysis 1 with Levels 1, 2 and 3. d) Daily liquid water flow density (W) estimated as a function of θ for Analysis 1 with Level 1, 2 and 3. The dashed line represents the separation of D and W.

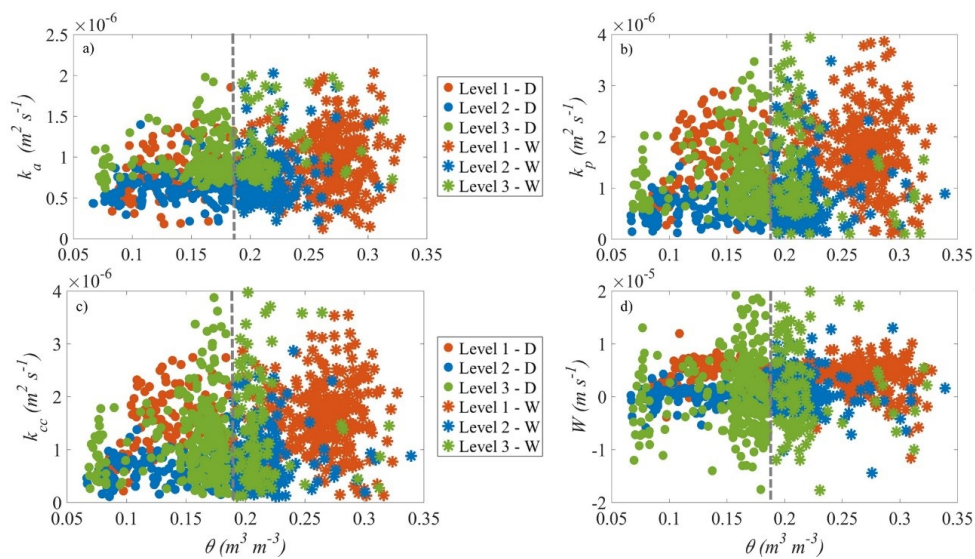


TABLE 4 – Mean values of soil thermal diffusivity (k , $\text{m}^2 \text{ s}^{-1}$) estimated by the amplitude (k_a), phase shift (k_p), and conduction-convection (k_{cc}) method in dry (D) and wet soil periods (W) for Analyses 1, 2 and 3.

Analysis	Level	k_a (10^{-6})		k_p (10^{-6})		k_{cc} (10^{-6})		W (10^{-5})	
		D	W	D	W	D	W	D	W
1	1	0.63	0.71	0.66	0.81	0.65	0.85	0.33	0.44
	2	0.81	0.97	1.21	1.31	1.30	1.41	0.38	0.68
	3	0.97	1.02	1.48	1.62	1.57	1.68	0.97	1.51
2	1.1	0.73	0.84	0.94	1.09	0.94	1.12	0.49	0.59
	2.2	1.02	1.09	1.13	1.16	1.29	1.42	1.62	1.68
3	Total	0.89	1.09	1.08	1.33	1.12	1.41	1.55	2.28

FIGURE 6 – Daily soil thermal diffusivity estimated as a function of soil moisture (θ) for dry (D) and wet (W) periods: a) by amplitude (k_a), b) phase shift (k_p), and c) conduction-convection (k_{cc}) methods for Analysis 2 with Levels 1.1 and 2.2. d) Daily liquid water flow density (W) estimated as a function of θ for Analysis 2 with Levels 1.1 and 2.2. The dashed line represents the separation of D and W.

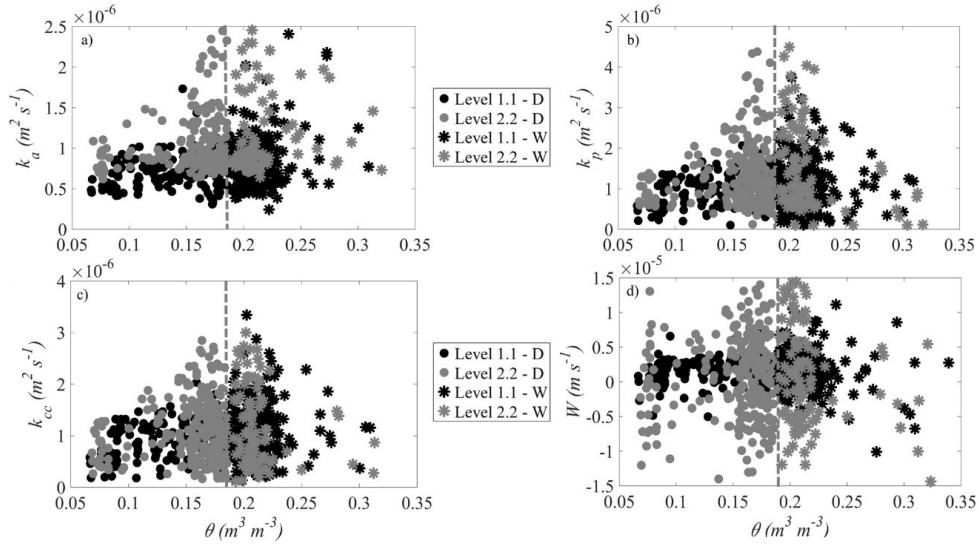
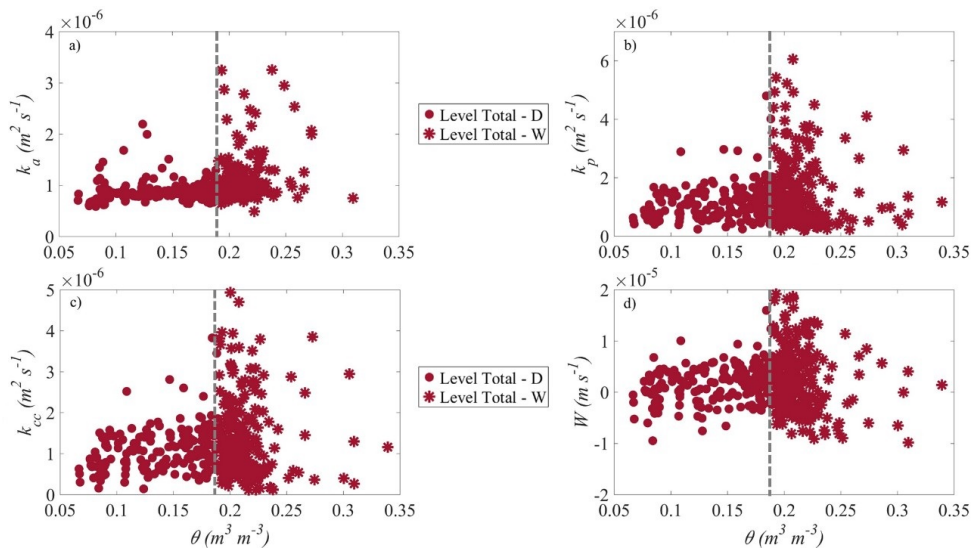


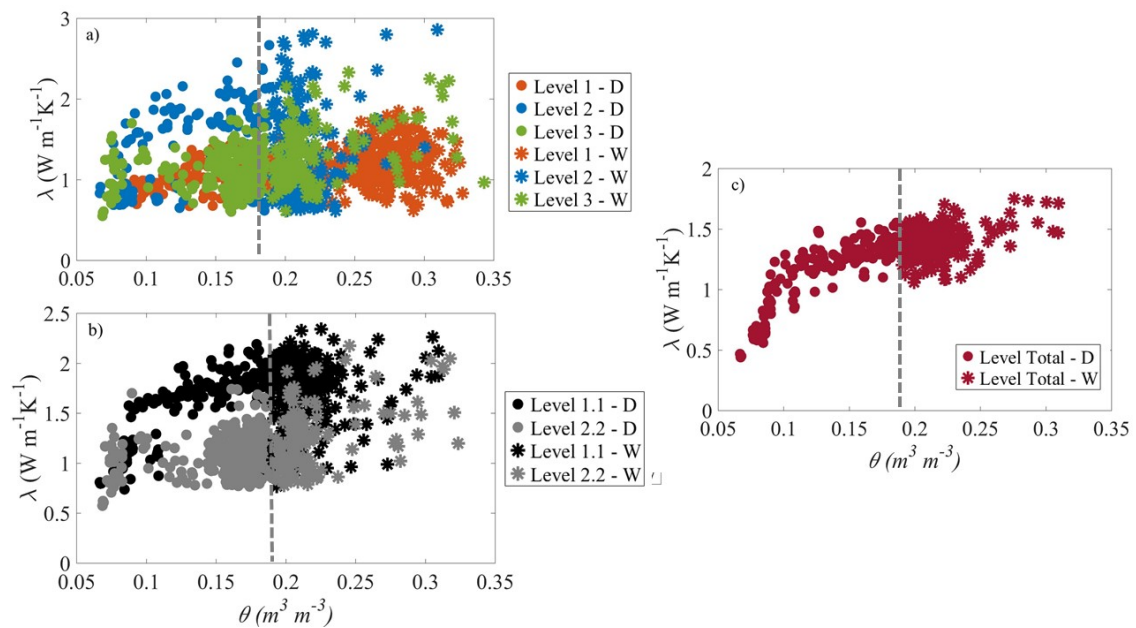
FIGURE 7 – Daily soil thermal diffusivity estimated as a function of soil moisture (θ) for dry (D) and wet (W) periods: a) by amplitude (k_a), b) phase shift (k_p), and c) conduction-convection (k_{cc}) methods for Analysis 3 with Total Level. d) Daily liquid water flow density (W) estimated as a function of θ for Analysis 3 with Total Level. The dashed line represents the separation of D and W.



3.3.2 | Soil Thermal Conductivity

The values of soil thermal conductivity (λ , $\text{W m}^{-1}\text{K}^{-1}$) for periods of dry (D) and wet (W) soil obtained by the conduction-convection method for the different analyses as a function of θ are shown in Figure 8. The λ increases at higher θ on a daily scale and with large variability for both values determined by Analyses 1, 2 and 3. The largest variability of λ occurs in Analysis 1 for Levels 2 and 3 at θ_{17} and θ_{34} , respectively. In all analyzed levels, λ increased rapidly when θ had low values (dry soil), especially Analyses 2 and 3. Nevertheless, for θ above $0.19 \text{ m}^3 \text{ m}^{-3}$, λ values showed a nearly constant behaviour. Roxy et al. (2014) analyzed the variation of λ as a function of θ and found a threshold (peak) near 22% ($0.22 \text{ m}^3 \text{ m}^{-3}$) of the water content in the soil. This can be explained by the fact that heat conduction in dry porous media occurs almost exclusively through the contact zones between solid particles (Sepaskhah and Boersma, 1979). As θ increases, water fills the spaces previously occupied by air and forms water bridges between solid soil particles. As a result, λ begins to increase rapidly due to greater contact between particles (Sepaskhah and Boersma, 1979; Tarnawski and Gori, 2002; Ewing and Horton, 2007; Zhao et al., 2019). This process continues until most of the solid particles are bonded together. Thereafter, as θ increases, the increase in λ depends largely on the displacement of the air by the water and, as a result, the increase in λ slows down and tends to become a constant, as shown more clearly in Figure 8 for Analysis 3. The results presented herein are similar to those demonstrated elsewhere (Usovicz et al., 2016; Zaibon et al., 2019; Zhao et al., 2019; Zimmer et al., 2020).

FIGURE 8 – Daily soil thermal conductivity estimated for dry (D) and wet (W) soil periods using the convection conduction method as a function of soil moisture: a) for Analysis 1 with Levels 1, 2, and 3, b) Analysis 2 with Levels 1.1 and 2.2, and c) Analysis 3 with Total Level of θ_{17} .



3.4 | Validation: Modeling soil temperature

The statistical indices for T_s determined experimentally and estimated from the previously determined k and W values (subsection 2.4) are listed in Table 5. We generally have a good estimate of T_s compared to the experimental data, with R^2 ranging from 0.79 to 0.99. The lowest R^2 was found for the T_{s34} estimate for Validation 3 using k_d for Total Level (Table 1). The best results for the T_s estimates were obtained using the conduction-convection method, which had the highest R^2 values and the lowest $RMSE$, followed by the phase or amplitude shift method. Gao et al. (2008b) recommended the conduction-convection method as the most accurate form of estimating soil temperature. This fact is related to the conduction-convection method using k and W values in its formulation and also considers the vertical heterogeneity of k .

The amplitude method had the poorest statistical indices because its formulation only considered the daily thermal amplitude (Eq.6), a parameter subject to greater amplitude variations over time, whereas, in the phase shift method, k is calculated from the phase of T_s (Eq.7), which, similar to the conduction-convection method, does not show large variations. Hu et al. (2016) estimated T_s at a depth of 0.10 m using the conduction method and found a value of 0.94 for R^2 , a similar result to this study for Validation 1 and 2 for T_{s9} . Wang et al. (2010) estimated T_s to be 0.10 m and found equal values for R^2 for the amplitude and phase shift methods (0.98), which is very close to the result for the conduction-convection method with $R^2 = 0.99$. In contrast to Wang et al. (2010), the conduction-convection heat transfer methods in our study had an average difference of $\sim 10\%$ in their statistical indices, except for Validation 1 (Table 5).

TABLE 5 – Statistical indices for validation against experimental data of soil temperature (T_s) and soil temperature modelled using Eq.(5), the amplitude (AM) and phase shift (PSM) method and Eq.(11) for the conduction-convection method (CCM).

Validation	Sub-Level	AM		PSM		CCM	
		R^2	RMSE ($^{\circ}\text{C}$)	R^2	RMSE ($^{\circ}\text{C}$)	R^2	RMSE ($^{\circ}\text{C}$)
1	T_{s9}	0.93	1.22	0.94	1.13	0.94	1.09
	T_{s17}	0.96	0.78	0.97	0.61	0.97	0.39
	T_{s34}	0.98	0.52	0.97	0.32	0.99	0.24
2	T_{s9}	0.89	1.51	0.93	1.22	0.94	1.10
	T_{s17}	0.88	1.53	0.92	1.21	0.97	0.61
	T_{s34}	0.97	0.62	0.98	0.52	0.99	0.26
3	T_{s9}	0.84	1.83	0.93	1.22	0.94	1.09
	T_{s17}	0.88	1.53	0.92	1.21	0.95	0.91
	T_{s34}	0.79	1.87	0.82	1.75	0.99	0.25

When analysing the T_s estimates of the levels, we found the lowest R^2 and the highest $RMSE$ near the surface, indicating worse statistical indices compared to lower levels. This could be related to the fact that larger temperature fluctuations occur at the surface during the day, and similar results were found by Holmes et al. (2008). In addition, vertical water flow may influence T_s , as there is greater influence on the diurnal variability of θ in near-surface layers.

4 | CONCLUSION

The amplitude of soil temperature fluctuations and the amount of water in the soil play a crucial role in the thermal behavior of the soil. The complexity of heat transfer processes in heterogeneous porous media hinders quantitatively evaluating the thermal properties, especially when conduction and convection processes are assumed to occur simultaneously.

In this study, we used heat transfer models by conduction and convection to estimate the thermal properties of soil in an area of the Brazilian Pampa biome. Using a time series of experimental data on soil temperature, soil heat flux, and soil moisture measured at different depths, we evaluated the influence of temperature gradient and moisture on estimating thermal properties. The variability of T_s and G showed a seasonal behavior with higher values during the spring/summer season. For T_{s17} , the highest amplitudes of variation were found during the day. In general, the daily mean values of G were negative during the autumn/winter seasons, indicating that the subsurface warms the surface. The θ data showed a large variability during the year for all analyzed levels, with 70% of the period classified as wet soil.

For all methods and soil levels, k showed an inverse seasonal variation of T_s . Analysis 1 showed the greatest temporal variation in k for all methods, from surface to subsoil (Level 1 to 3), indicating that k is vertically heterogeneous. The highest average estimates were observed for k_{cc} , about 6% higher than k_p and about 24% higher than k_a . The k values increased with the depth of the levels, which is directly related to the increase in θ or the change in soil composition. Nevertheless, the analyzed values are practically only found in one of the soil horizons (or layers), so only the surface layer could be affected by the more significant presence of organic matter.

The parameter W did not show a clear seasonality but decreased in periods with higher T_s values (Analysis 3). Another fact is that increasing W values increased the variability of k with depth. Both facts are related to a higher water evaporation rate from the soil surface, where there is an upward flow of water responding to a progressive increase in soil drying. In addition, the W parameter may also depend on other factors, such as the infiltration rate of liquids (η).

In general, λ values were highly similar across methods and varied only between levels, confirming the vertical heterogeneity of this property. We also observed that λ increases exponentially for low values of θ (dry period), while thermal diffusivity shows a behavior with greater variability for values corresponding to wet periods. We observed that the values increase linearly with increasing θ and soil depth for c_v .

Finally, the conduction-convection method provided the most accurate results for the estimates of T_s because it uses k and W values in its formulation (i.e., it considers the vertical heterogeneity of the soil and density of the liquid water flux. The amplitude method received the worst statistical indices in the validations for T_s , as it only considers the temperature amplitude. For all methods, the least accurate estimates for T_s occurred near the surface due to the larger differences in daily thermal amplitudes and the larger influence of daily θ variability. The thermal diffusivity of the soil controls the speed at which temperature waves travel through the soil and the depth of thermal influence of a surface.

Therefore, the study characterized the thermal dynamics of the soil in an area of native vegetation in the Brazilian Pampa biome. From the processes of heat transfer by conduction and convection, estimates of the thermal properties of the soil were obtained, which are fundamental for modeling the energy balance on the surface. The results obtained can thus contribute to the understanding of the biome and help research for the conservation of natural areas that are of economic and ecological importance for southern Brazil. In addition, it is possible to develop practices to protect ecosystems through an improved representation of the thermal dynamics of the soil in environmental models.

References

- Alkhaier, F., Flerchinger, G. and Su, Z. (2012) Shallow groundwater effect on land surface temperature and surface energy balance under bare soil conditions: modeling and description. *Hydrology and Earth System Sciences*, **16**, 1817–1831.
- Allen, R. G., Pereira, L. S., Raes, D., Smith, M. et al. (1998) Crop evapotranspiration-guidelines for computing crop water requirements-fao irrigation and drainage paper 56. *FAO, Rome*, **300**, D05109.
- An, K., Wang, W., Zhao, Y., Huang, W., Chen, L., Zhang, Z., Wang, Q. and Li, W. (2016) Estimation from soil temperature of soil thermal diffusivity and heat flux in sub-surface layers. *Boundary-layer meteorology*, **158**, 473–488.
- Andry, H., Yamamoto, T., Irie, T., Moritani, S., Inoue, M. and Fujiyama, H. (2009) Water retention, hydraulic conductivity of hydrophilic polymers in sandy soil as affected by temperature and water quality. *Journal of Hydrology*, **373**, 177–183.
- Campbell, G. (1985) Soil physics with basic; transport models for soil-plant systems. *Developments in Soil Science (Netherlands)*.
- Campbell, G. S. and Norman, J. M. (1998) Radiation fluxes in natural environments. In *An introduction to environmental biophysics*, 167–184. Springer.
- Carslaw, H. S. and Jaeger, J. C. (1959) Conduction of heat in solids. *Oxford: Clarendon Press*, 1959, 2nd ed.
- Clarke, B. G., Agab, A. and Nicholson, D. (2008) Model specification to determine thermal conductivity of soils. *Proceedings of the Institution of Civil Engineers-Geotechnical Engineering*, **161**, 161–168.
- Costello, T. and Horst, W. (1991) Soil temperature sensor installation: a comparison of two methods. *Transactions of the ASAE*, **34**, 904–0908.
- De Vries, D. and Peck, A. (1958) On the cylindrical probe method of measuring thermal conductivity with special reference to soils. i. extension of theory and discussion of probe characteristics. *Australian Journal of Physics*, **11**, 255–271.
- Evet, S. R., Agam, N., Kustas, W. P., Colaizzi, P. D. and Schwartz, R. C. (2012) Soil profile method for soil thermal diffusivity, conductivity and heat flux: Comparison to soil heat flux plates. *Advances in Water Resources*, **50**, 41–54.
- Ewing, R. P. and Horton, R. (2007) Thermal conductivity of a cubic lattice of spheres with capillary bridges. *Journal of Physics D: Applied Physics*, **40**, 4959.
- Gao, Z. (2005) Determination of soil heat flux in a tibetan short-grass prairie. *Boundary-Layer Meteorology*, **114**, 165–178.
- Gao, Z., Fan, X. and Bian, L. (2003) An analytical solution to one-dimensional thermal conduction-convection in soil. *Soil Science*, **168**, 99–107.
- Gao, Z., Horton, R., Wang, L., Liu, H. and Wen, J. (2008a) An improved force-restore method for soil temperature prediction. *European Journal of Soil Science*, **59**, 972–981.
- Gao, Z., Lenschow, D. H., Horton, R., Zhou, M., Wang, L. and Wen, J. (2008b) Comparison of two soil temperature algorithms for a bare ground site on the loess plateau in china. *Journal of Geophysical Research: Atmospheres*, **113**.
- Gao, Z., Tong, B., Horton, R., Mamtimin, A., Li, Y. and Wang, L. (2017) Determination of desert soil apparent thermal diffusivity using a conduction-convection algorithm. *Journal of Geophysical Research: Atmospheres*, **122**, 9569–9578.
- Graham, P. (2010) Bookham grazing demonstration results. *Department of Primary Industries: Yass, NSW*.
- Guntiñas, M. E., Leirós, M., Trasar-Cepeda, C. and Gil-Sotres, F. (2012) Effects of moisture and temperature on net soil nitrogen mineralization: A laboratory study. *European Journal of Soil Biology*, **48**, 73–80.
- Holmes, T., Owe, M., De Jeu, R. and Kooi, H. (2008) Estimating the soil temperature profile from a single depth observation: A simple empirical heatflow solution. *Water Resources Research*, **44**.

- Horton, R., Wierenga, P. and Nielsen, D. (1983) Evaluation of methods for determining the apparent thermal diffusivity of soil near the surface. *Soil Science Society of America Journal*, **47**, 25–32.
- Hu, G., Zhao, L., Wu, X., Li, R., Wu, T., Xie, C., Qiao, Y., Shi, J. and Cheng, G. (2016) An analytical model for estimating soil temperature profiles on the qinghai-tibet plateau of china. *Journal of Arid Land*, **8**, 232–240.
- Johansen, O. (1975) Thermal conductivity of soils. *Tech. rep.*, Cold Regions Research and Engineering Lab Hanover NH.
- Liu, H., Wang, B. and Fu, C. (2008) Relationships between surface albedo, soil thermal parameters and soil moisture in the semi-arid area of tongyu, northeastern china. *Advances in Atmospheric Sciences*, **25**, 757–764.
- Liu, Q., Chen, S., Jiang, L., Wang, D., Yang, Z. and Chen, L. (2019) Determining thermal diffusivity using near-surface periodic temperature variations and its implications for tracing groundwater movement at the eastern margin of the tibetan plateau. *Hydrological Processes*, **33**, 1276–1286.
- Lu, S., Lu, Y., Peng, W., Ju, Z. and Ren, T. (2019) A generalized relationship between thermal conductivity and matric suction of soils. *Geoderma*, **337**, 491–497.
- Lu, S., Ren, T., Gong, Y. and Horton, R. (2007) An improved model for predicting soil thermal conductivity from water content at room temperature. *Soil Science Society of America Journal*, **71**, 8–14.
- Lu, Y., Lu, S., Horton, R. and Ren, T. (2014) An empirical model for estimating soil thermal conductivity from texture, water content, and bulk density. *Soil Science Society of America Journal*, **78**, 1859–1868.
- Mellander, P.-E., Bishop, K. and Lundmark, T. (2004) The influence of soil temperature on transpiration: a plot scale manipulation in a young scots pine stand. *Forest Ecology and Management*, **195**, 15–28.
- Nerpin, S. and Chudnovskii, A. (1967) Physics of the soil: Israel program for scientific translations.
- Onwuka, M. and Nwangwu, B. (2016) Roles of biochar produced from animal and plant wastes on okra (*abelmoschus esculenta*) growth in umudike area of abia state, nigeria. *Journal of Agriculture and Sustainability*, **9**.
- Otunla, T. A. and Oladiran, E. O. (2013) Evaluation of soil thermal diffusivity algorithms at two equatorial sites in west africa. *Annals of Geophysics*, **56**, 0101.
- Peel, M. C., Finlayson, B. L. and McMahon, T. A. (2007) Updated world map of the köppen-geiger climate classification. *Hydrology and earth system sciences discussions*, **4**, 439–473.
- Peng, S., Piao, S., Wang, T., Sun, J. and Shen, Z. (2009) Temperature sensitivity of soil respiration in different ecosystems in china. *Soil Biology and Biochemistry*, **41**, 1008–1014.
- Rahi, G. and Jensen, R. (1975) Effect of temperature on soil-water diffusivity. *Geoderma*, **14**, 115–124.
- Romio, L. C., Roberti, D. R., Buligon, L., Zimmer, T. and Degrazia, G. A. (2019) A numerical model to estimate the soil thermal conductivity using field experimental data. *Applied Sciences*, **9**, 4799.
- Roxy, M., Sumithranand, V. and Renuka, G. (2014) Estimation of soil moisture and its effect on soil thermal characteristics at astronomical observatory, thiruvananthapuram, south kerala. *Journal of earth system science*, **123**, 1793–1807.
- Rubert, G. C., Roberti, D. R., Pereira, L. S., Quadros, F. L., Campos Velho, H. F. d. and Leal de Moraes, O. L. (2018) Evapotranspiration of the brazilian pampa biome: Seasonality and influential factors. *Water*, **10**, 1864.
- Seemann, J. (1979) Measuring technology. In *Agrometeorology*, 40–45. Springer.
- Sepaskhah, A. and Boersma, L. (1979) Thermal conductivity of soils as a function of temperature and water content. *Soil Science Society of America Journal*, **43**, 439–444.

- de Silans, A. M. P., Monteny, B. A. and Lhomme, J. P. (1996) Apparent soil thermal diffusivity, a case study: Hapex-sahel experiment. *Agricultural and Forest Meteorology*, **81**, 201–216.
- Tarnawski, V. and Gori, F. (2002) Enhancement of the cubic cell soil thermal conductivity model. *International journal of energy research*, **26**, 143–157.
- Uslowicz, B., Lipiec, J., Łukowski, M., Marczewski, W. and Uslowicz, J. (2016) The effect of biochar application on thermal properties and albedo of loess soil under grassland and fallow. *Soil and Tillage Research*, **164**, 45–51.
- Verhoef, A., van den Hurk, B. J., Jacobs, A. F. and Heusinkveld, B. G. (1996) Thermal soil properties for vineyard (efeda-i) and savanna (hapex-sahel) sites. *Agricultural and Forest Meteorology*, **78**, 1–18.
- Wang, C., Wan, S., Xing, X., Zhang, L. and Han, X. (2006) Temperature and soil moisture interactively affected soil net n mineralization in temperate grassland in northern china. *Soil Biology and Biochemistry*, **38**, 1101–1110.
- Wang, L., Gao, Z. and Horton, R. (2010) Comparison of six algorithms to determine the soil apparent thermal diffusivity at a site in the loess plateau of china. *Soil science*, **175**, 51–60.
- Wang, L., Gao, Z., Horton, R., Lenschow, D. H., Meng, K. and Jaynes, D. B. (2012a) An analytical solution to the one-dimensional heat conduction–convection equation in soil.
- Wang, W., Dai, Z., Li, J. and Zhou, L. (2012b) A hybrid laplace transform finite analytic method for solving transport problems with large pecllet and courant numbers. *Computers & geosciences*, **49**, 182–189.
- Wierenga, P., Nielsen, D. and Hagan, R. (1969) Thermal properties of a soil based upon field and laboratory measurements. *Soil science society of America Journal*, **33**, 354–360.
- Wu, S. H., Jansson, P.-E. and Kolari, P. (2012) The role of air and soil temperature in the seasonality of photosynthesis and transpiration in a boreal scots pine ecosystem. *Agricultural and Forest Meteorology*, **156**, 85–103.
- Xie, X., Lu, Y., Ren, T. and Horton, R. (2019) Soil temperature estimation with the harmonic method is affected by thermal diffusivity parameterization. *Geoderma*, **353**, 97–103.
- Xu, X., Luo, Y. and Zhou, J. (2012) Carbon quality and the temperature sensitivity of soil organic carbon decomposition in a tallgrass prairie. *Soil Biology and Biochemistry*, **50**, 142–148.
- Zaibon, S., Anderson, S. H., Veum, K. S. and Haruna, S. I. (2019) Soil thermal properties affected by topsoil thickness in switchgrass and row crop management systems. *Geoderma*, **350**, 93–100.
- Zhao, Y., Si, B., Zhang, Z., Li, M., He, H. and Hill, R. L. (2019) A new thermal conductivity model for sandy and peat soils. *Agricultural and Forest Meteorology*, **274**, 95–105.
- Zimmer, T., Buligon, L., de Arruda Souza, V., Romio, L. C. and Roberti, D. R. (2020) Influence of clearness index and soil moisture in the soil thermal dynamic in natural pasture in the brazilian pampa biome. *Geoderma*, **378**, 114582.

5 FINAL CONSIDERATIONS

The thermal regime of the soil and heat and moisture exchange between the surface and atmosphere play a key role in energy balances and weather and climate prediction models. Coupled models of heat and moisture transport in bare soils (NOVAK; BLACK, 1985; SILANS et al., 1989) or on vegetated surfaces (BRAUD et al., 1995; SMIRNOVA; BROWN; BENJAMIN, 1997) require information on soil temperature profiles and heat flux, which depend on soil thermal properties (thermal conductivity, thermal diffusivity, and volumetric heat capacity). In turn, these properties depend on soil moisture and soil composition and structure, which are coupled with soil vegetation and climatic conditions. Therefore, information on the thermal properties of the soil is crucial for detailed knowledge of heat transfer under different land cover conditions. It is also important for explaining the different chemical, physical, and biological processes in different types of ecosystems on Earth. In this regard, this study aimed to analyze the magnitude and dynamics of soil thermal properties throughout the year and under different climatic conditions at two experimental sites established in different locations of the Brazilian Pampa biome about 300 km apart: Pedras Altas and Santa Maria. The results were presented in two articles produced as part of a doctoral thesis.

The first article, entitled "*Influence of clearness index and soil moisture in the soil thermal dynamic in natural pasture in the Brazilian Pampa biome*" (Chapter 3), studied the influence of climatic conditions on soil thermal variables and properties in areas with natural vegetation in Pedras Altas and Santa Maria, considering two years of data from each site. The thermal properties of the soil were estimated using hybrid methods based on experimental data and analytical methods (the amplitude and phase-shift methods). The general heat transfer equation assumes that the thermal properties of the soil are independent of time and depth.

As shown in the results and underlined by various papers in the literature, soil moisture affects soil thermal parameters, which vary with time and depth. Hence, these results provide evidence for a new approach based on a hybrid model to account for the previously neglected physical processes, such as the convective effects of heat transfer in the soil.

With this background, the second article, entitled "*Estimation of soil thermal properties using conduction-convection heat transfer equations in the Brazilian Pampa biome*" (Chapter 4), presents the estimation of soil thermal properties and temperature using a new experimental setup based on the analytical solution of the conduction-convection heat transfer equation. The experimental data were obtained over one year and six months at the Santa Maria site. The results obtained shed more light on the thermal dynamics of the soil, considering the conductive and convective processes of heat transfer in the soil at different depths, as it was demonstrated that the thermal properties of the soil vary at

different levels and that there is vertical heterogeneity in the thermal properties of the soil as a function of soil moisture in dry and wet periods, and that the vertical movement of water in the soil has an influence on the thermal characterization of the soil. The results thus provide evidence that the process of heat convection also determines heat transfer in the soil.

BIBLIOGRAPHY

ACOSTA, R. et al. **Estimativas das interações biosfera-atmosfera em ecossistema de pastagem natural do bioma Pampa**. 2019. Tese (Doutorado) — Universidade Federal de Santa Maria, 2019.

ALKHAIER, F.; FLERCHINGER, G.; SU, Z. Shallow groundwater effect on land surface temperature and surface energy balance under bare soil conditions: modeling and description. **Hydrology and Earth System Sciences**, Copernicus GmbH, v. 16, n. 7, p. 1817–1831, 2012.

ALLEN, R. G. et al. Crop evapotranspiration-guidelines for computing crop water requirements-fao irrigation and drainage paper 56. **FAO, Rome**, v. 300, n. 9, p. D05109, 1998.

ALVALÁ, R. d. S. et al. Intradiurnal and seasonal variability of soil temperature, heat flux, soil moisture content, and thermal properties under forest and pasture in rondônia. **Journal of Geophysical Research: Atmospheres**, Wiley Online Library, v. 107, n. D20, 2002.

AN, K. et al. Estimation from soil temperature of soil thermal diffusivity and heat flux in sub-surface layers. **Boundary-layer meteorology**, Springer, v. 158, n. 3, p. 473–488, 2016.

AZEVEDO, L. **SABERES E PRÁTICAS TRADICIONAIS: uma análise do modo de apropriação da natureza pelos pecuaristas familiares da Serra do Sudeste/RS**. 2013. Tese (Doutorado) — Dissertação de mestrado. UFSM, 2013.

BARRIOS, M.; FRANCÉS, F. Spatial scale effect on the upper soil effective parameters of a distributed hydrological model. **Hydrological processes**, Wiley Online Library, v. 26, n. 7, p. 1022–1033, 2012.

BINKOWSKI, P. Conflitos ambientais e significados sociais em torno da expansão da silvicultura de eucalipto na "metade sul" do rio grande do sul. 2009.

BISHT, G. et al. Estimation of the net radiation using modis (moderate resolution imaging spectroradiometer) data for clear sky days. **Remote Sensing of Environment**, Elsevier, v. 97, n. 1, p. 52–67, 2005.

BOLDRINI, I. L. B. **Bioma Pampa: diversidade florística e fisionômica**. [S.l.]: Editora Pallotti, 2010.

BRAUD, I. et al. A simple soil-plant-atmosphere transfer model (sispat) development and field verification. **Journal of hydrology**, Elsevier, v. 166, n. 3-4, p. 213–250, 1995.

CAMPBELL, G. Soil physics with basic; transport models for soil-plant systems. **Developments in Soil Science (Netherlands)**, Elsevier, 1985.

CAMPBELL, K.; LONGWORTH, J. W. **Economía agrícola: fundamentos de agricultura moderna**. [S.l.], 1970.

CARSLAW, H. S.; JAEGER, J. C. Conduction of heat in solids. **Oxford: Clarendon Press, 1959, 2nd ed.**, 1959.

CHEN, H.; SHAO, M.; LI, Y. Soil desiccation in the loess plateau of china. **Geoderma**, Elsevier, v. 143, n. 1-2, p. 91–100, 2008.

CLARKE, B. G.; AGAB, A.; NICHOLSON, D. Model specification to determine thermal conductivity of soils. **Proceedings of the Institution of Civil Engineers-Geotechnical Engineering**, Thomas Telford Ltd, v. 161, n. 3, p. 161–168, 2008.

CÔTÉ, J.; KONRAD, J.-M. A generalized thermal conductivity model for soils and construction materials. **Canadian Geotechnical Journal**, NRC Research Press Ottawa, Canada, v. 42, n. 2, p. 443–458, 2005.

CULF, A. D.; FOKEN, T.; GASH, J. H. The energy balance closure problem. In: **Vegetation, water, humans and the climate**. [S.l.]: Springer, 2004. p. 159–166.

ECHER, M.; MARTINS, F.; PEREIRA, E. A importância dos dados de cobertura de nuvens e de sua variabilidade: Metodologias para aquisição de dados. **Revista Brasileira de Ensino de Física**, SciELO Brasil, v. 28, p. 341–352, 2006.

EVETT, S. R. et al. Soil profile method for soil thermal diffusivity, conductivity and heat flux: Comparison to soil heat flux plates. **Advances in Water Resources**, Elsevier, v. 50, p. 41–54, 2012.

FAROUKI, O. T. The thermal properties of soils in cold regions. **Cold Regions Science and Technology**, Elsevier, v. 5, n. 1, p. 67–75, 1981.

_____. Thermal properties of soils. Trans Tech Pub., Rockport, MA, 1986.

FOKEN, T. The energy balance closure problem: an overview. **Ecological Applications**, Wiley Online Library, v. 18, n. 6, p. 1351–1367, 2008.

GAO, Z. Determination of soil heat flux in a tibetan short-grass prairie. **Boundary-Layer Meteorology**, Springer, v. 114, n. 1, p. 165–178, 2005.

GAO, Z.; FAN, X.; BIAN, L. An analytical solution to one-dimensional thermal conduction-convection in soil. **Soil Science**, LWV, v. 168, n. 2, p. 99–107, 2003.

GAO, Z. et al. Determination of desert soil apparent thermal diffusivity using a conduction-convection algorithm. **Journal of Geophysical Research: Atmospheres**, Wiley Online Library, v. 122, n. 18, p. 9569–9578, 2017.

HEUSINKVELD, B. et al. Surface energy balance closure in an arid region: role of soil heat flux. **Agricultural and Forest Meteorology**, Elsevier, v. 122, n. 1, p. 21–37, 2004.

HORTON, R.; WIERENGA, P.; NIELSEN, D. Evaluation of methods for determining the apparent thermal diffusivity of soil near the surface. **Soil Science Society of America Journal**, Soil Science Society of America, v. 47, n. 1, p. 25–32, 1983.

IBGE. Mapa de vegetação do Brasil. **Instituto Brasileiro de Geografia e Estatística**, 2004.

IQBAL, M. An introduction to solar radiation. 1983. **Medium: X**, 1983.

JOHANSEN, O. **Thermal conductivity of soils**. [S.l.], 1975.

JR, J. A. S.; FRIEDL, M. A. Diurnal covariation in soil heat flux and net radiation. **Journal of Applied Meteorology**, v. 42, n. 6, p. 851–862, 2003.

KERSTEN, M. S. Thermal properties of soils. University of Minnesota, 1949.

KIMBALL, B. A. et al. Comparison of field-measured and calculated soil-heat fluxes. **Soil Science Society of America Journal**, Soil Science Society of America, v. 40, n. 1, p. 18–25, 1976.

KOJIMA, Y. et al. Bulk density effects on soil hydrologic and thermal characteristics: A numerical investigation. **Hydrological Processes**, Wiley Online Library, v. 32, n. 14, p. 2203–2216, 2018.

KUPLICH, T. M.; MOREIRA, A.; FONTANA, D. C. Série temporal de índice de vegetação sobre diferentes tipologias vegetais no rio grande do sul. **Revista Brasileira de Engenharia Agrícola e Ambiental**, SciELO Brasil, v. 17, p. 1116–1123, 2013.

KUSTAS, W. P.; DAUGHTRY, C. S. Estimation of the soil heat flux/net radiation ratio from spectral data. **Agricultural and Forest Meteorology**, Elsevier, v. 49, n. 3, p. 205–223, 1990.

LEUNING, R. Measurements of trace gas fluxes in the atmosphere using eddy covariance: Wpl corrections revisited. In: **Handbook of micrometeorology**. [S.l.]: Springer, 2004. p. 119–132.

LIU, Z. et al. Mechanisms of biochar effects on thermal properties of red soil in south china. **Geoderma**, Elsevier, v. 323, p. 41–51, 2018.

LU, S. et al. A generalized relationship between thermal conductivity and matric suction of soils. **Geoderma**, Elsevier, v. 337, p. 491–497, 2019.

_____. An improved model for predicting soil thermal conductivity from water content at room temperature. **Soil Science Society of America Journal**, Wiley Online Library, v. 71, n. 1, p. 8–14, 2007.

LU, Y. et al. An empirical model for estimating soil thermal conductivity from texture, water content, and bulk density. **Soil Science Society of America Journal**, Wiley Online Library, v. 78, n. 6, p. 1859–1868, 2014.

MARTHEWS, T. R.; MALHI, Y.; IWATA, H. Calculating downward longwave radiation under clear and cloudy conditions over a tropical lowland forest site: an evaluation of model schemes for hourly data. **Theoretical and applied climatology**, Springer, v. 107, n. 3, p. 461–477, 2012.

NABINGER, C. et al. Produção animal com base no campo nativo: aplicações de resultados de pesquisa. **Campos Sulinos: conservação e uso sustentável da biodiversidade**. Brasília: MMA, p. 175–197, 2009.

NERPIN, S.; CHUDNOVSKII, A. **Physics of the soil: Israel program for scientific translations**. [S.l.]: Keter press, Jerusalem, 1967.

NIKOOSOKHAN, S.; NOWAMOOZ, H.; CHAZALLON, C. Effect of dry density, soil texture and time-spatial variable water content on the soil thermal conductivity. **Geomechanics and Geoengineering**, Taylor & Francis, v. 11, n. 2, p. 149–158, 2016.

NOVAK, M.; BLACK, T. Theoretical determination of the surface energy balance and thermal regimes of bare soils. **Boundary-Layer Meteorology**, Springer, v. 33, n. 4, p. 313–333, 1985.

ONCLEY, S. P. et al. The energy balance experiment ebex-2000. part i: overview and energy balance. **Boundary-Layer Meteorology**, Springer, v. 123, n. 1, p. 1–28, 2007.

OTUNLA, T. A.; OLADIRAN, E. O. Evaluation of soil thermal diffusivity algorithms at two equatorial sites in west africa. **Annals of Geophysics**, v. 56, n. 1, p. 0101, 2013.

PEEL, M. C.; FINLAYSON, B. L.; MCMAHON, T. A. Updated world map of the köppen-geiger climate classification. **Hydrology and earth system sciences discussions**, v. 4, n. 2, p. 439–473, 2007.

PEREIRA, A. R. **Agrometeorologia: fundamentos e aplicações práticas**. [S.l.]: Agropecuária, 2002.

PLANA-FATTORI, A.; CEBALLOS, J. Glossário de termos técnicos em radiação atmosférica. **Série Ciências Atmosféricas**, n. 004, 1996.

PREVEDELLO, C. L. **Física do solo com problemas resolvidos-2ªEd**. [S.l.: s.n.], 2015.

REICHARDT, K. **A água em sistemas agrícolas**. [S.l.]: Manole, 1990.

REICHARDT, K.; TIMM, L. C. **Solo, planta e atmosfera: conceitos, processos e aplicações**. [S.l.]: Manole São Paulo, 2004.

ROESCH, L. F. W. et al. The brazilian pampa: a fragile biome. **Diversity**, Molecular Diversity Preservation International, v. 1, n. 2, p. 182–198, 2009.

ROMIO, L. C. et al. A numerical model to estimate the soil thermal conductivity using field experimental data. **Applied Sciences**, Multidisciplinary Digital Publishing Institute, v. 9, n. 22, p. 4799, 2019.

ROSA, M. Áreas prioritárias para conservação, uso sustentável e repartição de benefícios da biodiversidade brasileira. Brasília, DF (Brazil), 2008.

ROTH, K. Soil physics lecture notes. **Institute of Environmental Physics, Heidelberg University**, v. 2, 1995.

ROXY, M.; SUMITHRANAND, V.; RENUKA, G. Estimation of soil moisture and its effect on soil thermal characteristics at astronomical observatory, thiruvananthapuram, south kerala. **Journal of earth system science**, Springer, v. 123, n. 8, p. 1793–1807, 2014.

SEEMANN, J. Measuring technology. In: **Agrometeorology**. [S.l.]: Springer, 1979. p. 40–45.

SILANS, A. M. P. de; MONTENY, B. A.; LHOMME, J. P. Apparent soil thermal diffusivity, a case study: Hapex-sahel experiment. **Agricultural and Forest Meteorology**, Elsevier, v. 81, n. 3-4, p. 201–216, 1996.

SILANS, A. P. D. et al. Numerical modeling of coupled heat and water flows during drying in a stratified bare soil—comparison with field observations. **Journal of Hydrology**, Elsevier, v. 105, n. 1-2, p. 109–138, 1989.

SILANS, A. P. de; MONTENY, B. A.; LHOMME, J. P. The correction of soil heat flux measurements to derive an accurate surface energy balance by the bowen ratio method. **Journal of Hydrology**, Elsevier, v. 188, p. 453–465, 1997.

SMIRNOVA, T. G.; BROWN, J. M.; BENJAMIN, S. G. Performance of different soil model configurations in simulating ground surface temperature and surface fluxes. **Monthly Weather Review**, v. 125, n. 8, p. 1870–1884, 1997.

TAVARES, P. Observação e análise da radiação solar global e fotossinteticamente ativa na região de maceió. 2005.

TONG, B. et al. An empirical model for estimating soil thermal conductivity from soil water content and porosity. **Journal of Hydrometeorology**, v. 17, n. 2, p. 601–613, 2016.

TOULOUKIAN, Y. et al. **Thermophysical Properties of Matter, Volume 10-Thermal Diffusivity**. [S.l.]: IFI/Plenum Data Corporation, 1973.

VERHOEF, A. Remote estimation of thermal inertia and soil heat flux for bare soil. **Agricultural and forest meteorology**, Elsevier, v. 123, n. 3-4, p. 221–236, 2004.

VRIES, D. D.; PECK, A. On the cylindrical probe method of measuring thermal conductivity with special reference to soils. i. extension of theory and discussion of probe characteristics. **Australian Journal of Physics**, CSIRO Publishing, v. 11, n. 2, p. 255–271, 1958.

WANG, J.; BRAS, R. Ground heat flux estimated from surface soil temperature. **Journal of hydrology**, Elsevier, v. 216, n. 3, p. 214–226, 1999.

WANG, L.; GAO, Z.; HORTON, R. Comparison of six algorithms to determine the soil apparent thermal diffusivity at a site in the loess plateau of china. **Soil science**, LWW, v. 175, n. 2, p. 51–60, 2010.

WANG, L. et al. An analytical solution to the one-dimensional heat conduction–convection equation in soil. 2012.

WANG, W. et al. A hybrid laplace transform finite analytic method for solving transport problems with large pecllet and courant numbers. **Computers & geosciences**, Elsevier, v. 49, p. 182–189, 2012.

WIERENGA, P.; NIELSEN, D.; HAGAN, R. Thermal properties of a soil based upon field and laboratory measurements. **Soil science society of America Journal**, Soil Science Society of America, v. 33, n. 3, p. 354–360, 1969.

WILSON, K. et al. Energy balance closure at fluxnet sites. **Agricultural and Forest Meteorology**, Elsevier, v. 113, n. 1-4, p. 223–243, 2002.

WILSON, K. B. et al. A comparison of methods for determining forest evapotranspiration and its components: sap-flow, soil water budget, eddy covariance and catchment water balance. **Agricultural and forest Meteorology**, Elsevier, v. 106, n. 2, p. 153–168, 2001.

XIE, X. et al. Soil temperature estimation with the harmonic method is affected by thermal diffusivity parameterization. **Geoderma**, Elsevier, v. 353, p. 97–103, 2019.

ZHAO, Y. et al. A new thermal conductivity model for sandy and peat soils. **Agricultural and Forest Meteorology**, Elsevier, v. 274, p. 95–105, 2019.

ZIMMER, T. et al. Influence of clearness index and soil moisture in the soil thermal dynamic in natural pasture in the brazilian pampa biome. **Geoderma**, Elsevier, v. 378, p. 114582, 2020.